pôle de recherche et développement en **écohydraulique**

Cassiopée software

version 4.19.1
User documentation

MAY 6, 2025

DAVID DORCHIES, JEAN-PASCAL AUBRY, MATHIAS CHOUET, FRANÇOIS GRAND

Contents

1 Presentation of Cassiopée

1.1 Presentation of Cassiopée software

https://cassiopee.g-eau.fr

1.1.1 General characteristics

Cassiopée is a software dedicated to rivers hydraulics with especially some help for sizing fish passes, agricultural hydraulics and open-channel hydraulics in general. It comes in the form of independent calculation modules allowing one to solve a given problem. Calculation modules may be chained (parameters or calculation results may be "linked" from one module to another) in order to build complex calculation chains. Users may locally save the modules they use, in order to reuse them later.

1.1.2 Pre-requisites - installation

Cassiopée does not require any installation. It is available online using an up-to-date browser (tested with Firefox, Edge, Chrome and Chromium) by navigating to the following address: https://cassiopee.g-eau.fr.

Offline versions are available for the Windows, Linux, macOS, Android platforms. For details, see the "Installation" section in the documentation.

1.1.3 Documentation

Download documentation in PDF format

Download illustrated quick start guide (in french) in PDF format

1.1.4 Support and bug reports

To be kept informed of Cassiopée news or to benefit from the Cassiopée users' support network, subscribe to the Cassiopée users' mailing list: https://groupes.renater.fr/sympa/subscribe/cassiopee-users

Insiders can test the future version of Cassiopée under development at https://cassiopee-dev.g-eau.fr and provide feedback at bug@cassiopee.g-eau.fr.

To report a bug in the application, please use the "Report an issue" link in the main menu of the application or write directly to bug@cassiopee.g-eau.fr.

For questions concerning the design of fish crossing structures for upstream (basin, retarder, macro-roughness) and downstream migrations, please contact Sylvain Richard, pole OFB-IMFT Écohydraulique, sylvain.richard@imft.fr.

1.1.5 Citing Cassiopée

If you use Cassiopée in your work please remember to give appropriate credit by using the following reference:

Dorchies, David; Grand, François; Chouet, Mathias; Cassan, Ludovic; Courret, Dominique; Richard, Sylvain, 2022, "Cassiopée: tools for designing fish crossing devices for upstream and downstream migrations, and hydraulic calculation tools for environmental and agricultural engineering. Version 4.16.0", https://doi.org/10.15454/TLO5LX, Recherche Data Gouv, V1

1.2 Installation

Cassiopée can be installed for use without an internet connection as an executable program or as a progressive web app (PWA).

1.2.1 Installation of the Cassiopée progressive web application

A progressive web app (PWA) is a web application that consists of pages or websites, and can appear to the user in the same way as native applications or mobile applications.

PWAs are available for all platforms (Windows, Linux, MacOS, Android, and iOS) provided you have a compatible browser:

Plateforme	Chrome/Chromium	Edge	Firefox	Safari
Windows	Yes	Yes	via extension	
Linux	Yes		via extension	
MacOS	Yes		via extension	
Android	Yes		Yes	
iOS				Yes

The installation is done directly from the web browser at https://cassiopee.g-eau.net by clicking on a button located on the right of the address bar. The appearance of the button may vary depending on the browser used:

- Install a PWA with Chrome/Chromium: https://support.google.com/chrome/answer/9658361?hl=fr
- Installing a PWA with Edge: https://learn.microsoft.com/fr-fr/microsoft-edge/progressive-web-apps-chromium/ux
- Install a PWA (any browser and platform): https://developer.mozilla.org/en-US/docs/Web/Progressive_web_apps/Installing

After the installation, Cassiopée can be launched from the application icon on the desktop.

Updates are automatically detected and installed (the user is invited to restart Cassiopée after downloading the update).

N.B.: even without going through the PWA installation procedure, Cassiopée is available in the browser without an internet connection provided it has been previously loaded.

1.2.2 Installation of the Desktop application (obsolete)

Cassiopée is available as an executable program for Windows, Linux and MacOS platforms. The installation programs can be downloaded at the following address: https://cassiopee.g-eau.fr/cassiopee-releases/

The installation in the form of a progressive web application (see above) will definitely replace this installation mode in a future version of Cassiopée.

1.3 Principle of operation of a calculation module

Each Cassiopée calculation module allows you to calculate a parameter of your choice from those in one or more equations.

1.3.1 Open a new calculation module

Figure 1.1: Top banner of the application with the menu, the list of open modules and the button to add a new module

The list of modules is available when the application is launched. After opening a new calculation module, this list is available via the "+" button located in the upper banner or via the "≡" menu and then the "New calculation module" link located in the menu.

The list of open modules appears in the upper banner and allows you to navigate between open modules.

1.3.2 How are the choices made to perform a calculation or a series of calculations ?

The module is presented as a series of parameters involved in solving the equation of the calculation module.

For each of them, the user can choose to:

- Set the parameter's value ("FIXED" button);
- Vary the parameter to perform a series of calculations ("VARIATED" button);
- Choose the parameter that will be calculated ("CALCULATE" button).

The interface is designed so that one and only one parameter is chosen for the calculation. Parameters that cannot be calculated do not have a "CALCULATE" button.

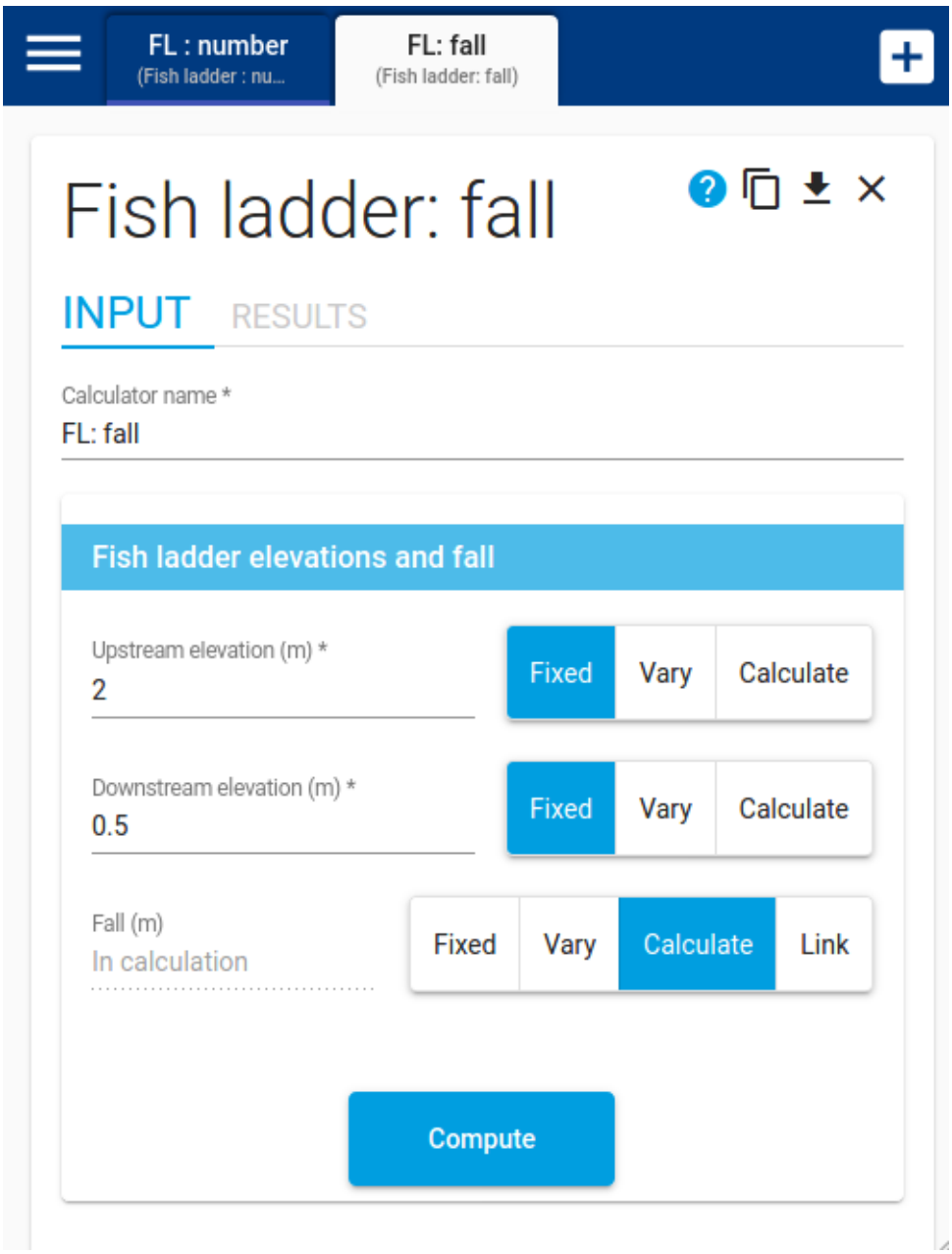

Figure 1.2: Parameters of the module for calculating the fall of a basin pass

1.3.3 How to vary a parameter to perform a series of calculations

A series of calculations can be triggered between a minimum value and a maximum value for a given step:

Or for a list of defined values:

Importing a values list is done either by typing or copy/pasting it in the “Values list” field, or by importing a text file. The decimal separator is configurable. Any character outside the numeric characters, the letter “E” and the decimal separator will be considered as separator between the values. Therefore, the separator could be comma, semicolon, space, tabulation, new line...

The window title contains the corresponding number of occurrences. Clicking on the graphic logo at the right of the window title displays a chart of the parameter variations.

In case several parameters vary and they do not have the same number of occurrences,

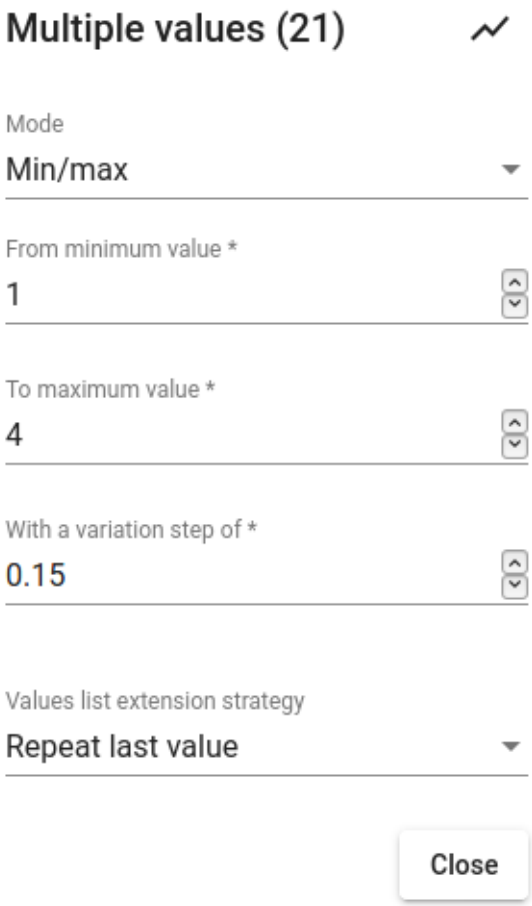

Figure 1.3: Define min, max and step values for a parameter to be varied

it is necessary to define a strategy to extend the shortest lists to fit the list of the parameter with the most occurrences. Two strategies are available: repeat the last value or reuse the values in the list since the first occurrence.

1.3.4 How to launch a calculation or a series of calculations

Press the [Enter] key or click on the “Calculate” button at the bottom of the page.

1.3.5 Calculation results

For fixed parameters, the results panel displays the fixed parameters and the calculated parameter as well as any additional results.

For one or more varying parameters, the results panel displays:

- an evolution graph on the which you can choose the parameter to use on the x-axis and y-axis;
- a table containing the parameters set;
- a table showing the parameters that vary and the calculated parameter as well as the values of any additional results.

The tables and charts are provided with different functionalities:

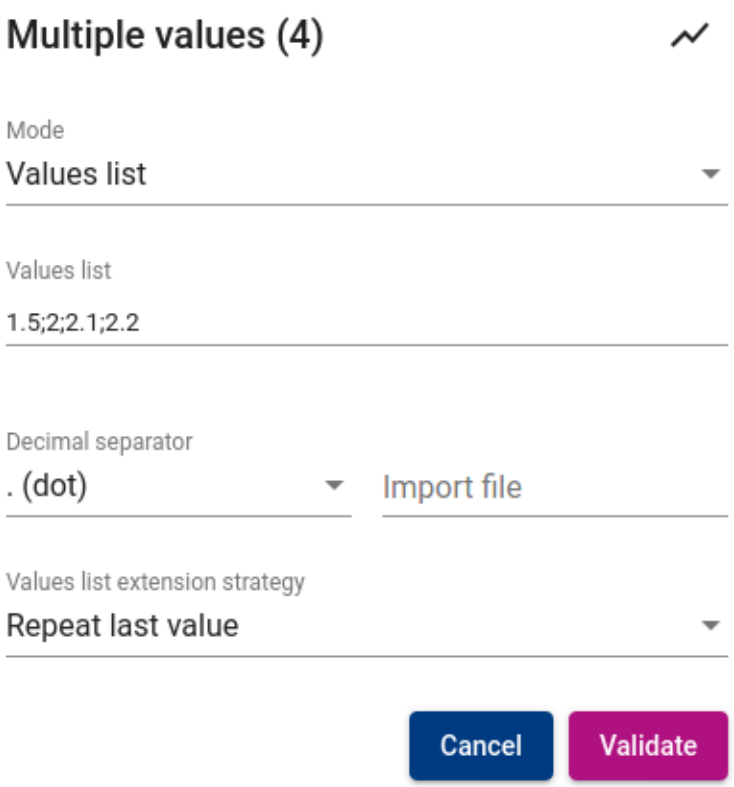

Figure 1.4: Defining a list of values for a parameter to be varied

Fixed parameters	Values
Upstream elevation (m)	2.000
Downstream elevation (m)	0.500
Fall (m)	**1.500**

Figure 1.5: Result of a calculation for fixed values

- a download button to retrieve the table content in XLSX format;
- a download button to retrieve the chart in PNG format;
- a button to display the table or chart in full screen.

The charts are zoomed in by making a mouse selection on some area. The button with the curved left-pointing arrow resets the zoom to its original position displaying all available values.

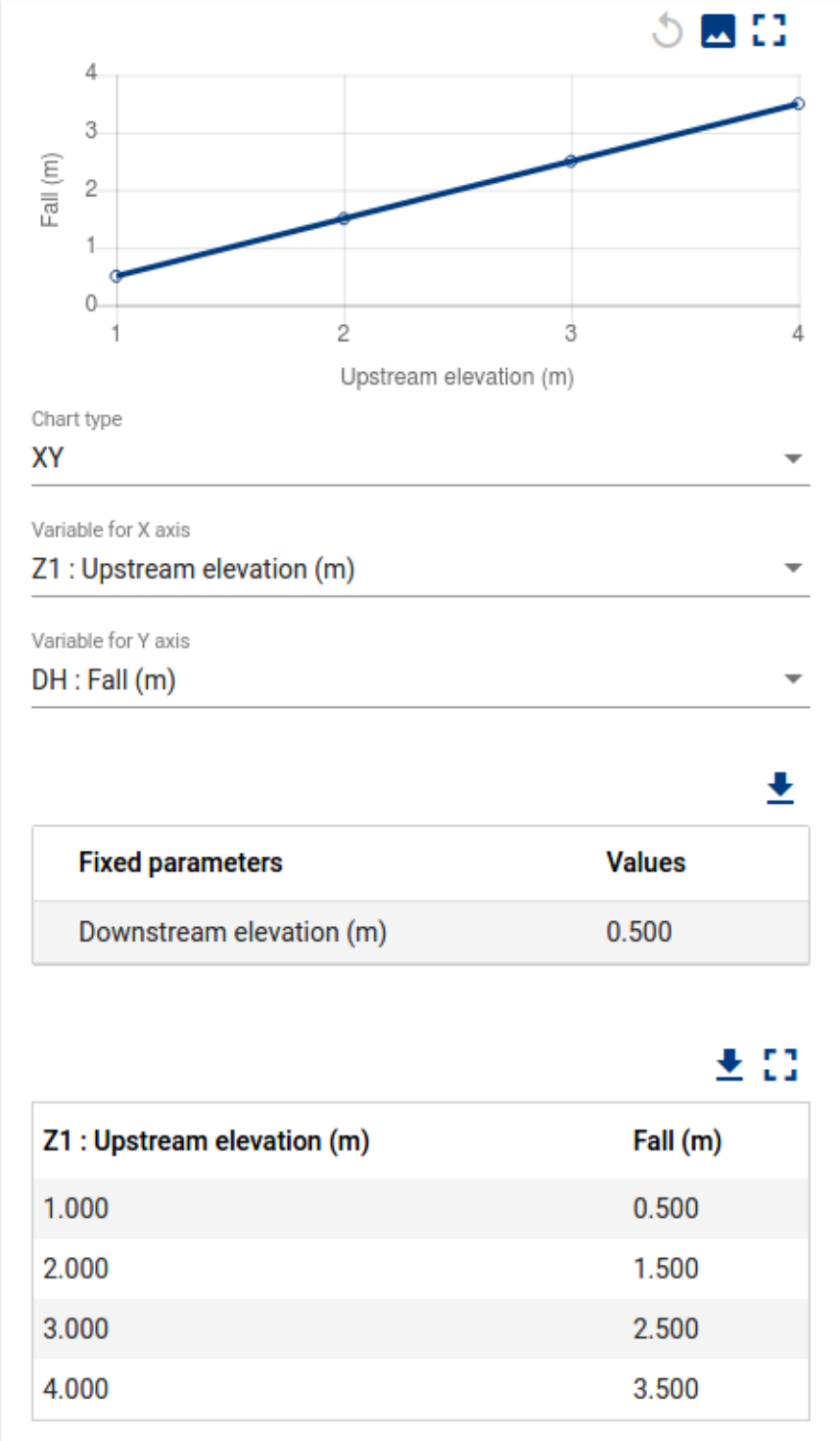

Figure 1.6: Results of a series of calculations for a varying parameter

1.4 Application parameters

Accessible from the left side menu, the application parameters that can be modified by the user are as follows:

- Number of displayed decimals: Number of displayed decimals for the calculation results. For numbers close to zero displayed in scientific notation, this option sets the number of significant digits displayed;

- Computation accuracy: Precision used for the convergence of numerical calculations (Brent's method or Newton's method);
- Solver iteration limit: Maximum iteration number of the numerical calculation;
- Enable on-screen notifications: allows notifications to be displayed during certain operations (warning when loading a session, calculation invalidation. . .);
- Enable keyboard shortcuts: allows the use of keyboard shortcuts (See list of available shortcuts);
- Create new calculators with empty fields (no default values): if unchecked, module parameters are pre-filled with default values;
- Language: defines the language of the software interfaces in French or English.

The save button at the top of the window allows you to save the user's preferences in your browser for future use. The "Reset" button restores the application's default settings.

1.5 Keyboard shortcuts list

To use keyboard shortcuts, the feature must be enabled in application parameters.

- Alt + S: Saves the current session
- Alt + O: Opens a session file
- Alt + Q: Empties the current session
- Alt + N: Adds a new calculation module to the current session
- Alt + ↩: Triggers calculation of the current module
- Alt + D: Duplicates the current module
- Alt + W: Closes the current module
- Alt + G: Shows modules diagram
- Alt + 1: Positions the page on the "Input" section of the current module
- Alt + 2: Positions the page on the "Results" section of the current module
- Alt + 3: Positions the page on the "Charts" section of the current module

2 Pipe flow

2.1 Pressure loss

This module computes linear head losses in a circular pipe with the following laws:

- Lechapt et Calmon
- Strickler

The following values can be computed:

- Flow (m3/s)
- Pipe diameter (m)
- Total pressure loss (m)
- Pipe length (m)
- Singular head loss coefficient

The total pressure loss is the sum of linear losses J_{lin}, according to the used law, and singular losses J_{loc} depending on the above coefficient.

2.1.1 Singular pressure loss

$$J_{loc} = K_{loc}\frac{V^2}{2g}$$

Given :

- K_{loc} : singular head loss coefficient
- V : water speed in the pipe ($V = 4Q/\pi/D^2$)

2.1.2 Linear head loss coefficient

$$K_{lin} = \frac{2gJ_{lin}}{V^2}$$

2.1.3 Darcy head loss coefficient

$$f_D = \frac{2gJD}{l_T V^2}$$

2.2 Lechapt and Calmon

This module allows to calculate the pressure losses in a circular pipe from the Lechapt and Calmon abacuses.

It allows the calculation of the value of one of the following quantities:

- Flow rate (m3/s)
- Pipe diameter (m)
- Total head loss (m)
- Pipe length (m)
- Singular pressure loss coefficient

The total head loss is the sum of the linear head losses J_L obtained from the Lechapt and Calmon abacuses and singular J_S depending on the above coefficient.

2.2.1 Lechapt and Calmon abacuses

Lechapt and Calmon formula is based on adjustements of Cyril Frank Colebrook formula:

$$J_L = l_T L.Q^M.D^{-N}$$

With:

- J_L: headloss in mm/m or m/km;
- l_T: pipe length in m;
- Q: flow in m3/s;
- D: pipe diameter in m;
- L, M and N coefficients depending on roughness {$\in$}.

The error made with respect to the Colebrook formula is less than 3% for speeds between 0.4 and 2 m/s.

The correlation table of the coefficients is as follows:

Table 2.1: Materials and coefficients used in the Lechapt and Calmon formula

Material	$\in$ (mm)	L	M	N
Uncoated cast iron or steel - Coarse concrete (corrosive water)	2	1.863	2	5.33
Uncoated cast iron or steel - Coarse concrete (low corrosive water)	1	1.601	1.975	5.25
Cast iron or steel with cement coating	0.5	1.40	1.96	5.19
Cast iron or steel bitumen coating - centrifuged concrete	0.25	1.16	1.93	5.11
Rolled steel - smooth concrete	0.1	1.10	1.89	5.01
Cast iron or steel centrifugal coating	0.05	1.049	1.86	4.93
PVC - polyethylene	0.025	1.01	1.84	4.88
Hydraulically smooth pipe - 0.05 $\leq$ D $\leq$ 0.2	0.00	0.916	1.78	4.78

Material	∈ (mm)	L	M	N
Hydraulically smooth pipe - 0.25 ≤ D ≤ 1	0.00	0.971	1.81	4.81

2.3 Strickler formula

This linear head loss law is parameterised by the Stricker coefficient K_S.

The other law parameters are shared with all pressure loss formulas:

- Q : flow (m3/s)
- D : pipe diameter (m)
- l_T : pipe length (m)

$$J_L = \frac{l_T.Q^2}{(K_S.\pi.D^2/4)^2.(D/4)^{4/3}}$$

2.4 Distributor pipe

Analytical relationship for the direct calculation of pressure drops in pipes distributing a flow rate in a homogeneous manner based on the Blasius formula.

2.4.1 Assumptions

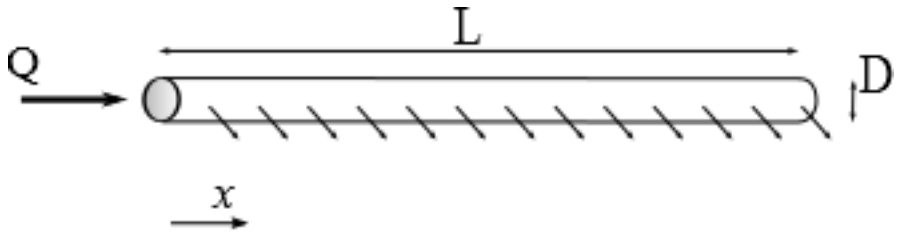

Figure 2.1: Conduct diagram

We assume a pipe length L, inner diameter D, with a flow rate at the top Q. We calculate the pressure drop between the two ends of the pipe. In a constant flow section q, the friction coefficient is evaluated with the Blasius formula, valid for moderate Reynolds numbers for smooth walls:

$$\lambda \simeq aRe^{-0.25}$$

2.4.2 Analytical development

We're recording the position from the downstream end of the pipe. The flow rate is supposed to vary linearly with x, and is then written:

$$q(x) = Qx/L$$

Let's note $S = \pi D^2/4$ the inner surface of the pipe. The pressure drop is obtained by integrating the Darcy-Weisbach relationship:

$$\Delta H = \int_{x=0}^{L} aRe^{-0.25} \frac{u^2(x)}{2gD} dx$$

Note the kinematic viscosity. We then replace Re with uD/ν, which gives

$$\Delta H = \int_{x=0}^{L} au(x)^{-0.25} D^{-0.25} \nu^{0.25} \frac{u^2(x)}{2gD} dx$$

By rearranging, we get:

$$\Delta H = \int_{x=0}^{L} a\nu^{0.25} \frac{u^{1.75}(x)}{2gD^{1.25}} dx$$

Let's use the flow equation to show the flow ($u(x) = q(x)/S$):

$$\Delta H = \int_{x=0}^{L} a\nu^{0.25} \frac{(Qx/(LS))^{1.75}}{2gD^{1.25}} dx$$

then the diameter:

$$\Delta H = \int_{x=0}^{L} a\nu^{0.25} \frac{(4Qx/(L\pi D^2))^{1.75}}{2gD^{1.25}} dx$$

We rearrange to get

$$\Delta H = a\nu^{0.25} \frac{(4/\pi)^{1.75} Q^{1.75}}{2gD^{4.75}} \int_{x=0}^{L} (x/L)^{1.75} dx$$

By integrating, we obtain

$$\Delta H = a\nu^{0.25} \frac{(4/\pi)^{1.75} Q^{1.75}}{2gD^{4.75}} \frac{L}{2.75}$$

$$\Delta H = a\nu^{0.25} \frac{4^{1.75}}{5.5g\pi^{1.75}} Q^{1.75} L D^{4.75}$$

2.4.3 Digital application

For water at 20°C: $\nu \simeq 10^{-6}$ m2/s, which gives

$$DeltaH = 0.323\ 10^{-3} \frac{Q^{1.75}}{D^{4.75}} L$$

with ΔH in meters.

For water at 50℃, $\nu \simeq 0.55610^{-6}$ m2/s, which means that the pressure drop is reduced by about 14%, or

$$DeltaH = 0.28\ 10^{-3} \frac{Q^{1.75}}{D^{4.75}} L$$

3 Open-channel flow

3.1 Uniform flow

The uniform flow is characterized by a water height called the normal height. The normal height is reached when the water line is parallel to the bottom, the load is then itself parallel to the water line and thus the head loss is equal to the slope of the bottom: $I_f = J$

With:

- I_f: bottom slope in m/m
- J: head loss in m/m

The head loss {J} is calculated here using Manning-Strickler's formula:

$$J = \frac{U^2}{K^2 R^{4/3}} = \frac{Q^2}{S^2 K^2 R^{4/3}}$$

With:

- K: Strickler coefficient in m1/3/s

In uniform flow, we obtain the formula:

$$Q = K R^{2/3} S \sqrt{I_f}$$

Based on the which, flow Q, slope I_f and Strickler calculation K can be calculated analytically.

To calculate normal height h_n , one can solve $f(h_n) = Q - K R^{2/3} S \sqrt{I_f} = 0$

using Newton's method:

$$h_{k+1} = h_k - \frac{f(h_k)}{f'(h_k)}$$

with:

- $f(h_k) = Q - K R^{2/3} S \sqrt{I_f}$
- $f'(h_k) = -K \sqrt{I_f} (\frac{2}{3} R' R^{-1/3} S + R^{2/3} S')$

To calculate the geometrical parameters of the section, the calculation module uses the flow calculation equation and solves the problem by dichotomy.

3.2 Backwater curve

The calculation of the backwater curve involves the following differential equation:

$$\frac{dy}{dx} = \frac{I_f - J(h)}{1 - F^2(h)}$$

where I_f is the slope of a canal, J the formula giving us the local pressure drop (depending on the water level), y here refers to the height of water.

Thus, for a rectangular channel of width b and a Strickler coefficient K:

$$J = \frac{Q^2(b+2y)^{4/3}}{K^2 b^{10/3} y^{10/3}}$$

and

$$F^2 = \frac{Q^2}{gb^2y^3}$$

The integration of the equation can be done by one of the following methods: Runge-Kutta 4, Explicit Euler, trapezes integration.

Depending on the flow regime, the calculation can be carried out:

- from downstream to upstream for subcritical flow with definition of a downstream boundary condition.
- from upstream to downstream for supercritical flow with definition of an upstream boundary condition

If we take the example of a rectangular channel, the proposed scilab code example for solving an ordinary differential equation is amended as follows:

```
b=0.3;
K=50;
If=0.005;
Q=0.01;
function z=DQ(y);
  z=Q-K*(b*y)^(5/3)/(b+2*y)^(2/3)*sqrt(If);
endfunction
yn=fsolve(0.5,DQ);
tmax=0;
t0=10;
dt=-0.5;
function z=f(y,t);
  z=(If-Q^2*(b+2*y)^(4/3)/(K^2*(b*y)^(10/3)))/(1-Q^2/(9.81*b^2*y^3));
endfunction
y0=0.12;
```

which gives us the normal depth, and the water line. Depending on the numerical method used, we can have large errors in the case of an F2 backwater curve (downstream condition

below normal height), because the waterline slopes are much steeper, and therefore much more prone to errors related to linear interpolation. We can therefore deduce that on the one hand the choice of the resolution method is important, and on the other hand it is essential to take a critical look at the solutions (with an interpretation of the processes we are trying to model).

3.3 Upstream / downstream elevations of a reach

This module is based on the equations of the backwater curves module and is used to calculate the following:

- The water elevation upstream of a reach of a fluvial backwater curve;
- The water elevation downstream of a reach of a torrential backwater curve;
- The flow that connects the upstream and downstream water elevations of a fluvial or torrential backwater curve.

The regime chosen on the type of water line determines whether the calculation is made from downstream to upstream (fluvial regime) and from upstream to downstream (torrential regime).

This calculation module is particularly useful for calculating the water line of a series of hydraulic structures or reaches (see the typical example “Flow of a channel with structures”).

3.4 Parametric section

This module calculates the hydraulic quantities associated to:

- a section with a defined geometrical shape (See section types managed by Cassiopée)
- a water depth y in m
- a flow Q in m3/s
- a bottom slope I_f in m/m
- a roughness expressed with the Strickler’s coefficient K in m1/3/s

The calculated hydraulic quantities are:

- Width at mirror (m)
- Wet perimeter (m)
- Hydraulic surface (m2)
- Hydraulic radius (m)
- Average speed (m/s)
- Specific head (m)
- Head loss (m)
- Linear variation of specific energy (m/m)
- Normal depth (m)
- Froude number
- Critical depth (m)
- Critical head (m)

- Corresponding depth (m)
- Impulsion (N)
- Conjugate depth
- Tractive force (Pa)

3.4.1 Bank height, overflow and closed-conduit flow

The sections are all provided with a bank height which is used at three levels in the free surface hydraulics calculation tools:

- It allows to define if the calculated water level overflows the section.
- Beyond this bank height the hydraulic calculations simulate a flow between two vertical walls. For example, a semi-circular pipe can be modelled by defining a bank height equal to the radius of the pipe.
- For a circular pipe, a bank height greater than or equal to the diameter of the pipe makes it possible to model a closed pipe. If the water level exceeds the diameter of the pipe, hydraulic calculations simulate a closed-conduit flow using the Preissmann slot technique.

3.4.2 Width at mirror, wet perimeter and surface

See the dedicated page for the parameters specific to each type of section

3.4.2.1 Rectangular section

- Width at mirror : $B = L$
- Surface : $S = L.y$
- Perimeter : $P = L + 2y$

3.4.2.2 Trapezoidal section

- Width at mirror : $B = L + 2..m.y$
- Surface : $S = (L + m.y)y$
- Perimeter : $P = L + 2y\sqrt{1 + m^2}$

3.4.2.3 Circular section

- Width at mirror : $B = D \sin\theta$
- Surface : $S = \frac{D^2}{4}(\theta - \sin\theta.\cos\theta)$
- Perimeter : $P = D.\theta$

3.4.2.4 Parabolic section

- Width at mirror : $B = \frac{B_b}{y_b^k} y^k$
- Surface : $S = \frac{B_b}{y_b^k} \frac{y^{k+1}}{k+1}$
- Perimeter : $P = 2\sum_{i=1}^{n} \sqrt{\frac{1}{n^2} + \frac{1}{4}\left(B\left(\frac{i.y}{n}\right) - B\left(\frac{(i-1).y}{n}\right)\right)^2}$ for n large enough

3.4.3 Hydraulic radius (m)

$$R = S/P$$

3.4.4 Average speed (m/s)

$$U = Q/S$$

3.4.5 Specific head (m)

$$H(y) = y + \frac{U^2}{2g}$$

3.4.6 Head loss (m/m)

Cassiopée uses Manning Strickler formula:

$$J = \frac{U^2}{K^2 R^{4/3}} = \frac{Q^2}{S^2 K^2 R^{4/3}}$$

3.4.7 Linear variation of specific energy (m/m)

$$\Delta E_s = I_f - J$$

3.4.8 Normal depth (m)

See the uniform flow calculation.

3.4.9 Froude number

The Froude number expresses the ratio between the mean fluid velocity and the surface wave velocity. c.

$$c = \sqrt{\frac{gS}{B}}$$

$$Fr = \frac{U}{c} = \sqrt{\frac{Q^2 B}{gS^3}}$$

3.4.10 Critical depth (m)

The critical height is reached when the average velocity of the fluid is equal to the velocity of the waves on the water surface.

The critical height is therefore reached when the Froude number $Fr = 1$.

For any section, the critical height is calculated as follows y_c by solving $f(y_c) = Fr^2 - 1 = 0$

We use Newton's method by posing $y_{k+1} = y_k - \frac{f(y_k)}{f'(y_k)}$ with : - $f(y_k) = \frac{Q^2 B}{gS^3} - 1$ - $f'(y_k) = \frac{Q^2}{g}\frac{B'.S - 3BS'}{S^4}$

3.4.11 Critical head (m)

This is the head calculated for a water depth equal to the critical depth. $H_c = H(y_c)$.

3.4.12 Corresponding depth (m)

For a fluvial (respectively torrential water depth) y, corresponding depth is the torrential (respectively fluvial) water depth for which $H(y) = H(y_{cor})$.

3.4.13 Hydraulic impulsion (N)

The impulsion I is the sum of the amount of movement and the resultant of the pressure force in a section:

$$I = \rho Q U + \rho g S y_g$$

With :

- ρ : the density of water (kg/m3)
- y_g : the distance from the centre of gravity of the section to the free surface (m)

The distance from the centre of gravity of the section to the free surface y_g can be found from the formula :

$$S.y_g = \int_0^y (y - z) B(z) dz$$

With y the depth and $B(z)$ the width at mirror for a water depth z

Formulas of $S.y_g$ for the different section shapes are :

- rectangular section: $S.y_g = \frac{L.y^2}{2}$
- trapezoidal section: $S.y_g = \left(\frac{L}{2} + \frac{m.y}{3}\right) y^2$
- circular section: $S.y_g = \frac{D^3}{8}\left(\sin\theta - \frac{\sin^3\theta}{3} - \theta\cos\theta\right)$
- parabolic section: $S.y_g = \frac{B_b.y^{k+2}}{y_b^k(k+1)(k+2)}$

3.4.14 Conjugate depth (m)

For a fluvial (respectively torrential water depth) y, conjugate depth is the torrential (respectively fluvial) water depth for which $I(y) = I(y_{con})$.

3.4.15 Tractive force (Pa)

$$\tau_0 = \rho g R J$$

3.5 Slope

3.5.1 Definition

The slope used in all Cassiopée's modules is the topographic slope:

> The grade (also called slope, incline, gradient, mainfall, pitch or rise) of a physical feature, landform or constructed line refers to the tangent of the angle of that surface to the horizontal. (Source: Wikipedia)

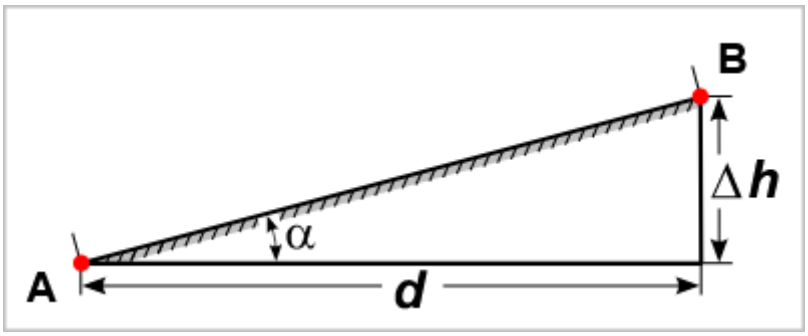

Figure 3.1: Longitudinal cross-sectional scheme of a rectilinear section

The slope (I) in m/m used in Cassiopee's modules is:

$$I = \Delta h/d = \tan(\alpha)$$

Important:

All calculation modules consider a descending slope as positive except for the "Jet Impact" module where a positive slope will be considered as rising and vice versa. To invert the slope in a calculation sequence of linked modules, use the "linear function" module with $a = -1$ and $b = 0$.

3.5.2 The "Slope" module

This tools allows to calculate the missing value of the four quantities:

- upstream elevation (Z_1) in m;
- downstream elevation (Z_2) in m;
- length (d) in m;
- slope (I) in m/m, with $I = \frac{(Z_1 - Z_2)}{d}$.

3.6 Section types

3.6.1 Rectangular section

The rectangular section is characterized by the following parameters:

- width at bottom L (in m)

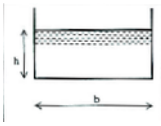

Figure 3.2: Rectangular section

3.6.2 Circular section

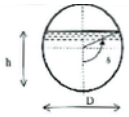

Figure 3.3: Circular section

The circular section is characterized by the following parameters:

- the pipe diameter D (in m)
- the angle θ between the pipe bottom and the junction point between water surface and pipe (in Rad)

$$\theta = \arccos\left(1 - \frac{y}{D/2}\right)$$

$$\theta' = \frac{2}{D\sqrt{1-\left(1-\frac{2y}{D}\right)^2}}$$

3.6.3 Trapezoidal section

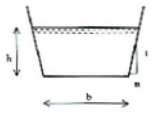

Figure 3.4: Trapezoidal section

The trapezoidal section is characterized by the following parameters:

- width at bottom L (in m)
- bank slope (inclination to the vertical: widening between the top and bottom of the slope divided by the depth.) m (in m/m)

3.6.4 Parabolic section

The parabolic section is characterized by a mirror width that can be expressed in the form:

$B = \Lambda.y^k$.

With k: coefficient between 0 and 1. $k = 0.5$ corresponds to the true parabolic form.

Λ can be calculated by giving:

- y_b: bank height (in m)
- B_b: embankment width (in m)

We then have: $\Lambda = \frac{B_b}{y_b^k}$

3.7 Manning-Strickler's formula

3.7.1 Definition

Manning-Strickler formula is written as follows:

$$V = K_s R_h^{2/3} i^{1/2}$$

with:

- V la vitesse moyenne de la section transversale en m/s
- K_s Strickler's coefficient
- R_h Hydraulic radius in m
- i slope en m/m

The Strickler coefficient K_s varies from 20 (rough stone and rough surface) to 80 (smooth concrete and cast iron).

Manning's coefficient n is obtained by :

$$n = \frac{1}{K_s}$$

3.7.2 Chow's table (1959)

Table 3.1: Chow's table (1959)

Type of channel and description	K_S min.	K_S normal	K_S max.
1. Main channels			
a. clean, straight, full stage, no rifts or deep pools	30	33	40
b. same as above, but more stones and weeds	25	29	33
c. clean, winding, some pools and shoals	22	25	30
d. same as above, but some weeds and stones	20	22	29
e. same as above, lower stages, more ineffective slopes and sections	18	21	25
f. same as "d" with more stones	17	20	22
g. sluggish reaches, weedy, deep pools	13	14	20
h. very weedy reaches, deep pools, or floodways with heavy stand of timber and underbrush	7	10	13
2. Mountain streams, no vegetation in channel, banks usually steep, trees and brush along banks submerged at high stages			
a. bottom: gravels, cobbles, and few boulders	20	25	33
b. bottom: cobbles with large boulders	14	20	25
3. Floodplains			

Type of channel and description	K_S min.	K_S normal	K_S max.
a. Pasture, no brush			
1. short grass	29	33	40
2. high grass	20	29	33
b. Cultivated areas			
1. no crop	25	33	50
2. mature row crops	22	29	40
3. mature field crops	20	25	33
c. Brush			
1. scattered brush, heavy weeds	14	20	29
2. light brush and trees, in winter	17	20	29
3. light brush and trees, in summer	13	17	25
4. medium to dense brush, in winter	9	14	22
5. medium to dense brush, in summer	6	10	14
d. Trees			
1. dense willows, summer, straight	5	7	9
2. cleared land with tree stumps, no sprouts	20	25	33
3. same as above, but with heavy growth of sprouts	13	17	20
4. heavy stand of timber, a few down trees, little undergrowth, flood stage below branches	22	21	20
5. same as 4. with flood stage reaching branches	6	8	10
4. Excavated or Dredged Channels			
a. Earth, straight, and uniform			
1. clean, recently completed	50	56	63
2. clean, after weathering	40	45	56
3. gravel, uniform section, clean	33	40	45
4. with short grass, few weeds	30	37	45
b. Earth winding and sluggish			
1. no vegetation	33	40	43
2. grass, some weeds	30	33	40
3. dense weeds or aquatic plants in deep channels	25	29	33
4. earth bottom and rubble sides	29	33	36
5. stony bottom and weedy banks	25	29	40
6. cobble bottom and clean sides	20	25	33
c. Dragline-excavated or dredged			
1. no vegetation	30	36	40
2. light brush on banks	17	20	29
d. Rock cuts			
1. smooth and uniform	25	29	40
2. jagged and irregular	20	25	29
e. Channels not maintained, weeds and brush uncut			
1. dense weeds, high as flow depth	8	13	20
2. clean bottom, brush on sides	13	20	25
3. same as above, highest stage of flow	9	14	22
4. dense brush, high stage	7	10	13
5. Lined or Constructed Channels			

Type of channel and description	K_S min.	K_S normal	K_S max.
a. Cement			
1. neat surface	77	91	100
2. mortar	67	77	91
b. Wood			
1. planed, untreated	71	83	100
2. planed, creosoted	67	83	91
3. unplaned	67	77	91
4. plank with battens	56	67	83
5. lined with roofing paper	59	71	100
c. Concrete			
1. trowel finish	67	77	91
2. float finish	63	67	77
3. finished, with gravel on bottom	50	59	67
4. unfinished	50	59	71
5. gunite, good section	43	53	63
6. gunite, wavy section	40	45	56
7. on good excavated rock		50	59
8. on irregular excavated rock		37	45
d. Concrete bottom float finish with sides of:			
1. dressed stone in mortar	50	59	67
2. random stone in mortar	42	50	59
3. cement rubble masonry, plastered	42	50	63
4. cement rubble masonry	33	40	50
5. dry rubble or riprap	29	33	50
e. Gravel bottom with sides of:			
1. formed concrete	40	50	59
2. random stone mortar	38	43	50
3. dry rubble or riprap	28	30	43
f. Brick			
1. glazed	67	77	91
2. in cement mortar	56	67	83
g. Masonry			
1. cemented rubble	33	40	59
2. dry rubble	29	31	43
h. Dressed ashlar/stone paving	59	67	77
i. Asphalt			
1. smooth		77	77
2. rough		63	63
j. Vegetal lining	2		33

4 Parallel structures

4.1 Parallel structures

4.1.1 Description of the calculation module

This calculation module allows to simulate the hydraulic operation of valves and thresholds placed in parallel. All the flow laws present in Cassiopée are grouped in this module, which makes it possible in particular to easily compare the flow laws between them.

This module allows to calculate any missing parameter among them:

- Boundary conditions (water level upstream and downstream of the structures);
- The flow through the structures;
- Parameters of the structures (crest elevation, width, flow coefficient. . .).

The module calculates the requested parameter and displays for each structure present:

- The flow passing through the structure;
- The type of flow: under load (flow pinched under a gate), or free surface;
- The speed: flooded, partially flooded or dewatered;
- The type of jet for free surface flows: surface or submerged.

4.1.2 Jet type

For the definition of the type of jet (plunging or surface), see: Larinier, M., 1992. Successive basin transitions, pre-dams and artificial rivers. Bulletin Français de la Pêche et de la Pisciculture 45-72. https://doi.org/10.1051/kmae:1992005.

Excerpt from Larinier, M., 1992. Passages to successive basins, pre-dams and artificial rivers. Bulletin Français de la Pêche et de la Pisciculture 45-72. https://doi.org/10.1051/kmae:1992005

The definition used in Cassiopée is as follows:

- if $DH \geq 0.5H1$ then the jet is plunging;
- if $DH < 0.5H1$ then the jet is surface.

With $H1$, the upstream head over the weir and DH the head drop across the weir.

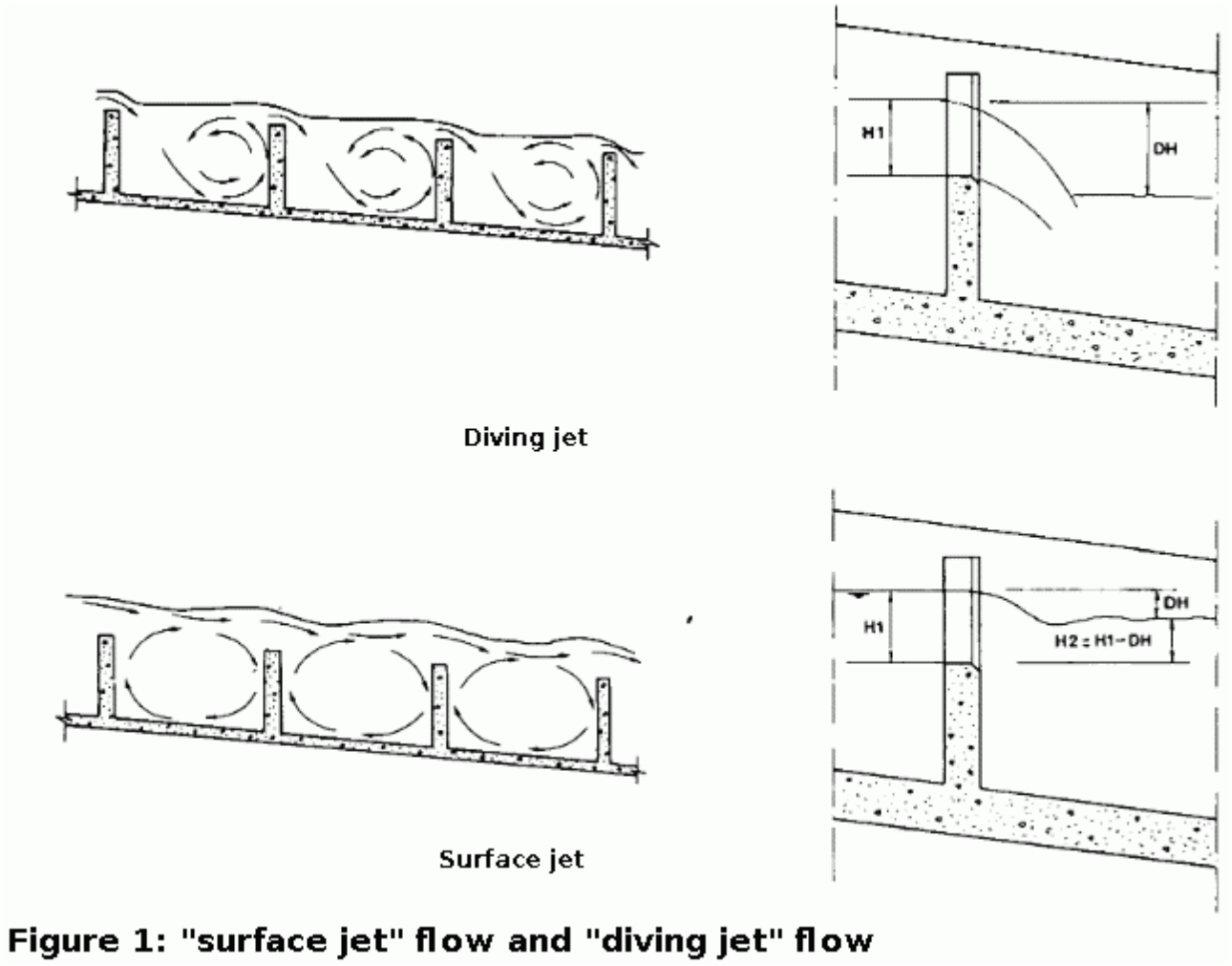

Figure 4.1: Diagram of jet type

4.2 Free flow weir stage-discharge laws

This calculation module is similar to that of the Parallel structures, except that it simulates only free flows and refine by using the upstream approach speed.

It can be used to calculate the relationship between water level upstream of a weir and flow. It is most often used to assess the upstream-flow rating relationship at a weir or structure evacuator of a development. The facility may have several distinct discharge levels and Rectangular (with horizontal discharge side), triangular, semi-triangular weirs or truncated triangles.

The classical use consists in entering the extreme levels (min/max) of the upstream water level and the calculation step for which flow estimates are desired.

The upstream characteristics (upstream width and bed elevation) make it possible to estimate the approach speed and upstream kinetic energy, expressed in metres, and to calculate total flow from the total head at a non-negligible approach speed.

$$V = \frac{Q}{L \times (Z_1 - Z_{lit})}$$

with V the approach speed, Q the flow, Z_1 the upstream water elevation, $Zlit$ the upstream river bed elevation.

$$E_c = \frac{V^2}{2g}$$

with E_c the upstream cinetic energy in metres, and g the acceleration of gravity (9.81 m.s-2).

Head H used for flow calculation then is:

$$H = Z_1 + E_c$$

The difficulty of the calculation lies in the fact that the flow rate to be calculated is involved in the calculation of the head. This problem is solved with the fixed point algorithm where the flow rate calculation is repeated several times by updating the head at each iteration until the calculation converges to the final value of the flow rate.

The approach speed correction coefficient Cv is then calculated by relating the flow rate obtained with the head H to the flow rate calculation with the upstream dimension Z_1.

4.3 Cross walls

This tool, which is similar to the Parallel Structures tool, is an aid to the hydraulic predimensioning of a fish pass: it is most often used for the dimensioning of notches, slots, orifices, etc. characterizing the walls of a pass as well as for the setting in altitude of the notches, slots and apron of the upstream basin of a pass.

It allows to calculate the missing value of the 7 values characterizing the fall, the surface of the submerged orifice, the width of the slot, the load on the slot, the width of the notch, the load on the notch and the flow rate.

Mandatory data to be provided are the dimensions of the basins (width and length) and the average draught in metres. These data associated with the fall between basins allow us to calculate the power dissipation.

Once the module is calculated, the tool proposes to create a basin pass from this cross wall by specifying the upstream water elevation, the number of falls in the pass and the downstream water elevation.

4.3.1 Hydraulic structures that can be part of the cross wall

The tool allows you to place one or more structures in parallel among the following types of structures:

4.3.1.1 Submerged orifice

Excerpt from Larinier, M., Travade, F., Porcher, J.-P., Gosset, C., 1992. Fish passage: expertise and design of crossing structures. CSP. (page 94).

The submerged orifice equation is described on the submerged orifice formula page.

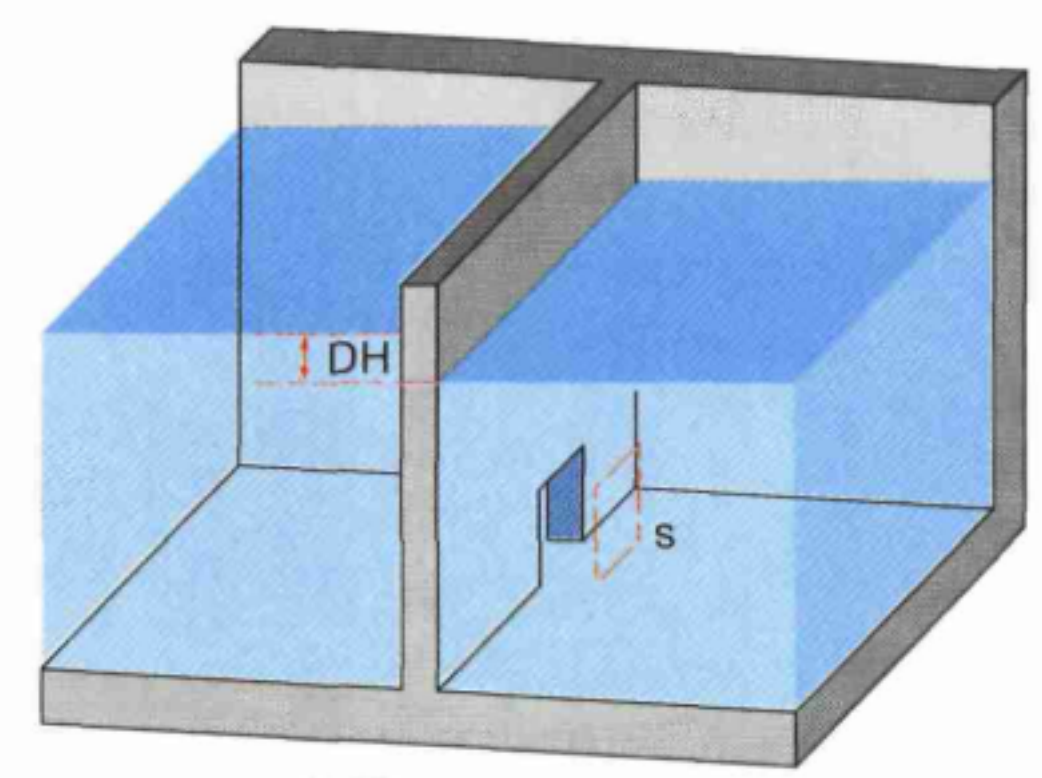

Figure 4.2: Submerged orifice diagram

4.3.1.2 Submerged Slot

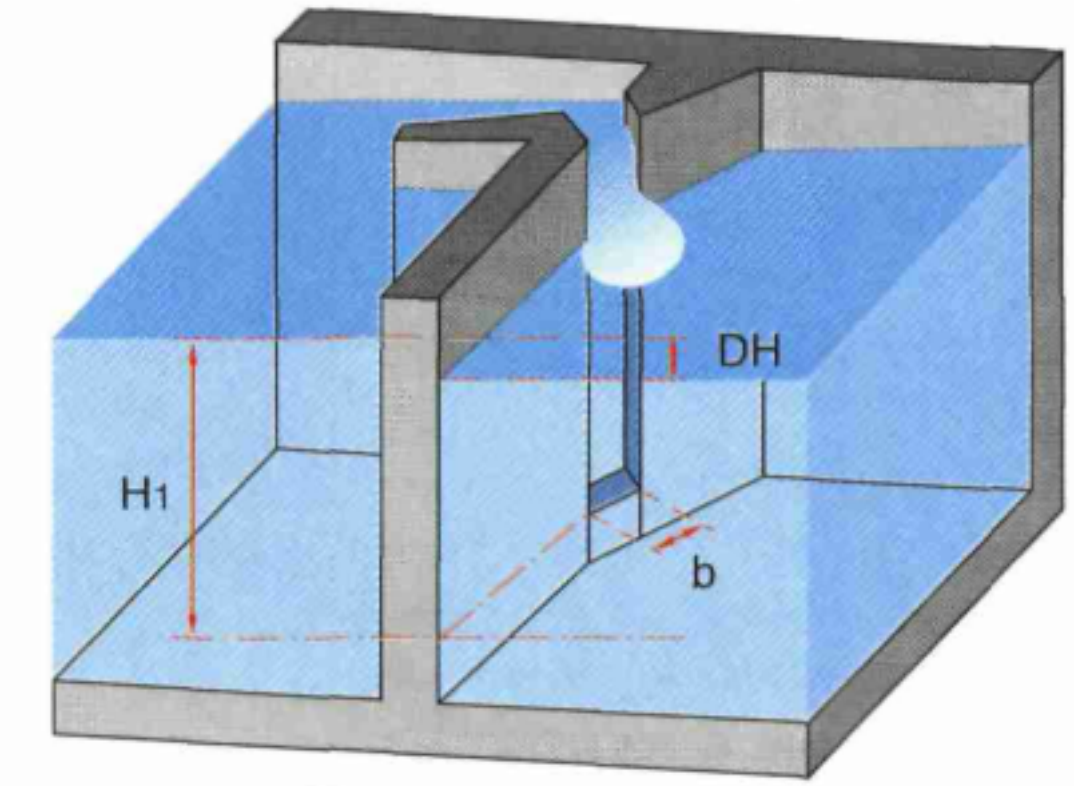

Figure 4.3: Schematic of the submerged slot

Excerpt from Larinier, M., Travade, F., Porcher, J.-P., Gosset, C., 1992. Fish passage: expertise and design of crossing structures. CSP. (page 94).

The submerged slot equation is described on the sumberged slot formula page.

4.3.1.3 Notch

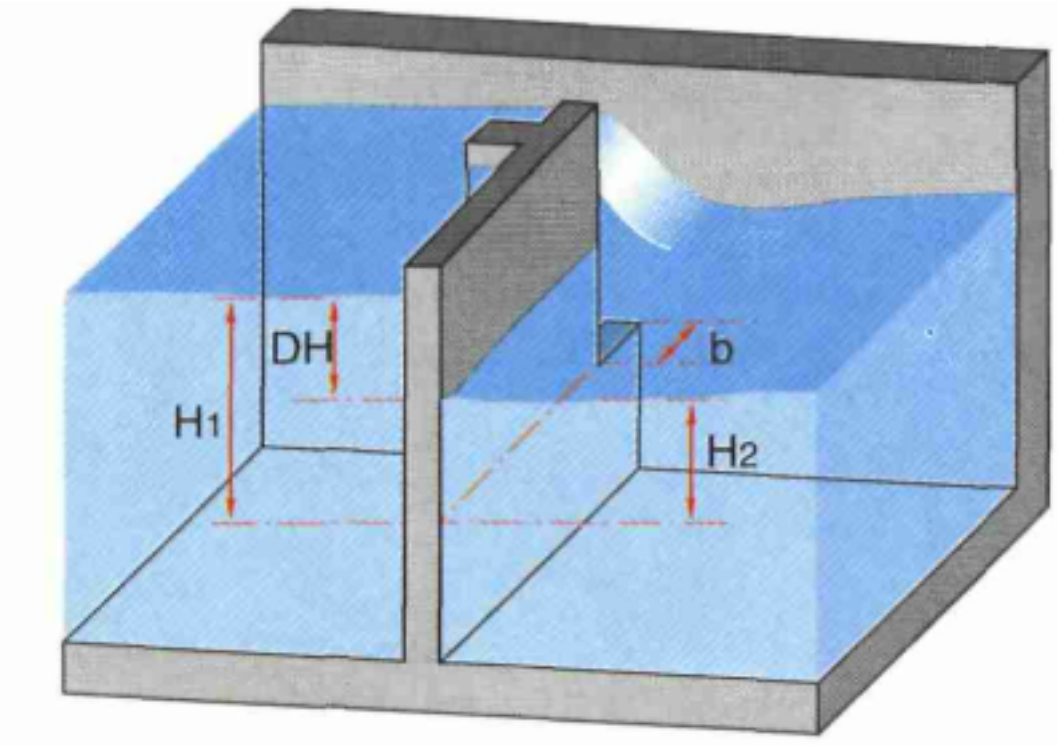

Figure 4.4: Notch diagram

Excerpt from Larinier, M., Travade, F., Porcher, J.-P., Gosset, C., 1992. Fish passage: expertise and design of crossing structures. CSP. (page 94).

The equation used for the notch is that of Kindsvater-Carter and Villemonte.

4.4 Device equations

4.4.1 Stage-discharge equations list

Table 4.1: Stage-discharge equations list

Structure typology	Structure geometry	Structure type	Flow regimes	Name of equation	Default flow coefficient	Modules
Weir	Rectangular	Sharp-crested weir (notch)	Free	Poleni	0.4	Parallel structures, free flow weir stage-discharge laws

Structure typology	Structure geometry	Structure type	Flow regimes	Name of equation	Default flow coefficient	Modules
		Sharp-crested weir (slot)	Submerged	Rajaratnam	0.9	Parallel structures
		Sharp-crested weir (slot)	Submerged	Lagarier slot	to be defined by designer	Parallel structures, cross walls, downwall
		Sharp-crested weir (notch)	Submerged / free	Kindsvater-Carter & Villemonte	α = 0.4; ß = 0.001	Parallel structures
		Sharp-crested weir (notch)	Submerged / free	Villemonte	0.4	Parallel structures, cross walls, downwall
		Sharp-crested regulated weir (notch)	Submerged / free	Villemonte	0.4	Downwall
		Sharp-crested regulated weir (slot)	Submerged	Lagarier slot	To be defined by designer	Downwall
	Triangular	Sharp-crested weir (notch)	Submerged / free	Villemonte	1.36	Parallel structures, free flow weir stage-discharge laws, cross walls, downwall
		Broad-crested weir (notch)	Submerged / free	Bos	1.36	Parallel structures, free flow weir stage-discharge laws, cross walls, downwall
	Triangular truncated	Sharp-crested weir (notch)	Submerged / free	Villemonte	1.36	Parallel structures, free flow weir stage-discharge laws, cross walls, downwall
Orifice / Sluice gate handling free surface weir flow	Rectangular	Broad-crested weir (notch) / orifice	Submerged / free	Cunge-Lagaref-D	0.4	Parallel structures, cross walls, pre-dams

Structure typology	Structure geometry	Structure type	Flow regimes	Name of equation	Default flow coefficient	Modules
	Rectangular	Broad-crested weir (notch) / orifice	Submerged / free	Cemagref	1	Parallel structures, pre-dams
	Rectangular	Broad-crested weir (notch) / bottom gate	Submerged / free	Cemagref-V	0.6	Parallel structures, downwall, pre-dams
Orifice / Sluice gate	Rectangular	Sluice gate	Free	Free flow sluice gate	0.6	Parallel structures
	Rectangular	Sluice gate	Submerged	Submerged sluice gate	0.8	Parallel structures
	Undefined	Orifice	Submerged	Free flow orifice	0.7	Parallel structures, cross walls, downwall
	Undefined	Orifice	Free	Submerged orifice	0.7	Parallel structures

4.4.1.1 Relationship between water level and load

Most of the flow laws in this documentation refer to the **water level** or to the **head**. These two concepts are generally confused because kinetic energy is neglected (See the detailed calculation of the load in the tool 'Free flow weir stage-discharge laws'). These quantities correspond to the difference in elevation between the upstream free surface Z_1 or downstream Z_2 and the base of the weir Z_d.

We then have:

$$h_1 = Z_1 - Z_d$$

and

$$h_2 = Z_2 - Z_d$$

4.4.1.2 Sharp-crested or broad-crested weir?

Extract from CETMEF, 2005. Note on weirs : synthesis of flow laws at the right of weirs and spillways. Centre d'Études Techniques Maritimes Et Fluviales, Compiègne.

The type of weir is related to the flow at the right of the structure.

Indeed, the more the breadth of the crest of the weir is negligible compared to the upstream water height above it, the more the weir appears transparent to the flow and thus the sharper the crest of the weir appears.

On the other hand, the closer the upstream water line is to the weir crest, the greater the width of the weir appears in relation to the breadth of the water flowing over it and therefore the broader the weir crest appears. A weir in a river thus belongs to one of the three following categories:

- sharp-crested weir
- broad-crested weir
- weir with undefined crest

In order to determine the type of weir studied, the following conditions must be verified:

- if $C < \frac{H_1}{2}$, then the threshold is sharp-crested;
- if $C > \frac{2H_1}{3}$, then the threshold is broad-crested.

4.4.2 Kindsvater-Carter and Villemonte formula

The calculation module allows hydraulic calculations to be carried out for several structures in parallel.

4.4.2.1 Kindsvater-Carter formula (1957)

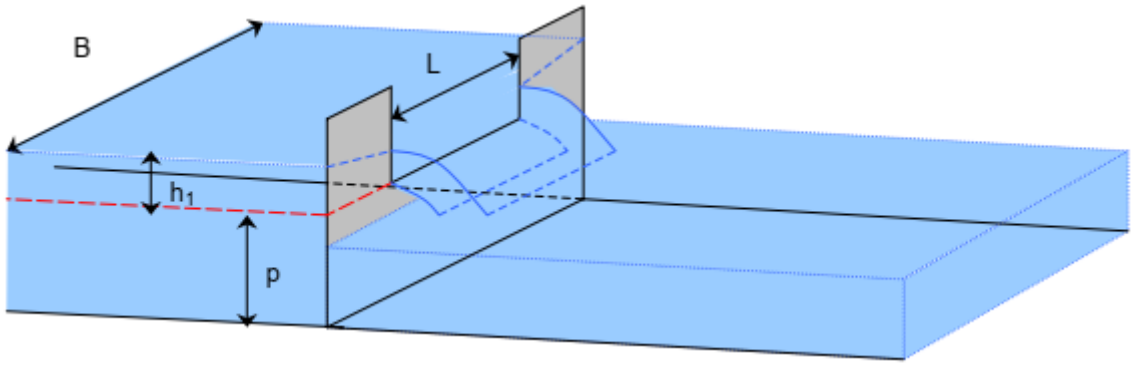

Figure 4.5: Kindsvater-Carter formula: weir diagram

Perspective view of a rectangular weir with lateral contraction from CETMEF (2005)

Kindsvater-Carter formula corresponds to the classic weir formula:

$$Q = \mu L \sqrt{2g} h_1^{1.5}$$

With:

- μ the discharge coefficient $\mu = \alpha + \beta h_1/p$
- L the width of the weir
- h_1 the water level above the weir crest

- p the sill or weir crest height

The coefficients α and β depend on the ratio between the width of the weir (L) and the width of the basin (B). Their values are given in the abacuses below (Excerpt from *Larinier, M., Porcher, J.-P., 1986. Programmes de calcul sur HP86 : hydraulique et passes à poissons*):

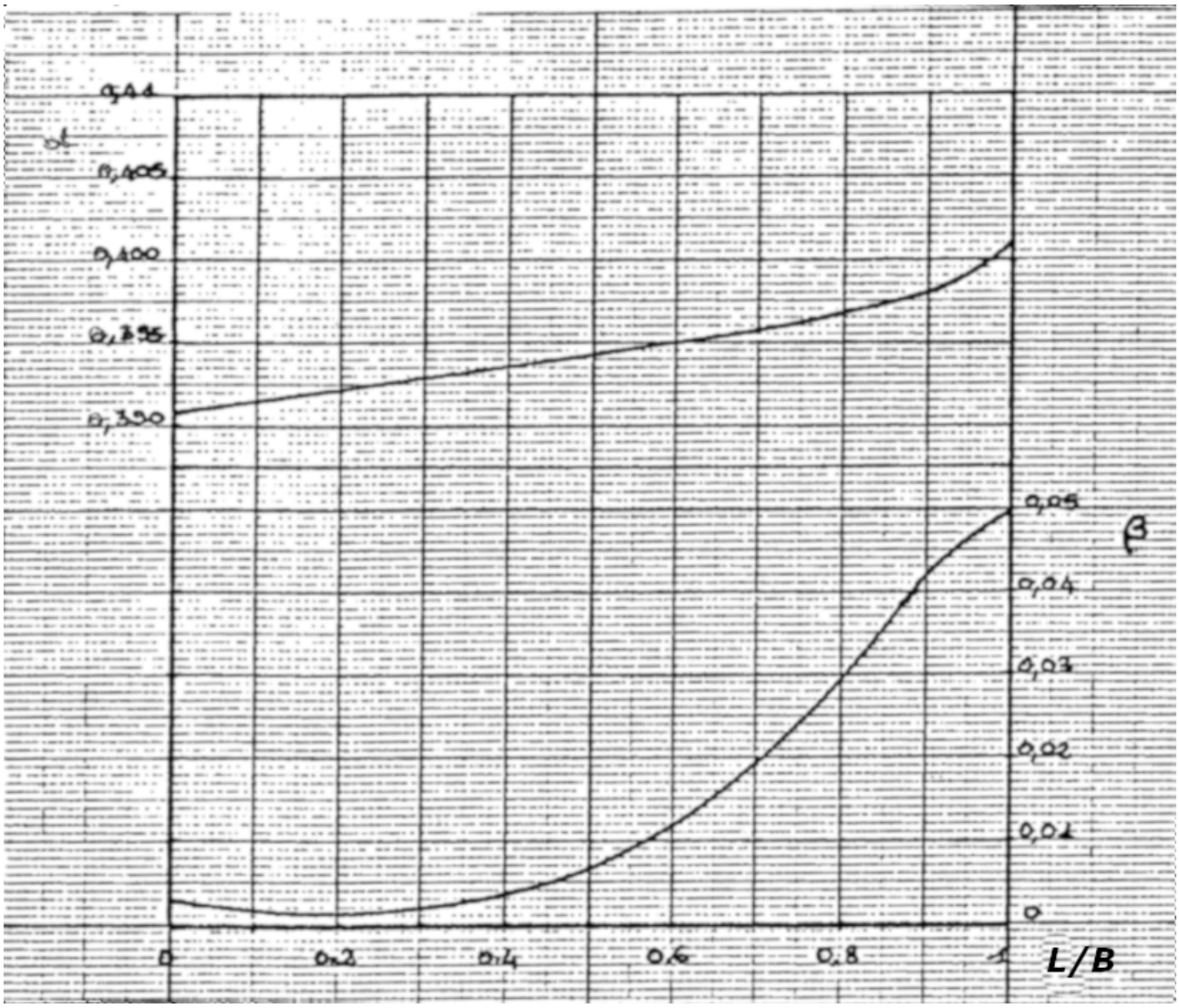

Figure 4.6: Kindsvater-Carter formula: abacuses

4.4.2.2 Submerged flow: Villemonte formula (1947)

Excerpt from CETMEF (2005)

For a downstream water elevation higher than the elevation of the weir crest, the flow is submerged and a flooding coefficient is applied to the flow coefficient.

Villemonte proposes the following formula:

$$K = \frac{Q_{submerged}}{Q_{free}} = \left[1 - \left(\frac{h2}{h1}\right)^{n}\right]^{0.385}$$

With:

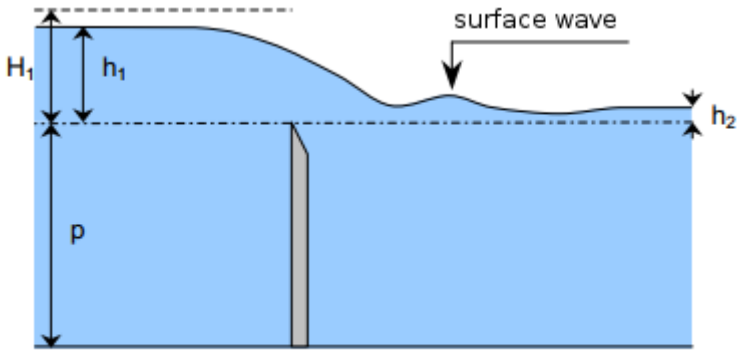

Figure 36: longitudinal section of a thin-crested weir in submerged flow

Figure 4.7: Villemonte formula: submerged weir diagram

- h_1 the upstream water level above the weir crest
- h_2 the downstream water level above the weir crest
- n the exponent in free flow relationships (rectangular=1.5, triangular=2.5, parabolic=2)

4.4.2.3 References

CETMEF. Notice sur les déversoirs : synthèse des lois d'écoulement au droit des seuils et déversoirs. Compiègne: Centre d'Études Techniques Maritimes Et Fluviales, 2005. http://www.side.developpement-durable.gouv.fr/EXPLOITATION/DEFAULT/doc/IFD/IFD_REFDOC_0513410/notice-sur-les-deversoirs-synthese-des-lois-d-ecoulement-au-droit-des-seuils-et-deversoirs

4.4.3 Submerged orifice formula

Excerpt from Larinier, M., Travade, F., Porcher, J.-P., Gosset, C., 1992. Passes à poissons : expertise et conception des ouvrages de franchissement. CSP. (page 94)

The equation corresponds roughly to that of the calculation module for the submerged rectangular gate with the difference that the area of the orifice is given directly rather than by the ratio of width to height:

$$Q = \mu S \sqrt{2g\Delta H}$$

With:

- *Q* the flow in m3/s;
- μ the discharge coefficient (equal to 0.7 by default);
- *S* the orifice surface in m2;
- ΔH the head loss *H1 - H2* in m(named "Fall" in Cassiopée).

4.4.4 Free orifice formula

Excerpt from CARLIER, M. (1972). Hydraulique générale et appliquée. OCLC : 421635236. Paris : Eyrolles

The general formula for a free orifice or nozzle is as follows (CARLIER, 1972):

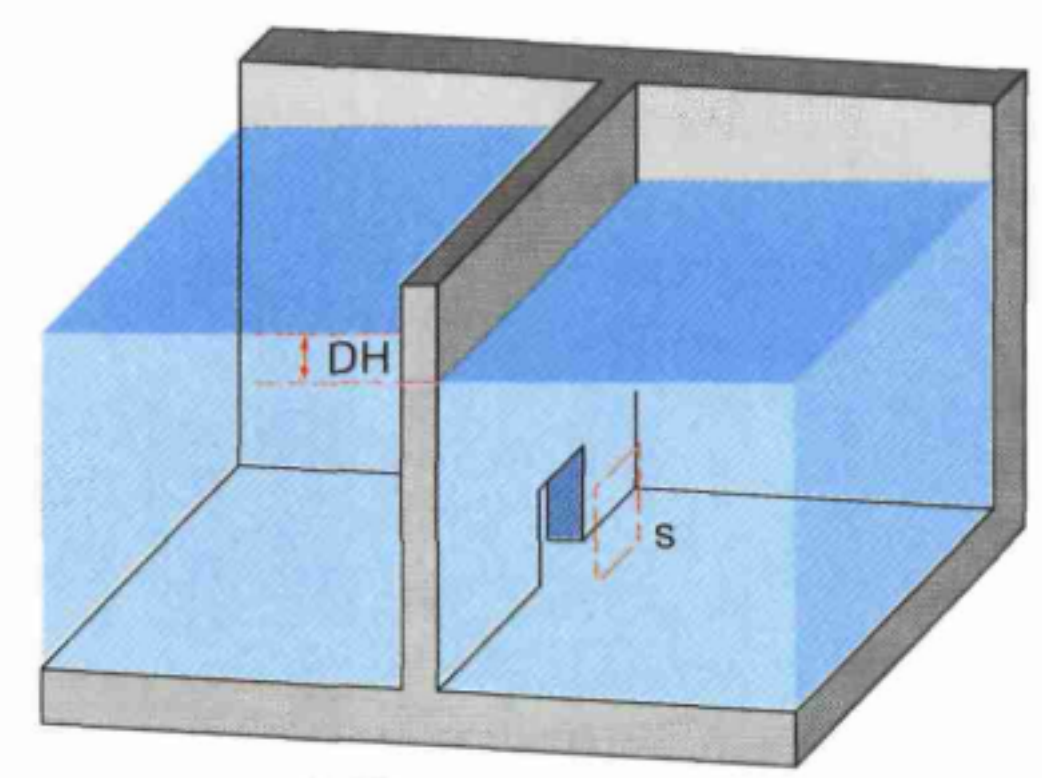

Figure 4.8: Submerged orifice diagram

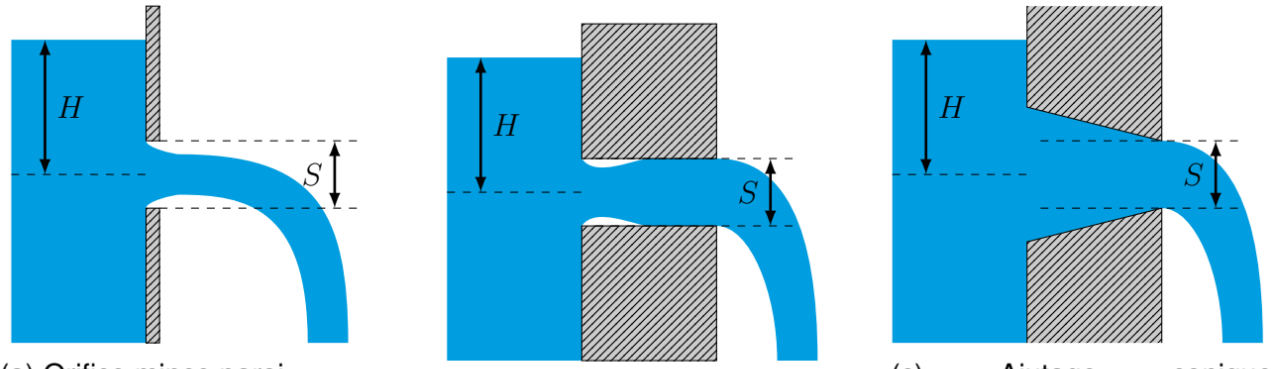

(a) Orifice mince paroi $C_d = 0.6$

(b) Ajutage $C_d = 0.8$

(c) Ajutage conique convergent $C_d = 0.97$

FIGURE 5.12 – Schémas explicatifs des écoulements à travers des orifices ou ajutages dénoyés

Figure 4.9: Free orifice diagram

$$Q = C_d S \sqrt{2gH}$$

With:

- Q the flow in m3/s;
- C_d the discharge coefficient;
- S the orifice surface in m2;
- g the acceleration of gravity 9.81 m/s2
- H The water level measured from the surface of the water to the centre of the orifice in meters.

The area S to be considered is the smallest cross-sectional area of the orifice or nozzle (Figure 5.12c). The discharge coefficient C_d varies depending on the type of orifice or nozzle. Figure 5.12 shows the most common shapes and discharge coefficients (Source: CARLIER, 1972).

4.4.5 Submerged slot formula

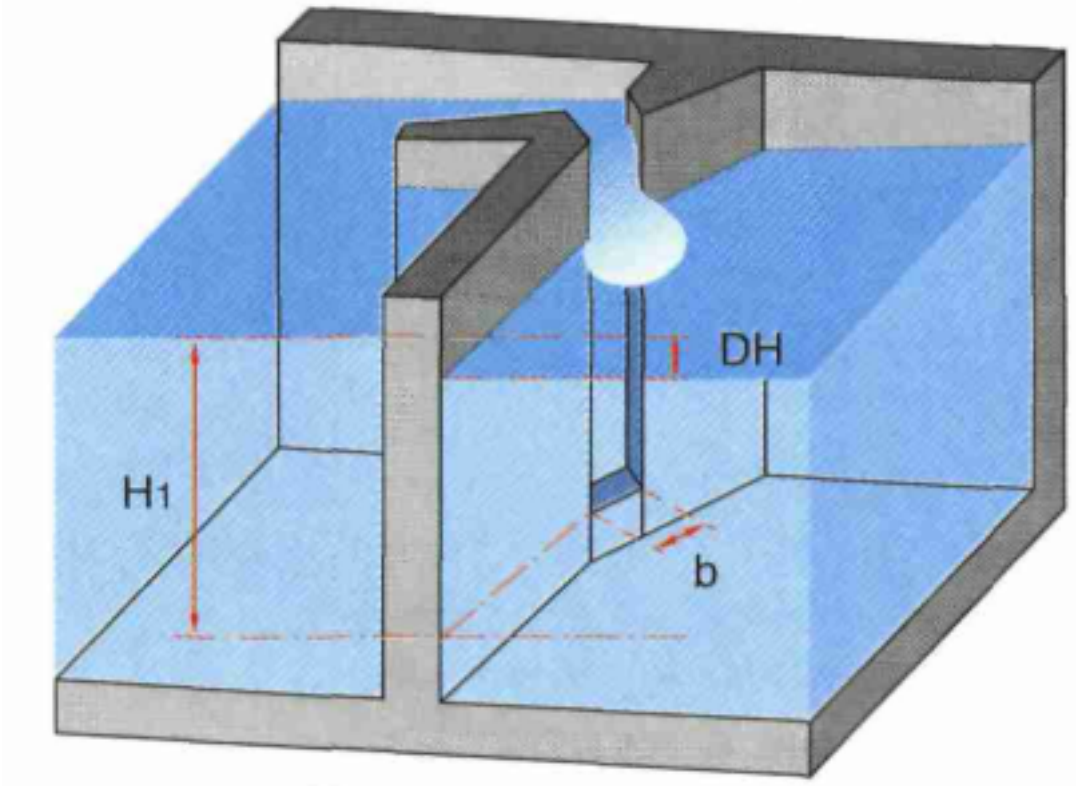

Figure 4.10: Submerged slot diagram

Excerpt from Larinier, M., Travade, F., Porcher, J.-P., Gosset, C., 1992. Passes à poissons : expertise et conception des ouvrages de franchissement. CSP. (page 94)

Larinier (1992) suggests the following equation:

$$Q = C_d b H_1 \sqrt{2g\Delta H}$$

With:

- *b* the slot width in m
- *H1* the head on the slot m
- *Cd* the discharge coefficient.

4.4.6 Discharge coefficient Cd for the submerged slot formula (vertical slot fish ladder)

The discharge coefficient **Cd** is an important parameter for the design of vertical slot weirs. This term is integrated in the formula of conveyance of a submerged slot, which connects the transited flow with the fall between basins, the upstream head on the slot and its width.

For single vertical slot weirs, model-reduced studies and numerical simulations have determined average values of discharge coefficients for different configurations, for a typical slot and baffle geometry defined from vertical slot weirs built in France (Figure 1). A different slot and baffle geometry can induce deviations from the average values of the discharge coefficients according to the configurations indicated below.

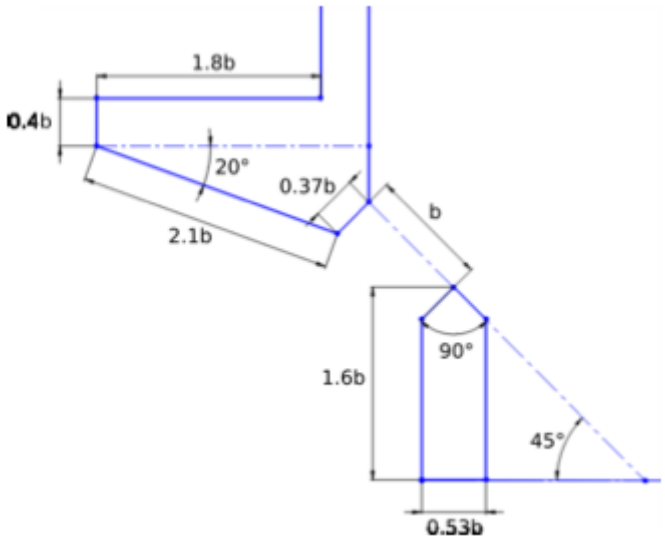

Figure 4.11: Figure 1

Figure 1: typical slot and baffle geometry from which the discharge coefficient values were determined (Ballu, 2017)

- **Under smooth apron conditions (no bottom roughness) and in the absence of a weir in the slot**, Wang *et al.* (2010) and Ballu *et al.* (2017) showed that the value of **Cd** is not significantly influenced by discharge and depends mainly on the slope **S** (%) and the ratio of the basin width **B** to the slot width **b** (**B**/**b**).
- **Under smooth invert conditions (no bottom roughness) with the presence of a weir in the slot**, under 3 configurations of weir heights **hs**/**b** related to slot width **b** (**hs**/**b** = 0.5, 1, and 1.5), Ballu *et al.* (2015) and Ballu (2017) showed that the value of **Cd** is not significantly influenced by discharge, and is mainly influenced by slope **S**, aspect ratio **B**/**b**, and weir height **hs**/**b**.
- **Under apron conditions with precast bottom roughnesses and in the absence of a weir in the slot**, with evenly distributed roughnesses of height **hr**/**b** = 2/3 and diameter **Ør**/**b** = 1/2, under 2 configurations of densities **dr** of 10% and 15%, Ballu *et al.* (2017) and Ballu (2017) showed that the value of **Cd** is not significantly influenced by discharge, and is mainly influenced by slope **S**, aspect ratio **B**/**b**, and the presence of the bottom roughness **dr**.

Depending on these different configurations, the average values of the discharge coefficient range from about 0.62 to nearly 0.88 (Figure 2).

Figure 2: average values and uncertainties (95% confidence intervals, k = 2) of the discharge coefficients according to the slope S and the shape ratio B/b, for different configurations: (A) smooth raft without weir in the slot, (B) bottom roughness dr = 10% without weir in the slot, (C) bottom roughness dr = 15% without weir in the slot, (D) weir in the slot hs/b =

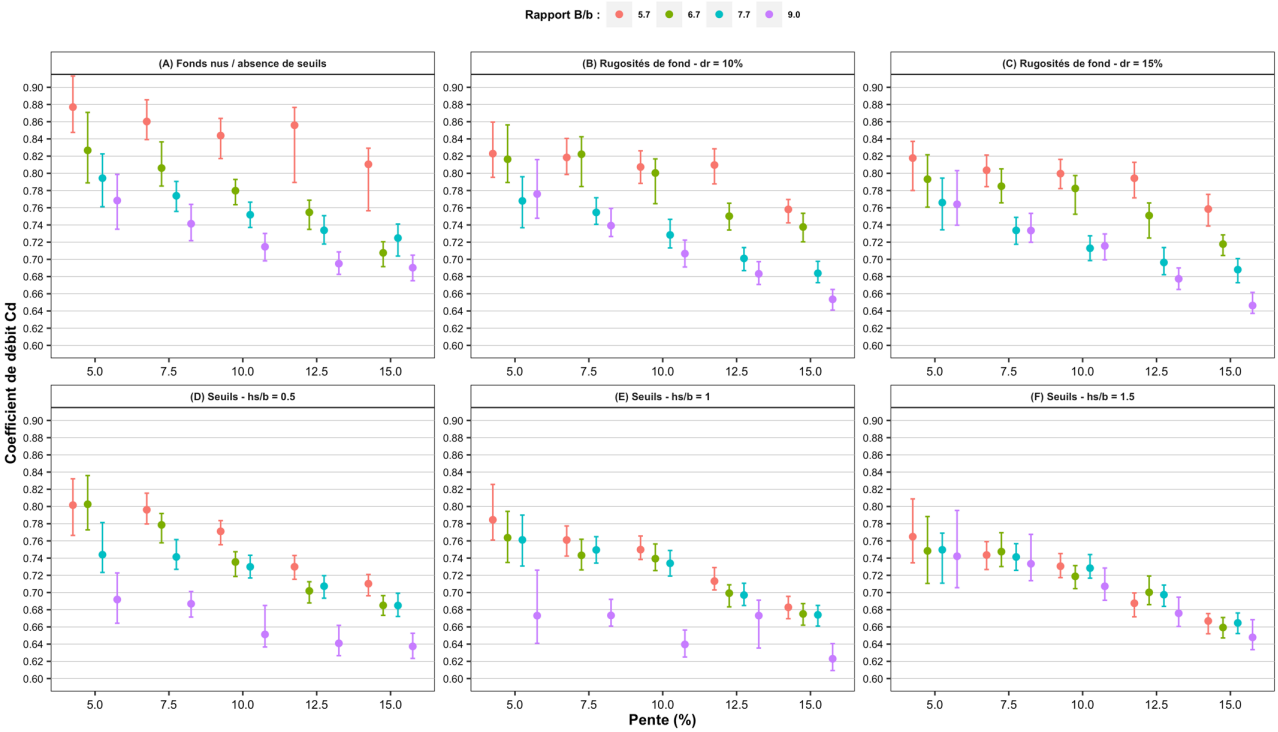

Figure 4.12: Figure 2

0.5 and smooth raft, (E) weir in the slot hs/b = 1 and smooth raft, (F) weir in the slot hs/b = 1.5 and smooth raft

For passes with double vertical slots, **Cd** values between 0.75 and 0.80 are commonly used for recently constructed devices with longitudinal slopes between 4% and 5.5%. Studies are under way to clarify the influence of different configurations on discharge coefficients and their corresponding values.

Bibliography:

Ballu A., Pineau G., Calluaud D., David L. (2015). Experimental study of the influence of sills on vertical slot fishway flow. *36th IAHR World Congress*, 7p.

Ballu A. (2017). Étude numérique et expérimentale de l'écoulement turbulent au sein des passes à poissons à fentes verticales. Analyse de l'écoulement tridimensionnel et instationnaire. *Thèse de l'Université de Poitiers*, 223p.

Ballu A., Calluaud D., Pineau G., david L. (2017). Experimental study of the influence of macro-roughnesses on vertical slot fishway flows. *La Houille Blanche*, 2: 9-14.

Wang R.W., David L., Larinier M. (2010). Contribution of experimental fluid mechanics to the design of vertical slot fish passes. *Knowledge and Management of Aquatic Ecosystems*, 396(2).

4.4.7 Submerged weir formula

Excerpt from: Rajaratnam, N., Muralidhar, D., 1969. Flow below deeply submerged rectangular weirs. Journal of Hydraulic Research 7, 355–374.

In submerged flow, the flow rate depends on the upstream water level h_1 and the downstream water level h_2 (Rajaratnam et al., 1969):

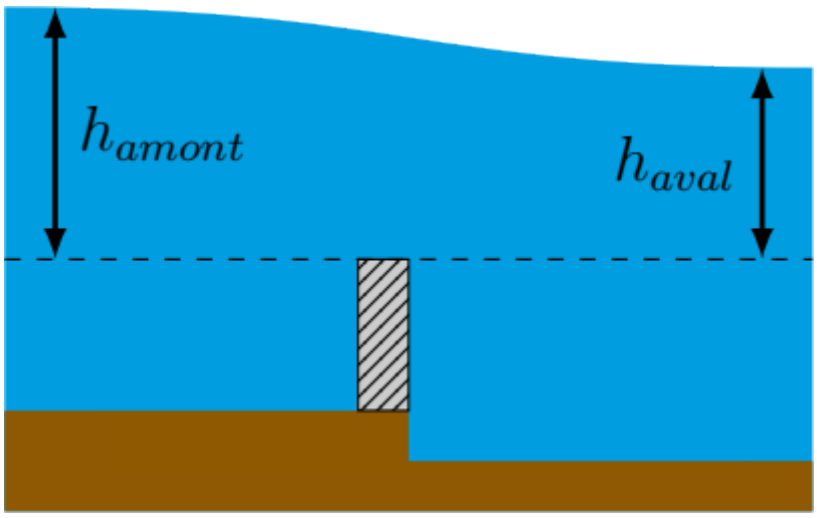

Figure 4.13: Submerged weir diagram

$$Q = Cd\sqrt{2g}Lh_2\sqrt{h_1 - h_2}$$

With:

- *L* the weir width in m
- *hamont* the upstream head on the weir in m
- *haval* the downstream head on the weir in m
- *Cd* the discharge coefficient (equal to 0.9 by default).

This formula is not recommended for flooding below 80%.

Rajaratnam, N., Muralidhar, D., 1969. Flow below deeply submerged rectangular weirs. Journal of Hydraulic Research 7, 355–374.

4.4.8 Free weir formula

The formula is derived from the original formula of Poleni (1717).

In a free flow, the flow rate depends only on the upstream water level h_1:

$$Q = Cd\sqrt{2g}Lh_1^{3/2}$$

With:

- *Q* the flow in m3/s
- *Cd* the discharge coefficient
- g the acceleration of gravity 9.81 m/s2
- *L* the width of the weir in m
- *hamont* the upstream water level above the crest of the weir in m

A flow coefficient value $C_d = 0.4$ is generally a good approximation for a rectangular weir. For more complex weir shapes (trapezoidal, circular...) or to take into account the

characteristics of the longitudinal profile (thin-crested weir, thick-crested weir), one can refer to the CETMEF weir leaflet (CETMEF, 2005).

CETMEF (2005). Notice sur les déversoirs : synthèse des lois d'écoulement au droit des seuils et déversoirs. Compiègne : Centre d'Études Techniques Maritimes Et Fluviales. 89 p.

4.4.9 V-notch weir formula

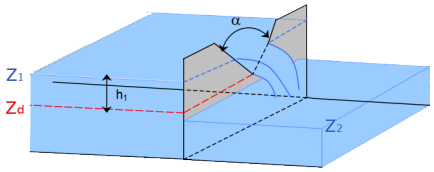

Figure 4.14: Perspective view of a triangular weir

*Perspective view of a triangular weir (from CETMEF, 2005

4.4.9.1 Free flow formula

$$Q = C_d * \tan\left(\frac{\alpha}{2}\right)(Z_1 - Z_d)^{2.5}$$

Avec:

- C_d : discharge coefficient
- $\alpha/2$: half-angle at the apex of the triangle
- Z_1 : upstream water elevation
- Z_d : spill elevation at the tip of the triangle

The discharge coefficient C_d depends, among other things, on the thickness of the weir:

- Sharp-crested weir : C_d = 1.37
- Broad-crested weir (rounded off $r > 0.1 * h1$) : C_d = 1.27
- triangular profile weir : (1/2 upstream, 1/2 or 1/5 downstream) : C_d = 1.68 and 1.56

4.4.9.2 Submergence of a V-notch sharp-crested weir

The weir is submerged as soon as $Z_2 > Z_d$ and the Villemonte reduction coefficient is then applied to the discharge calculated in free flow.

4.4.9.3 Submergence of a V-notch broad-crested weir

Submergence occurs for $h_2/h_1 > 4/5$ with $h_1 = Z_1 - Z_d$ and $h_2 = Z_2 - Z_d$, and with Z_2 the downstream water elevation.

The reduction coefficient proposed by Bos (1989) is then applied:

Submergence reduction factor for a V-notch broad-crested weir (from Bos, 1989)

The abacus is approximated by the following formula:

$$K_s = sin(3.9629(1 - h_2/h_1)^{0.575})$$

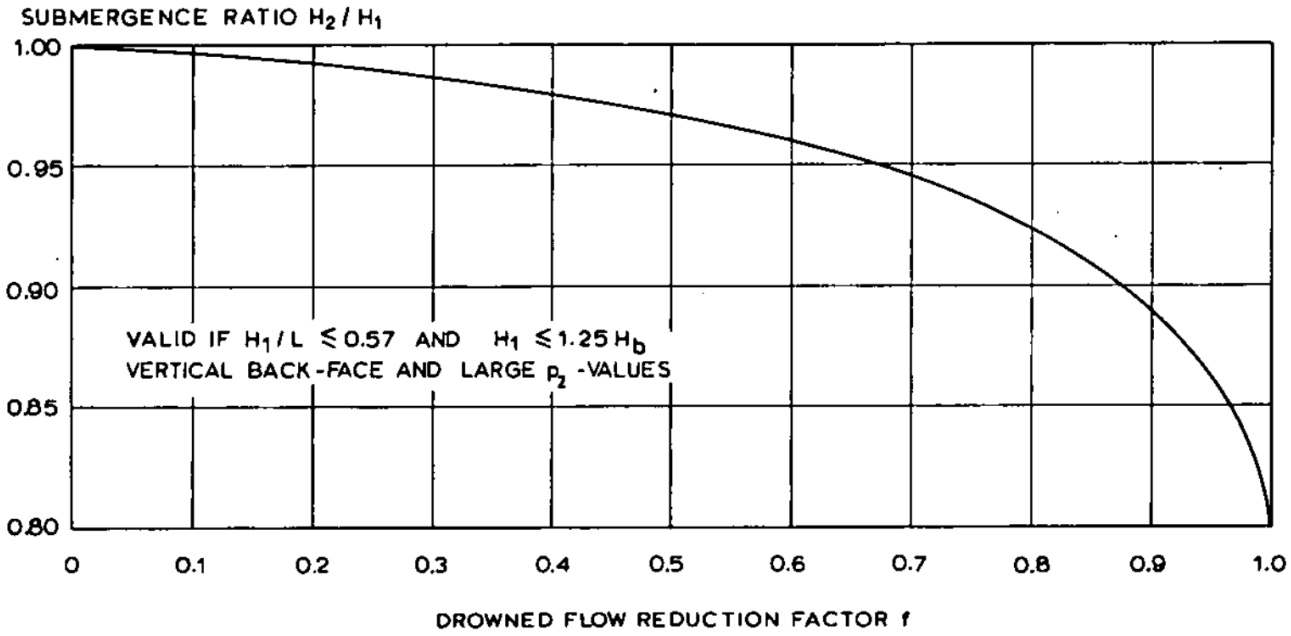

Figure 4.15: Submergence reduction factor for a V-notch broad-crested weir (from Bos, 1989)

4.4.9.4 References

CETMEF, 2005. Notice sur les déversoirs : synthèse des lois d'écoulement au droit des seuils et déversoirs. Centre d'Études Techniques Maritimes Et Fluviales, Compiègne.

Bos, M.G., 1989. Discharge measurement structures., 3rd edition. ed, Publication. International Institute for Land Reclamation and Improvement, Wageningen, The Netherlands.

4.4.10 Truncated triangular weir formula

The truncated triangular weir is characterized by the following parameters:

- C_d: discharge coefficient
- Z_d: triangle's lower overflow elevation
- Z_t: triangle's higher overflow elevation
- $B/2$: half-opening of the triangle

4.4.10.1 Formula

for $Z_1 \leq Z_t$

$$Q = C_d \frac{B}{2(Z_t - Z_d)} (Z_1 - Z_d)^{2.5}$$

for $Z_1 > Z_t$

$$Q = C_d \frac{B}{2(Z_t - Z_d)} \left((Z_1 - Z_d)^{2.5} - (Z_1 - Z_t)^{2.5}\right)$$

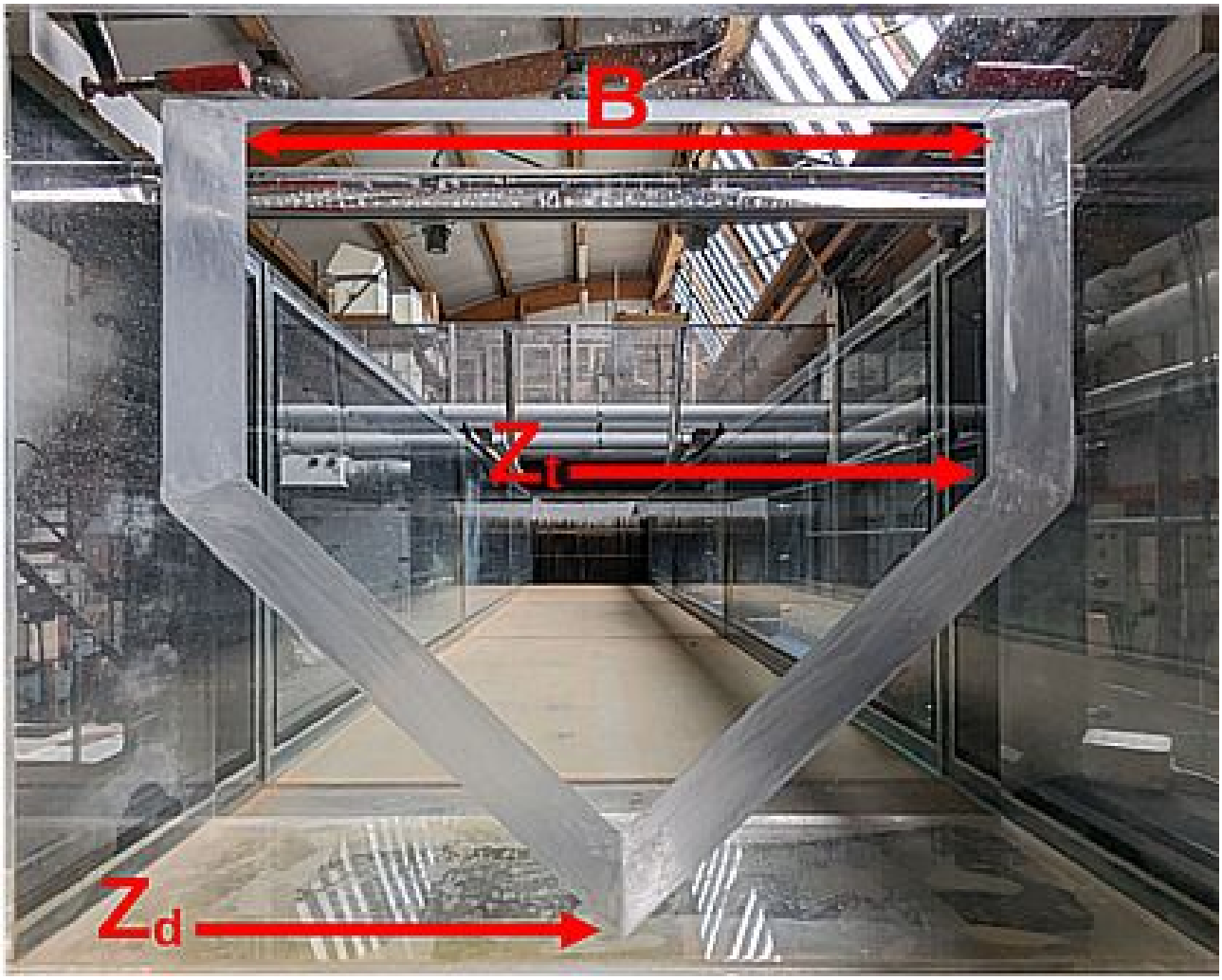

Figure 4.16: Diagram of a truncated triangular weir

Thin wall weir: C_d = 1.37

Thick weir without contraction (rounded $r > 0.1 * h1$): C_d = 1.27

Triangular profile weir: (1/2 upstream, 1/2 or 1/5 downstream): C_d = 1.68 and 1.56

4.4.11 CEM88(D) : Weir / Orifice (low sill)

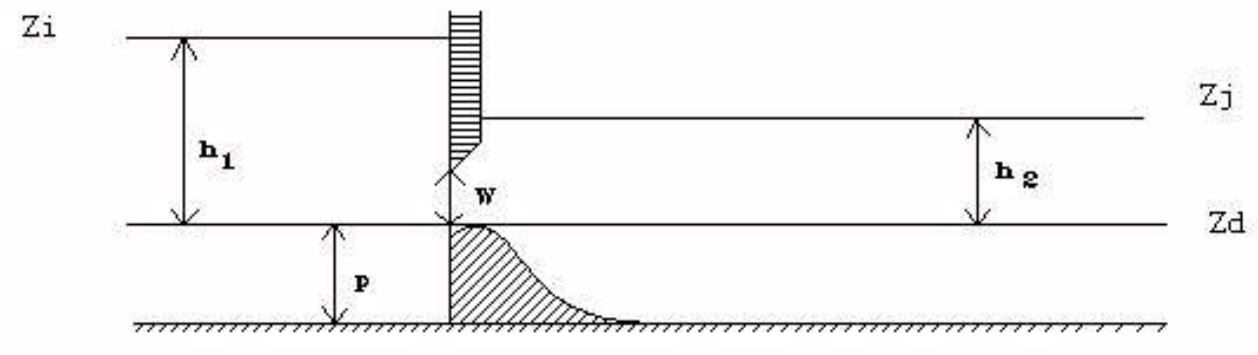

Figure 4.17: CEM 88 V diagram

4.4.11.1 Weir - free flow

$$Q = \mu_f L \sqrt{2g} h_1^{3/2}$$

4.4.11.2 Weir - submerged flow

$$Q = k_F \mu_F L \sqrt{2g} h_1^{3/2}$$

k_F flow reduction coefficient in submerged flow. The flow reduction coefficient is a function of $\frac{h_2}{h_1}$ and the value α of this ratio when switching from submerged flow to free flow. Flooding is achieved when $\frac{h_2}{h_1} > \alpha$. Variation law of k_F was ajusted to experimental results ($\alpha = 0.75$).

Let's put $x = \sqrt{1 - \frac{h_2}{h_1}}$:

- If $x > 0.2 : k_F = 1 - \left(1 - \frac{x}{\sqrt{1-\alpha}}\right)^{\beta}$
- If $x \leq 0.2 : k_F = 5x \left(1 - \left(1 - \frac{0.2}{\sqrt{1-\alpha}}\right)^{\beta}\right)$

With $\beta = -2\alpha + 2.6$, an equivalent free flow coefficient is calculated as above.

4.4.11.3 Undershot gate - free flow

$$Q = L\sqrt{2g}\left(\mu h_1^{3/2} - \mu_1 (h_1 - W)^{3/2}\right)$$

Experimentally, the flow coefficient of a valve is found to increase with $\frac{h_1}{W}$. A law of variation ofμ was adjusted, in the form of:

$\mu = \mu_0 - \frac{0.08}{\frac{h_1}{W}}$ with : $\mu_0 \simeq 0.4$

so $\mu_1 = \mu_0 - \frac{0.08}{\frac{h_1}{W} - 1}$

To ensure continuity with the free surface for $\frac{h1}{W} = 1$, $\mu_F = \mu_0 - 0.08$ then has to be $\mu_F = 0.32$ for $\mu_0 = 0.4$

4.4.11.4 Undershot gate - submerged flow

Partially submerged flow

$$Q = L\sqrt{2g}\left[k_F \mu h_1^{3/2} - \mu_1 \left(h_1 - W\right)^{3/2}\right]$$

k_F being the same as for free surface.

The switching from submerged flow to free flow was adjusted to experimental results, we then have a law like:

$\alpha = 1 - 0.14\frac{h_2}{W}$

$0.4 \leq \alpha \leq 0.75$

In order to ensure continuity with free surface operation, the free surface sumbmerged-free switch must therefore be for $\alpha = 0.75$ instead of $2/3$ in the orifice weir formulation.

Totally submerged flow

$$Q = L\sqrt{2g}\left(k_F \mu h_1^{3/2} - k_{F1}\mu_1 \left(h_1 - W\right)^{3/2}\right)$$

Formulation of k_{F1} is the same as the one of k_F replacing h_2 with $h_2 - W$ (and h_1 with $h_1 - W$) for the calculation of coefficient x and of α (and therefore of k_{F1}).

Switching to totally submerged occurs for:

$h_2 > \alpha_1 h_1 + (1 - \alpha_1)W$

with : $\alpha_1 = 1 - 0.14\frac{h_2 - W}{W}$

$(\alpha_1 = \alpha(h_2 - W))$

Weir gate operation is represented by the above equations and Figure below. Regardless of the type of flow under load, an equivalent free flow coefficient is calculated corresponding to a conventional free flow gate design:

$C_F = \frac{Q}{L\sqrt{2g}W\sqrt{h_1}}$

The default master coefficient for the device is a coefficient of C_G usually close to 0.6. We then transform it into $\mu_0 = \frac{2}{3}C_G$, which allows to calculate μ and μ_1 of the equation of the free flow gate.

Note: it is possible to obtain $C_F \neq C_G$, even under free flow conditions, as long as the discharge coefficient increases with the ratio $\frac{h_1}{W}$.

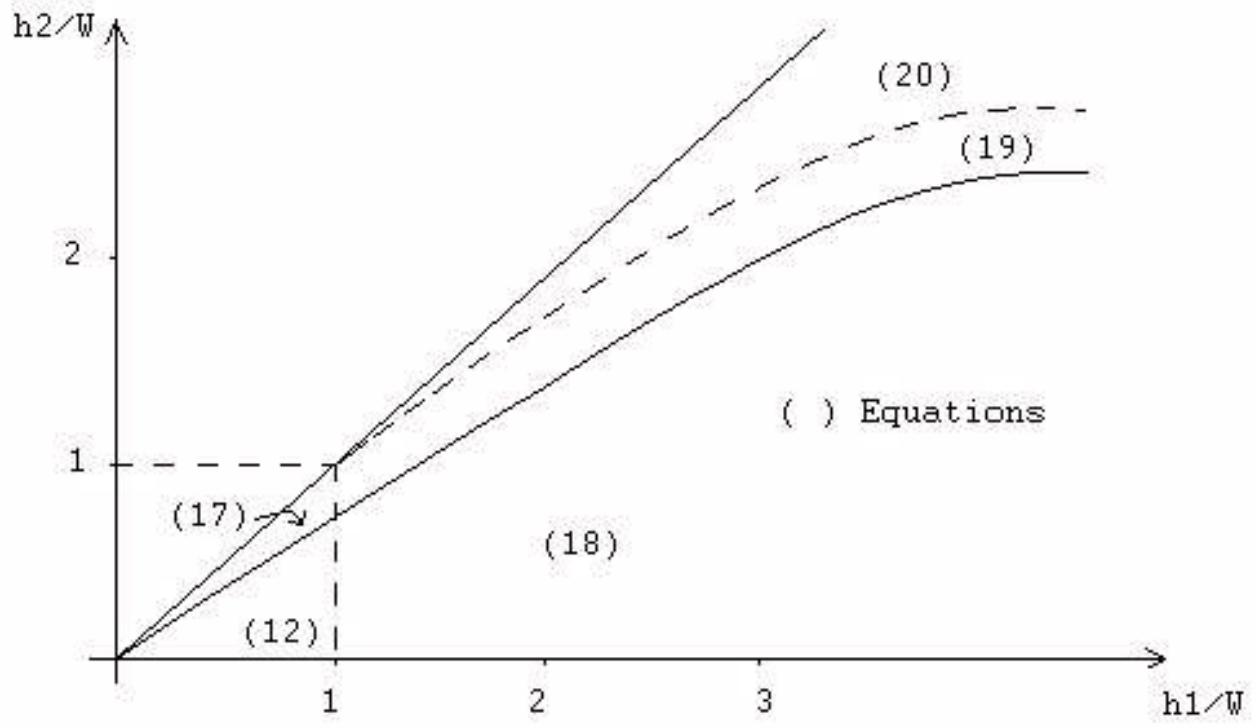

Figure 4.18: CEM 88 V chart

- (12) : Weir - free flow
- (19) : Orifice - partially submerged
- (17) : Weir - submerged

- (20) : Orifice - totally submerged
- (18) : Orifice - free flow

4.4.11.5 References

Baume, Jean-Pierre. 1988. « Modélisation des ouvrages de type : déversoir, vanne, orifice, dans les modèles d'hydraulique à surface libre ». Montpellier n°205-Document de travail 87.1. Montpellier, France: CEMAGREF. https://hal.inrae.fr/hal-04970129

4.4.12 CEM88(D) : Weir / Orifice (important sill)

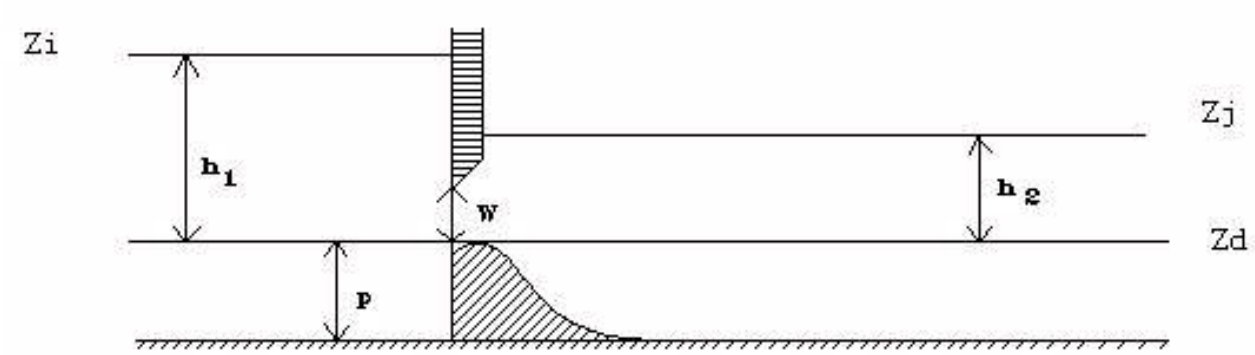

Figure 4.19: CEM 88 D diagram

4.4.12.1 Weir - free flow

($h_1 < W and h_2 \leq \frac{2}{3}h_1$)

$Q = \mu_F L\sqrt{2g}h_1^{3/2}$

Classical formulation of the free flow weir ($\mu_F \simeq 0.4$).

4.4.12.2 Weir - submerged flow

($h_1 < W$ and $h_2 \geq \frac{2}{3}h_1$)

$$Q = \mu_S L\sqrt{2g}(h_1 - h_2)^{1/2}h_2$$

Classical formulation of the submerged weir.

The switch from submerged to free flow occurs for $h_2 = \frac{2}{3}h_1$, we then have:

$\mu_S = \frac{3\sqrt{3}}{2}\mu_F$ for $\mu_F = 0.4 \Rightarrow \mu_S = 1.04$

An equivalent free flow coefficient can be calculated:

$\mu_F = \frac{Q}{L\sqrt{2g}h_1^{3/2}}$

which makes it possible to evaluate the degree of flooding of the threshold by comparing it to the free coefficient μ_F introduces. Indeed, the master coefficient of the structure introduced is that of the free weir. (μ_F close to 0.4).

4.4.12.3 Orifice - free flow

($h_1 \geq W$ and $h_2 \leq \frac{2}{3}h_1$)

We take a formulation like:

$Q = \mu L\sqrt{2g}\left(h_1^{3/2} - (h_1 - W)^{3/2}\right)$

This modeling applies well to large rectangular orifices.

Continuity to free surface operation is ensured when:

$\frac{h1}{W} = 1$, we then have $\mu = \mu_F$.

4.4.12.4 Orifice - submerged flow

There are two formulations depending on whether the orifice is partially submerged or totally submerged.

Partially submerged flow

($h_1 \geq W$ and $\frac{2}{3}h_1 < h_2 < \frac{2}{3}h_1 + \frac{W}{3}$)

$Q = \mu_F L\sqrt{2g}\left[\frac{3\sqrt{3}}{2}\left((h_1 - h_2)^{1/2}\, h_2\right) - (h_1 - W)^{3/2}\right]$

Totally submerged flow

($h_1 \geq W$ and $\frac{2}{3}h_1 + \frac{W}{3} < h_2$)

$$Q = \mu' L\sqrt{2g}(h_1 - h_2)^{1/2}\left[h_2 - (h_2 - W)\right] \Rightarrow Q = \mu' L\sqrt{2g}(h_1 - h_2)^{1/2}W$$

Classical formulation of submerged orifices, with $\mu' = \mu_S$.

Orifice weir operation is represented by the equations above and Figure below. Regardless of the type of flow under load, an equivalent free flow coefficient is calculated corresponding to the conventional free orifice formulation:

$C_F = \frac{Q}{L\sqrt{2g}W(h_1 - 0.5W)^{1/2}}$

- (12) : Weir - free flow
- (15) : Orifice - partially submerged
- (13) : Weir - submerged
- (16) : Orifice - totally submerged
- (14) : Orifice - free flow

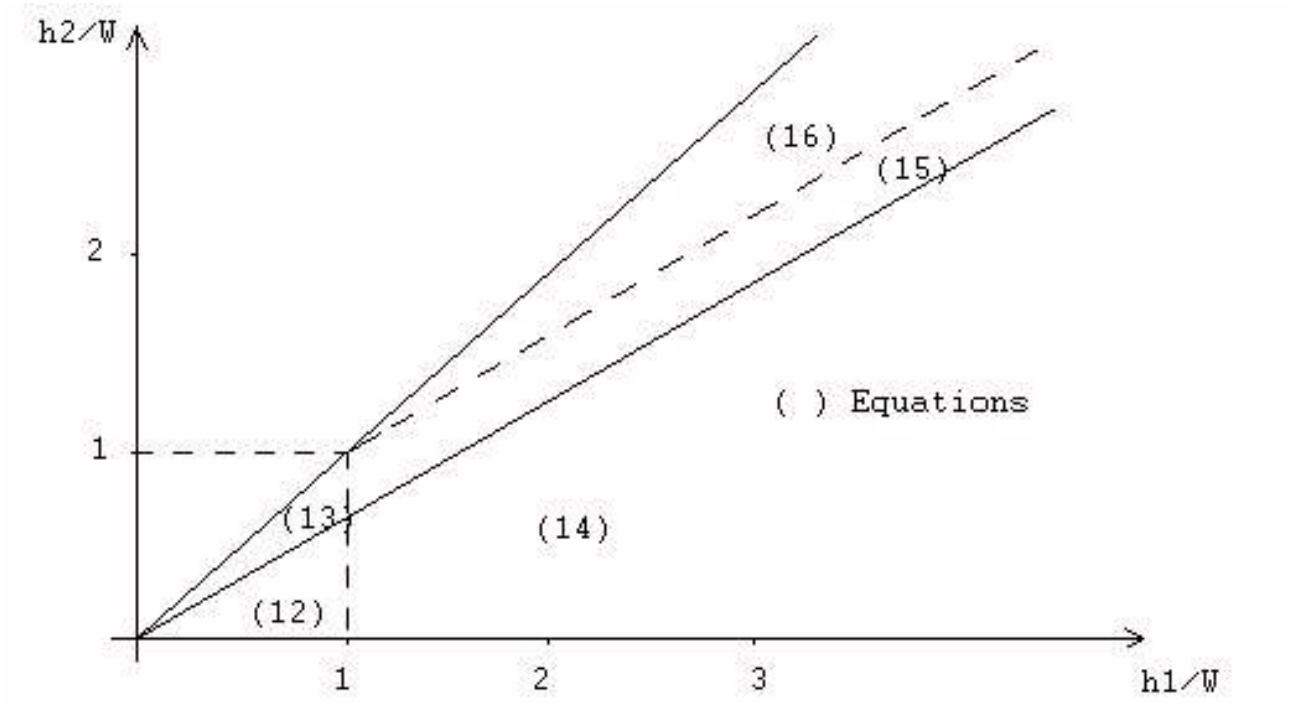

Figure 4.20: CEM 88 D chart

4.4.12.5 References

Baume, Jean-Pierre. 1988. « Modélisation des ouvrages de type : déversoir, vanne, orifice, dans les modèles d'hydraulique à surface libre ». Montpellier n°205-Document de travail 87.1. Montpellier, France: CEMAGREF. https://hal.inrae.fr/hal-04970129

4.4.13 Cunge 1980 formula

This stage discharge equation is based on the equations described by Cunge in his book [1], or in more detail in an article by Mahmood and Yevjevich [2]. This law is a compilation of the classical laws taking into account the different flow conditions: submerged, free flow, free surface and in charge as well as the equations CEM88(D) : Weir / Orifice (important sill) and CEM88(D) : Weir / Orifice (low sill). However, contrary to these equations, it does not provide any continuity between free surface and in charge flow conditions. This can lead to design problems in the vicinity of this transition.

This law is suitable for a broad-crested rectangular weir, possibly in combination with a valve. The default discharge coefficient $C_d = 1$ corresponds to the following discharge coefficients for the classical equations:

- $C_d = 0.385$ for the free flow weir.
- $C_d = 1$ for the submerged weir.
- $C_d = 1$ for the submerged gate.
- $C_c = 0.611$ for the free flow gate with C_d calculated from C_c (See below).

[1] Cunge, Holly, Verwey, 1980, "Practical aspects of computational river hydraulics", Pitman, p. 169 for weirs and p. 266 for gates.

[2] Mahmood K., Yevjevich V., 1975, "Unsteady flow in open channels, Volume 1 and 2", Water resources publications, Fort Collins, USA, 923 p.

4.4.13.1 Free flow / submerged regime detection

The flow regime is in free flow as long as the downstream water level is below critical height:

$$(Z_2 - Z_{dv}) < \frac{2}{3}(Z_1 - Z_{dv})$$

with Z_1 upstream water elevation, Z_2 downstream water elevation, et Z_{dv} apron or sill elevation of the hydraulic structure.

4.4.13.2 Free flow / in charge flow detection

The water level at the gate when the gate is open is considered here to be equal to:

- the critical height in the case of a free flow regime;
- the downstream water height in the case of a submerged regime.

The flow becomes in charge when the gate touches the surface of the water at this point.

In free flow, the flow is in charge when:

$$W \leq \frac{2}{3}(Z_1 - Z_{dv})$$

In submerged flow, the condition becomes:

$$W \leq Z_2$$

4.4.13.3 Discharge equations

The free flow gate equation uses a fixed contraction coefficient C_c with:

$C_d = \frac{C_c}{\sqrt{1+C_c W/h_1}}$

For all other flow regimes, used equations here are the following as they can be used independently:

	Free surface	In charge
Free flow	Free flow weir	free flow gate
Submerged	Submerged weir	Submerged gate

4.4.14 Free flow sluice gate

Excerpt from Baume, J.-P., Belaud, G., Vion, P.-Y., 2013. Hydraulique pour le génie rural, Formations de Master, Mastère Spécialisé, Ingénieur agronome. UMR G-EAU, Irstea, SupAgro Montpellier.

W is the gate opening, h_1 the upstream water level and L the date width. The stage-discharge equation of the free flow sluice gate is derived from Bernoulli's load conservation relationship between the upstream side of the valve and the contracted section.

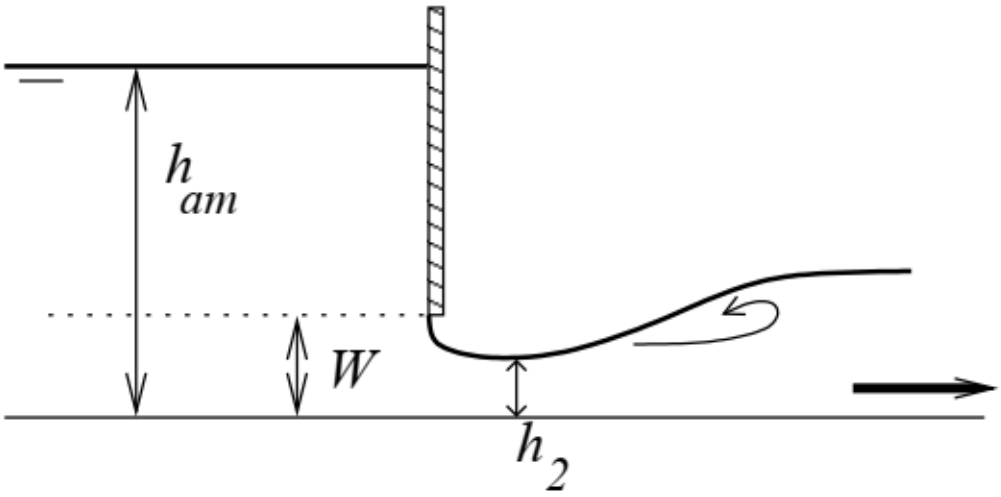

Figure 4.21: Free flow sluice gate diagram

The height h_2 corresponds to the contracted section and is equal to C_cW where C_c is the contraction coefficient. The stage-discharge equation is often expressed as a function of a flow coefficient C_d in the form of:

$Q = C_dLW\sqrt{2g}\sqrt{h_1}$

So we have the relationship between C_d and C_c :

$C_d = \frac{C_c}{\sqrt{1+C_cW/h_1}}$

Numerous experiments were conducted to evaluate C_d, which varies little around 0.6. As a first approximation, for a low W/h_1 (undershot gate, most frequent case), C_d is close to C_c and can be chosen equal to 0.6.

Discharge coefficients C_d are given by abacuses, which can be found in specialized books if necessary. They range from 0.5 to 0.6 for a vertical sluice gate, from 0.6 to 0.7 for a radial gate, up to 0.8 for an inclined sluice gate.

4.4.15 Submerged sluice gate

Excerpt from Baume, J.-P., Belaud, G., Vion, P.-Y., 2013. Hydraulique pour le génie rural, Formations de Master, Mastère Spécialisé, Ingénieur agronome. UMR G-EAU, Irstea, SupAgro Montpellier.

4.4.15.1 Submerged sluice gate equation

$Q = C'_dLW\sqrt{2g}\sqrt{h_1 - h_2}$

Coefficient C'_d is around 0.8.

4.4.16 Villemonte 1947

The “Villemonte (1947)” equation uses the equation of the Free weir to which the flooding coefficient proposed by Villemonte applies (see explanations below). This flooding coefficient is also used for the triangular and truncated triangular weir formulas.

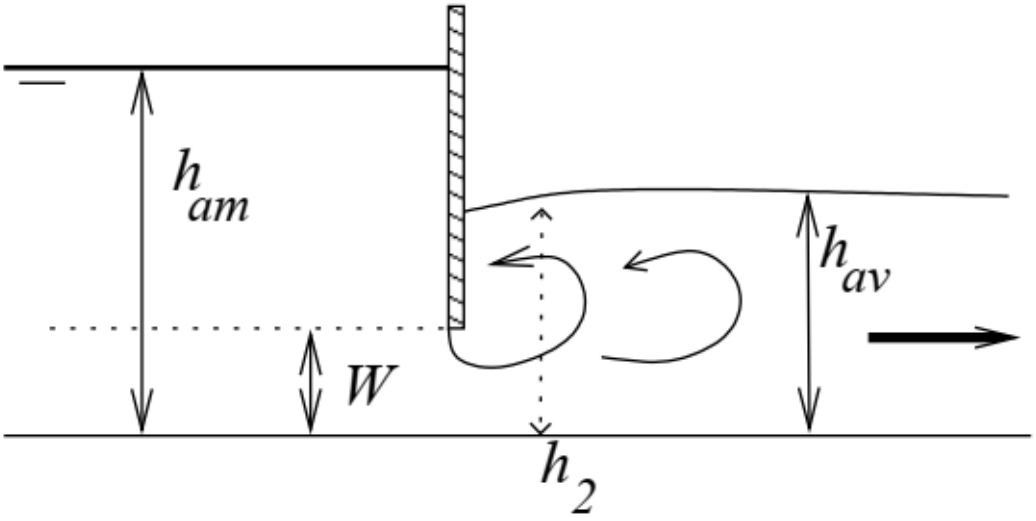

Figure 4.22: Submerged gate diagram

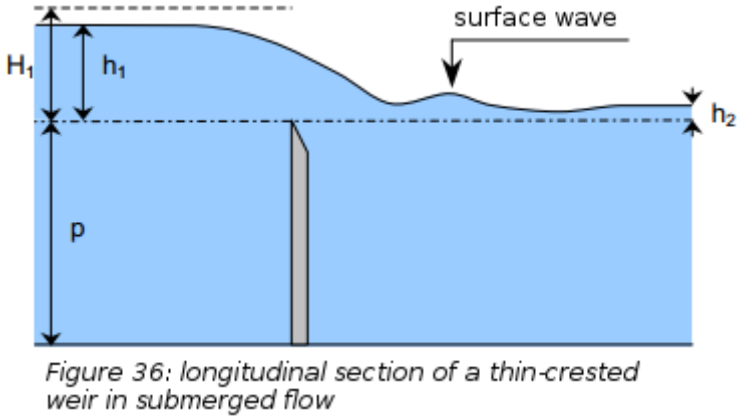

Figure 4.23: Villemonte formula: submerged weir diagram

Excerpt from CETMEF (2005)

For a downstream water elevation higher than the crest elevation of the weir, the flow is flooded and a flooding coefficient is applied to the flow coefficient.

Villemonte proposes the following formula:

$$K = \frac{Q_{submerged}}{Q_{free}} = \left[1 - \left(\frac{h2}{h1}\right)^{n}\right]^{0.385}$$

With:

- h_1 the upstream water level above the crest of the weir
- h_2 the downstream water level above the crest of the weir
- n the exponent in free flow relationships (rectangular=1.5, triangular=2.5, parabolic=2)

4.4.16.1 References

CETMEF. Notice sur les déversoirs : synthèse des lois d'écoulement au droit des seuils et déversoirs. Compiègne: Centre d'Études Techniques Maritimes Et Fluviales, 2005. http://

www.side.developpement-durable.gouv.fr/EXPLOITATION/DEFAULT/doc/IFD/IFD_REFDOC_0513410/notice-sur-les-deversoirs-synthese-des-lois-d-ecoulement-au-droit-des-seuils-et-deversoirs

Villemonte, J.R., 1947. Submerged weir discharge studies. Engineering news record 866, 54–57.

5 Fish ladders

5.1 Fish ladders: Fall

This tool is an aid for the pre-dimensioning of a fish ladder: it allows to calculate the missing value of the three quantities:

- the upstream dimension (Z_1) in m;
- the downstream dimension (Z_2) in m;
- the fall (ΔH) in m;

5.1.1 Formula

$$\Delta H = Z_1 - Z_2$$

5.2 Fish ladders: Number of falls

This tool is an aid for the pre-dimensioning of a fish ladder: it allows to calculate the missing value of the three quantities:

- the total fall (ΔH_T) in m;
- the fall between basins (ΔH) in m;
- the number of falls (N);

as well as the residual fall (ΔH_R) in m.

5.2.1 Formula

$$\Delta H_T = (\Delta H * N) + \Delta H_R$$

5.3 Fish ladders: Power dissipation

This tool is an aid for the pre-dimensioning of a fish ladder: it allows to calculate the missing value of the four quantities:

- the fall between the basins (ΔH) in m;
- the flow rate (Q) in m3/s;

- the volume of the basins (V) in m3;
- the power density (P_v) in W/m3.

The formula for calculating the power dissipation is then:

$$P_v = \frac{\rho g Q \Delta H}{V}$$

with:

- ρ: the density of water;
- g: the acceleration of the Earth's gravity = 9.81 m.s-2

5.4 Fish ladders: Dimensions

This tool is an aid for dimensioning the basins of a pass: it allows to calculate the missing value of the four quantities:

- the volume of water (V) in m3;
- the mean draught (Y_{mean}) in m;
- the length of the basin (L) in m;
- the width of the basin (B) in m.

The calculation is carried out by applying the formula:

$$V = Y_{mean} \times L \times B$$

5.5 Cross walls

This tool, which is similar to the Parallel Structures tool, is an aid to the hydraulic pre-dimensioning of a fish pass: it is most often used for the dimensioning of notches, slots, orifices, etc. characterizing the walls of a pass as well as for the setting in altitude of the notches, slots and apron of the upstream basin of a pass.

It allows to calculate the missing value of the 7 values characterizing the fall, the surface of the submerged orifice, the width of the slot, the load on the slot, the width of the notch, the load on the notch and the flow rate.

Mandatory data to be provided are the dimensions of the basins (width and length) and the average draught in metres. These data associated with the fall between basins allow us to calculate the power dissipation.

Once the module is calculated, the tool proposes to create a basin pass from this cross wall by specifying the upstream water elevation, the number of falls in the pass and the downstream water elevation.

5.5.1 Hydraulic structures that can be part of the cross wall

The tool allows you to place one or more structures in parallel among the following types of structures:

5.5.1.1 Submerged orifice

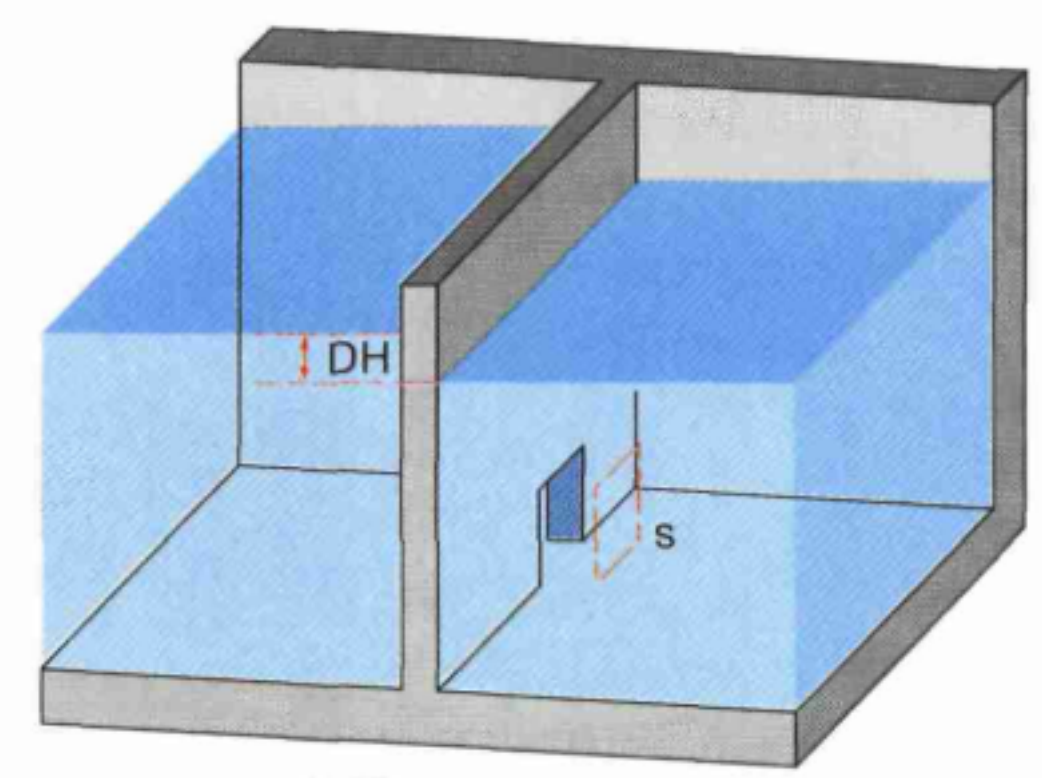

Figure 5.1: Submerged orifice diagram

Excerpt from Larinier, M., Travade, F., Porcher, J.-P., Gosset, C., 1992. Fish passage: expertise and design of crossing structures. CSP. (page 94).

The submerged orifice equation is described on the submerged orifice formula page.

5.5.1.2 Submerged Slot

Excerpt from Larinier, M., Travade, F., Porcher, J.-P., Gosset, C., 1992. Fish passage: expertise and design of crossing structures. CSP. (page 94).

The submerged slot equation is described on the sumberged slot formula page.

5.5.1.3 Notch

Excerpt from Larinier, M., Travade, F., Porcher, J.-P., Gosset, C., 1992. Fish passage: expertise and design of crossing structures. CSP. (page 94).

The equation used for the notch is that of Kindsvater-Carter and Villemonte.

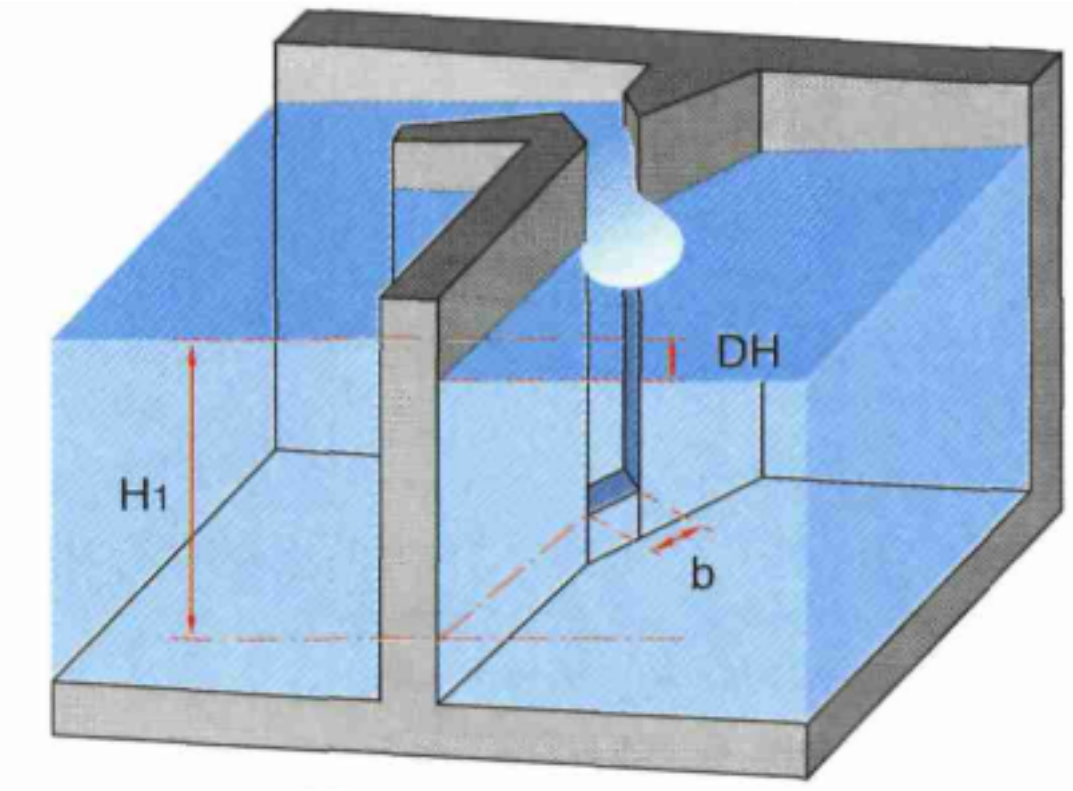

Figure 5.2: Schematic of the submerged slot

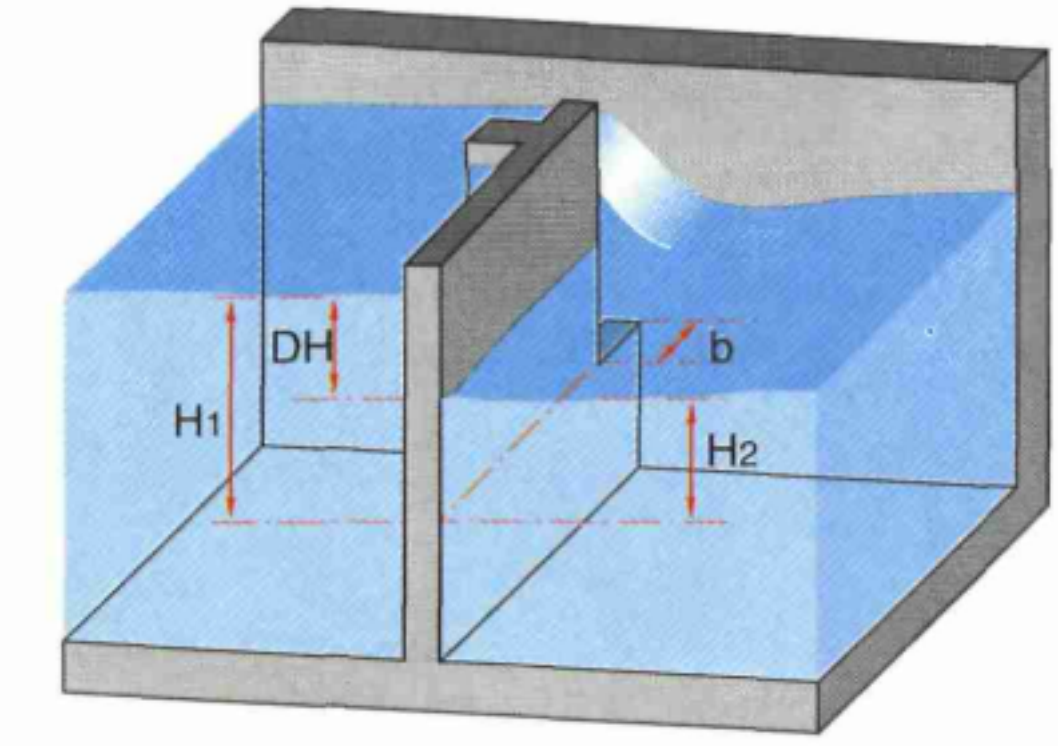

Figure 5.3: Notch diagram

5.6 Fish ladder

5.6.1 General presentation

This module calculates the water line of a fish ladder with successive basins. Two calculation possibilities are offered: calculation of the inflow into the channel from the upstream and downstream water levels, calculation of the upstream water level from the inflow into the channel and the downstream water level.

The creation of a channel can be done from scratch or from a wall model created with the Cross walls tool.

Input parameters are divided into two steps:

- The hydraulic parameters which include the boundary conditions (water level upstream and downstream of the fish ladder) and the inflow into the fish ladder.
- The parameters of the basins, which include the geometry of the basins and the parameters of the hydraulic structures constituting the walls.

It is possible to vary one or two hydraulic parameters so as to obtain a series of results for several boundary conditions or flows.

5.6.2 Input of the pass geometry

The geometry table has a line for each basin and a final line to describe the downstream wall. For each basin, the parameters present are

- length of the basin (m)
- basin width (m)
- attraction flow (m3/s)
- Mid-basin invert rating (m)
- Upstream invert elevation (m)

To these are added the parameters of the structures of the upstream wall of each basin.

5.6.2.1 Modification of the pass structure

The structure of the pass, i.e. the number of basins or the number of structures in a wall can be changed using the toolbar at the top right of the table:

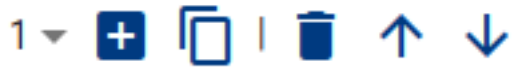

Figure 5.4: Edit toolbar for the geometry of the pass

This bar is activated when you select:

- a basin (which includes its upstream wall) or the downstream wall by clicking on the first column of a row
- a structure by clicking on an uneditable cell of a structure in a wall
- all structures in a column of the table by clicking on the header of the column to be selected

It is also possible to expand an existing selection by pressing the Ctrl] key to add a new item to the selection, or by pressing the [Shift] key to expand the selection between two rows or two columns.

Depending on the elements selected in the table, the toolbar indicates whether the proposed actions will apply to the selected basins or structures.

The toolbar consists of the following buttons:

1. Number of basins or structures to be added or duplicated
2. Add *n* basins or *n* structures with *n* the number indicated on the first button.
3. Duplicate *n* basins or *n* structures with *n* the number indicated on the first button.
4. Delete selected basins or structures
5. 1. Move the selected pools (or structures) upwards (or to the left).
6. 1. Move the selected basins (or structures) downwards (or to the right).

5.6.2.2 Advanced modification of the pass geometry

The selection of basins or structures gives access to a button “Modify values” which allows to modify a parameter among all the variables of the selected cells in the geometry table.

For this variable to be modified, one can:

- define a fixed value;
- apply a delta;
- calculate an interpolation between the basin selected upstream and downstream.

5.6.2.3 The downstream wall

The downstream wall, in addition to the laws of structures available on the walls, allows the use of a “lift gate” in the form of two laws:

- Regulated notch (Villemonte 1957);
- Regulated submerged slot (Larinier 1992).

The lift gate is a structure where the crest of the weir is regulated to maintain a setpoint waterfall between the last basin and the downstream water level. In addition to the conventional parameters of the flow laws, it includes:

- a *DH* setpoint waterfall (m)
- a minimum crest elevation *minZDV* (m);
- a maximum crest elevation *maxZDV* (m);

During the calculation, if the calculated crest elevation is less than *minZDV* (resp. greater than *maxZDV*), the value is locked at *minZDV* (resp. *maxZDV*) and a warning appears in the calculation log.

5.6.3 Calculation results

The results are presented in the form of a summary table of hydraulic calculations for all basins and walls. It contains all the data calculated by the modules [Cross walls and Power dissipation.

Two graphs are present:

- A profile along the channel with the apron elevation of the basins and the water elevation in each basin.
- A general graph allowing the selection of any parameter from the result table in abscissa and ordinate.

If several results are available due to the variation of one or two hydraulic parameters of the pass, all calculated water lines are displayed in the long profile, and a drop-down list allows to select the result to be displayed in the generalist table and graph.

5.6.4 Example session

An example illustrating the conception of a fish ladder can be directly loaded through this link.

5.7 Pre-barrages

Pre-barrages are a type of basin pass used for crossing low obstacles. They are made up of several walls or thresholds dividing the fall into several large basins in parallel and in series.

5.7.1 General presentation

This module calculates the flow distribution and the water line of the basins of a pre-barrage. Two calculation possibilities are offered: calculation of the channel flow into knowing the upstream and downstream water level, calculation of the upstream water level knowing the channel flow and the downstream water level.

The input of the pre-barrage parameters is divided into two parts:

- The composition of the pre-barrage in basins and the walls connecting the basins, on the first part of the screen.
- The input of the pre-barrage parameters: boundary conditions, basin parameters and walls parameters, on the second part of the screen.

It is possible to vary any parameter in order to obtain a series of results.

The pre-barrage composition scheme can be displayed in full screen and exported to PNG image format.

5.7.2 Pre-barrage composition

At its creation, the pre-barrage consists of an upstream boundary condition, a basin, a downstream boundary condition and walls joining these three elements.

The buttons “Add new basin” and “Add new wall” are used to add respectively a basin and a wall to the pre-barrage. When adding a wall, you are asked to which boundary conditions or basins the wall is connected. When entering the connections to the walls, the user must follow the numbering of the basins, which necessarily respects an upstream-downstream order.

A toolbar allows to duplicate and delete a selected wall or basin and to change the order of a basin.

5.7.3 Entering parameters of the pre-barrage elements

The entry of the parameters of the upstream or downstream boundary condition, of a basin or a wall is made by selecting the desired element in the diagram in the first part of the screen.

The entry of the elements is then carried out as for any Cassiopée module. For the entry of walls, refer to the module Parallel structures.

5.7.4 Launching the calculation

The calculate button is activated from the moment all the basins are connected by walls from upstream to downstream of the pre-barrage and all the parameters have been entered.

5.7.5 Visualization of the results

After the calculation, the interface displays two tabs “Input” and “Results” that allow to navigate between the pre-barrage input and the calculation results.

If the calculation produces a series of results, a drop-down list allows you to choose which result to display for each parameter that has changed.

The first part of the screen shows a synoptic of the pre-barrage with the flows and falls at the walls, the average power dissipated and the average depth at the basins, and the flow and water levels at the upstream and downstream boundary conditions. To view the numerical results at basin level, the user must click on one of these items on the diagram. To view the numerical results at a wall, click on the corresponding wall on the diagram.

An “Export all results” button allows you to retrieve a table in Excel format containing the results of boundary conditions, basins and walls for the whole calculation series.

5.8 Nature-like fish passage with riprap in periodic rows

It is stated on p.16 of the design guide for nature-like fishways (Larinier et al., 2006) that rock-rigged fishways in periodic rows are similar to fish ladders, and their design criteria are identical to those of.

It is therefore possible to use the various tools in the “fish ladder” module module to design this type of device. In particular, the “cloisons” tool can be used to enter the various dimensional characteristics of weirs (widths, overflow dimensions) and pseudo-basins pseudo-basins (length, width, mid-radius), which can be used to indirectly indirectly retrieve the sill height (p) and useful block height (k) parameters in the generated geometry table. Porosity (ratio between the free passage between the blocks and the total width width of the pseudo-wall) is not entered directly, but this parameter can be be deduced and examined elsewhere if necessary.

According to this principle, each overhanging portion of the partition must be entered as an indentation or slot, as well as the dimension of the top of the blocks if the latter are flooded within the operating range of the device. In the case of notches, particular attention should be paid to the type of (thick or thin) in order to accurately reflect the conditions of flooding by the downstream of the weir.

It is also possible to use the “pre-dams” tool (the equations implemented are the same as in the “cloisons” tool), if the device is affected by complex feed modes, with, for example, overflows from the weir to different basins in the system (a less frequent case for a riprap pass in periodic rows).

An example of a pass can be accessed directly via this link.

5.8.1 References

Larinier, Michel, Dominique Courret, et Peggy Gomes. 2006. « Guide technique pour la conception des passes à poissons “naturelles” ». Rapport GHAPPE RA. Compagnie Nationale du Rhône / Agence de l’Eau Adour Garonne. http://dx.doi.org/10.13140/RG.2.1.1834.8562

6 Rock-ramp fishpasses

6.1 Rock-ramp fishpasses

The rock-ramp fishpass calculation module makes it possible to calculate the characteristics of a rock-ramp pass made up of uniformly distributed blocks with equal transverse ax and longitudinal ay spacings.

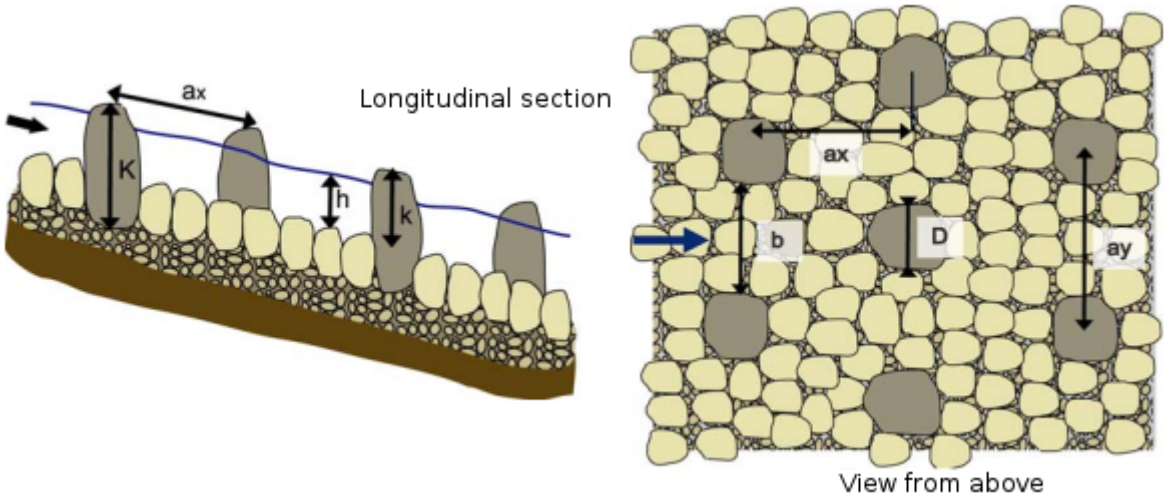

Figure 6.1: Schematic of a regular arrangement of rockfill and notations

Excerpt from Larinier et al., 2006

The tool allows you to calculate one of the following values:

- The width of the pass (m);
- The slope of the pass (m);
- The flow rate (m3/s);
- The depth h (m);
- The concentration of the blocks.

It requires the following values to be entered:

- The upstream bottom coordinate (m);
- The length of the pass (m);
- The background roughness (m);
- The width of the blocks D facing the flow (m);
- The useful height of the blocks k (m);
- The drag coefficient of a single block (1 for round, 2 for square).

6.2 Bed roughness

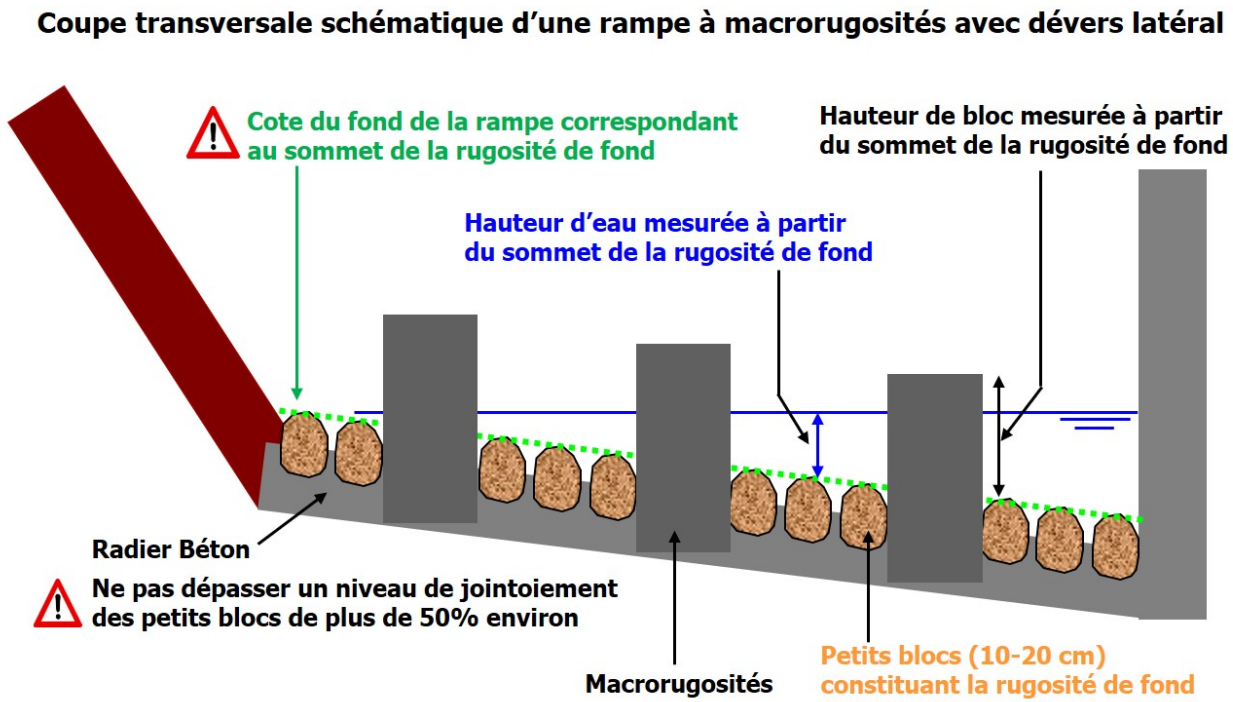

6.2.1 References

Larinier, Michel, Courret, D., Gomes, P., 2006. Technical guide for the design of "natural" fish passes, GHAPPE RA Report. Compagnie Nationale du Rhône / Adour Garonne Water Agency. http://dx.doi.org/10.13140/RG.2.1.1834.8562

6.3 Calculation of the flow rate of a rock-ramp pass

The calculation of the flow rate of a rock-ramp pass corresponds to the implementation of the algorithm and the equations present in Cassan et al. (2016).

6.3.1 General calculation principle

After Cassan et al., 2016

There are three possibilities:

- the submerged case when $h \geq 1.1 \times k$
- the emergent case when $h \leq k$
- the quasi-emergent case when $k < h < 1.1 \times k$

In the quasi-emergent case, the calculation of the flow corresponds to a transition between emergent and submerged case formulas:

$$Q = a \times Q_{submerge} + (1 - a) \times Q_{emergent}$$

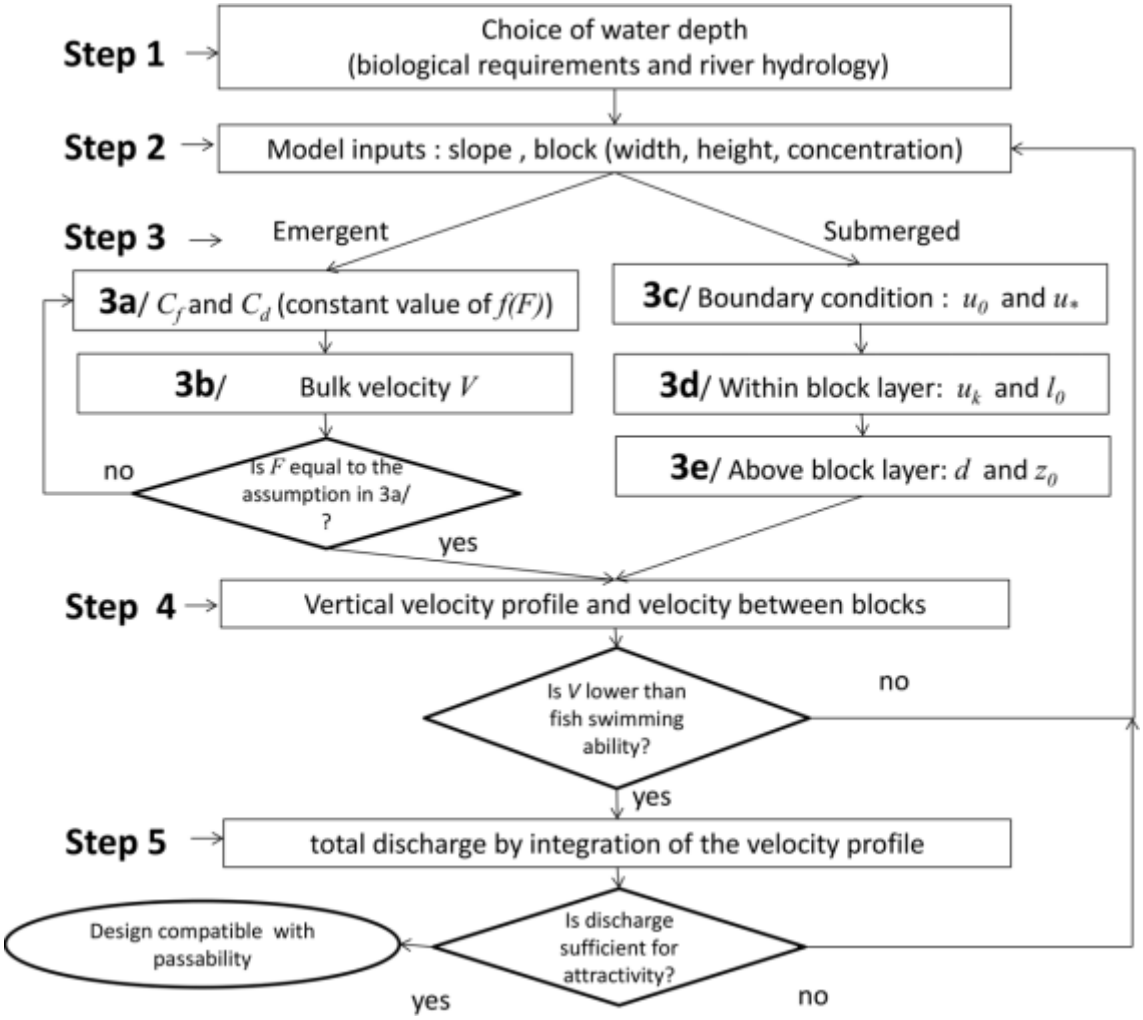

Figure 6.2: Organigramme de la méthode de calcul

with $a = \dfrac{h/k - 1}{1.1 - 1}$

6.3.2 Submerged case

The calculation is done by integrating the velocity profile in and above the macro-roughnesses. The calculated velocities are the temporal and spatial averages per plane parallel to the bottom.

In macro-roughnesses, velocities are obtained by double averaging the Navier-Stokes equations in uniform regime with a mixing length model for turbulence.

Above the macro-roughnesses, the classical turbulent boundary layer analysis is maintained. The velocity profile is continuous at the top of the macro-roughnesses and is dependent on the boundary conditions set by the hydraulics:

- velocity at the bottom (without turbulence) in m/s:

$$u_0 = \sqrt{2gSD(1 - \sigma C)/(C_d C)}$$

- total shear stress at the top of the roughnesses in m/s:

$$u_* = \sqrt{gS(h-k)}$$

The average bed velocity is given by integrating the flows between and above the blocks:

$$\bar{u} = \frac{Q_{inf} + Q_{sup}}{h}$$

with respectively Q_{inf} and Q_{sup} the unit flows for the part in the canopy and the part above the canopy.

6.3.2.1 Calculation of the unit flow rate Qinf *in the canopy*

The flow in the canopy is obtained by integrating the velocity profile (Eq. 9, Cassan et al., 2016):

$$Q_{inf} = \int_0^1 u(\tilde{z}) d\tilde{z}$$

with

$$u(\tilde{z}) = u_0 \sqrt{\beta \left(\frac{h}{k} - 1\right) \frac{\sinh(\beta \tilde{z})}{\cosh(\beta)} + 1}$$

with

$$\beta = \sqrt{(k/\alpha_t)(C_d C k/D)/(1-\sigma C)}$$

with

$$C_d = C_x f_{h_*}(h_*)$$

and α_t obtained by solving the following equation:

$$\alpha_t u(1) - l_0 u_* = 0$$

with

$$l_0 = \min(s, 0.15k)$$

with

$$s = D\left(\frac{1}{\sqrt{C}} - 1\right)$$

6.3.2.2 Calculation of the unit flow Qsup above the canopy

$$Q_{sup} = \int_k^h u(z)dz$$

with (Eq. 12, Cassan et al., 2016)

$$u(z) = \frac{u_*}{\kappa} \ln\left(\frac{z-d}{z_0}\right)$$

with (Eq. 14, Cassan et al., 2016)

$$z_0 = (k-d)\exp\left(\frac{-\kappa u_k}{u_*}\right)$$

and (Eq. 13, Cassan et al., 2016)

$$d = k - \frac{\alpha_t u_k}{\kappa u_*}$$

which gives

$$Q_{sup} = \frac{u_*}{\kappa}\left((h-d)\left(\ln\left(\frac{h-d}{z_0}\right)-1\right) - \left((k-d)\left(\ln\left(\frac{k-d}{z_0}\right)-1\right)\right)\right)$$

6.3.3 Emerging case

The calculation of the flow rate is done by successive iterations which consist in finding the flow rate value allowing to obtain the equality between the flow velocity V and the average velocity of the bed given by the equilibrium of the friction forces (bottom + drag) with gravity:

$$u_0 = \sqrt{\frac{2gSD(1-\sigma C)}{C_d f_F(F) C(1+N)}}$$

with

$$N = \frac{\alpha C_f}{C_d f_F(F) C h_*}$$

with

$$\alpha = 1 - (a_y/a_x \times C)$$

6.3.4 Formulas used

6.3.4.1 Bulk velocity V

$$V = \frac{Q}{B \times h}$$

6.3.4.2 Average speed between blocks Vg

From Eq. 1 Cassan et al (2016) and Eq. 1 Cassan et al (2014):

$$V_g = \frac{V}{1 - \sqrt{(a_x/a_y)C}}$$

6.3.4.3 Drag coefficient of a single block Cd0

C_{d0} is the drag coefficient of a block considering a single block infinitely high with $F << 1$ (Cassan et al, 2014).

Block shape	Cylinder	"Rounded face" shape	Square-based parallelepiped	"Flat face" shape
	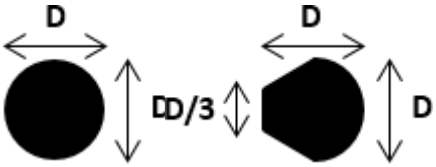		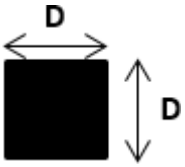	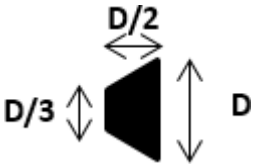
Value of C_{d0}	1.0	1.2-1.3	2.0	2.2

When establishing the statistical formulae for the 2006 technical guide (Larinier et al. 2006), the definition of the block shapes to be tested was based on the use of quarry blocks with neither completely round nor completely square faces. The so-called "rounded face" shape was thus not completely cylindrical, but had a trapezoidal bottom face (seen in plan). Similarly, the "flat face" shape was not square in cross-section, but also had a trapezoidal bottom face. These differences in shape between the "rounded face" and a true cylinder on the one hand, and the "flat face" and a true parallelepiped with a square base on the other hand, result in slight differences between them in the shape coefficients C_{d0}.

6.3.4.4 Block shape coefficient σ

Cassan et al. (2014), et Cassan et al. (2016) define σ as the ratio between the block area in the x, y plane and D^2. For the cylindrical form of the blocks, σ is equal to $\pi/4$ and for a square block, $\sigma = 1$.

6.3.4.5 Ratio between the average speed downstream of a block and the maximum speed r

The values of r depends on the block shapes (Cassan et al., 2014 et Tran et al. 2016):

- round : $r_Q = 1.1$
- "rounded face" shape : $r = 1.2$
- square-based parallelepiped : $r = 1.5$
- "flat face" shape : $r = 1.6$

Cassiopée implements a formula depending on $Cd0$:

$$r = 0.4C_{d0} + 0.7$$

6.3.4.6 *Froude* F

$$F = \frac{V_g}{\sqrt{gh}}$$

6.3.4.7 *Froude-related drag coefficient correction function* fF(F)

If $F < 1$ (Eq. 19, Cassan et al., 2014):

$$f_F(F) = \min\left(\frac{r}{1 - \frac{F_g^2}{4}}, \frac{1}{F^{\frac{2}{3}}}\right)^2$$

otherwise $f_F(F) = 1$ because a torrential flow upstream of the blocks is theoretically impossible because of the hydraulic jump caused by the downstream block.

6.3.4.8 *Maximum speed* umax

According to equation 19 of Cassan et al, 2014 :

$$u_{max} = V_g\sqrt{f_F(F)}$$

6.3.4.9 *Drag coefficient correction function linked to relative depth* fh*(h*)

The equation used in Cassiopeia differs slightly from equation 20 of Cassan et al. 2014 and equation 6 of Cassan et al. 2016. This formula is a fit to the experimental measurements on circular blocks used in Cassan et al. 2016:

$$f_{h*}(h_*) = (1 + 1/h_*^2)$$

6.3.4.10 *Coefficient of friction of the bed* Cf

If $k_s < 10^{-6}\mathrm{m}$ then we use Blasius' formula

$$C_f = 0.3164/4 * Re^{-0.25}$$

with

$$Re = u_0 \times h/\nu$$

Else (Eq. 3, Cassan et al., 2016 d'après Rice et al., 1998)

$$C_f = \frac{2}{(5.1\log(h/k_s) + 6)^2}$$

6.3.5 Notations

- α: ratio of the area affected by the bed friction to $a_x \times a_y$
- α_t: length scale of turbulence in the block layer (m)
- β: ratio between drag stress and turbulence stress
- κ: Von Karman constant = 0.41
- σ: ratio between the block area in the plane X,y et D^2
- a_x: cell width (perpendicular to the flow) (m)
- a_y: length of a cell (parallel to the flow) (m)
- B: pass width (m)
- C: blocks concentration
- C_d: drag coefficient of a block under current flow conditions
- C_{d0}: drag coefficient of a block considering an infinitely high block with $F \ll 1$
- C_f): bed friction coefficient
- d: displacement in the zero plane of the logarithmic profile (m)
- D: width of the block facing the flow (m)
- F: Froude number based on h and V_g
- g: acceleration of gravity = 9.81 m.s-2
- h: average depth (m)
- h_*: dimensionless depth (h/D)
- k: useful block height (m)
- k_s: roughness height (m)
- l_0: length scale of turbulence at the top of the blocks (m)
- N: ratio between bed friction and drag force
- Q: flow (m3/s)
- S: pass slope (m/m)
- u_0: average bed speed (m/s)
- u_*: shear velocity (m/s)
- V: flow velocity (m/s)
- V_g: velocity between blocks (m/s)
- s: minimum distance between blocks (m)
- z: vertical position (m)
- z_0: hydraulic roughness (m)
- $\tilde{z}$: dimensionless stand $\tilde{z} = z/k$

6.3.6 References

Cassan L, Laurens P. 2016. Design of emergent and submerged rock-ramp fish passes. Knowl. Manag. Aquat. Ecosyst., 417, 45. https://doi.org/10.1051/kmae/2016032

Cassan, L., Tien, T.D., Courret, D., Laurens, P., Dartus, D., 2014. Hydraulic Resistance of Emergent Macroroughness at Large Froude Numbers: Design of Nature-Like Fishpasses. Journal of Hydraulic Engineering 140, 04014043. https://doi.org/10.1061/(ASCE)HY.1943-7900.0000910

Larinier, Michel, Courret, D., Gomes, P., 2006. Guide technique pour la conception des passes à poissons “naturelles,” Rapport GHAPPE RA. Compagnie Nationale du Rhône / Agence de l’Eau Adour Garonne. http://dx.doi.org/10.13140/RG.2.1.1834.8562

Rice C. E., Kadavy K. C., et Robinson K. M., 1998. Roughness of Loose Rock Riprap on Steep Slopes. Journal of Hydraulic Engineering 124, 179-85. https://doi.org/10.1061/(ASCE)0733-9429(1998)124:2(179)

Tran, T.D., Chorda, J., Laurens, P., Cassan, L., 2016. Modelling nature-like fishway flow around unsubmerged obstacles using a 2D shallow water model. Environmental Fluid Mechanics 16, 413–428. https://doi.org/10.1007/s10652-015-9430-3

6.4 Compound rock-ramp fishpasses

This calculation module allows to calculate the flow passing through a rock-ramp pass called “complex” because it has an inclined apron or multiple aprons.

6.4.1 General characteristics

The parameters to be entered are the same as for the so-called “simple” macro-roughness pass. Concerning the apron of the pass two choices are offered:

- Multiple aprons: it is possible to create, duplicate, delete, change the order of as many aprons as necessary. For each apron, the parameters to be entered are: the width of the apron and the dimension of the apron upstream of the pass.
- The inclined apron: in addition to the width of the apron, the right and left sides of the apron must be entered upstream of the pass.

The calculated data are the same as for the so-called “simple” macro-roughness pass. The results display the different data for each apron and the graph allows you to view this data for each apron (transverse profile). In the event that at least one of the calculation parameters varies, the results are available individually via a drop-down list.

6.4.2 Inclined apron case

The calculation of an inclined apron pass consists in discretizing the pass into several horizontal aprons. The width of the created aprons is fixed at the distance between two blocks with an adjustment of the uppest apron to obtain the total width of the pass. It is possible to edit the created aprons by selecting “Multiple aprons” after performing a calculation with an inclined apron.

6.5 Blocks concentration

This module makes it possible to calculate the concentration of uniformly distributed blocks in a rock-ramp fish pass.

It allows to calculate one of the following values:

- The width of the pass (m) ;
- The number of blocks ;
- The diameter of the blocks (m) ;
- The concentration of the blocks C.

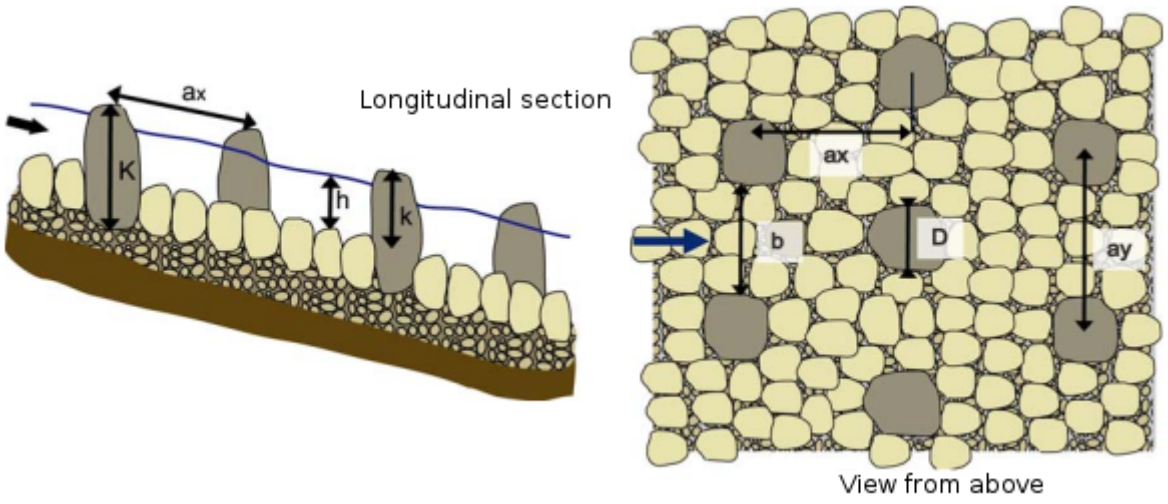

Figure 6.3: Schematic of a regular arrangement of rockfill and notations

6.5.1 Formula

Excerpt from Larinier et al., 2006

The spacing between the blocks is then calculated with the following formula:

$$ax = ay = \frac{D}{\sqrt{C}}$$

With :

- ax and ay respectively the longitudinal and lateral distances between the centres of the blocks (m);
- the width of the blocks facing the flow (m);
- the concentration of the blocks (-).

The number of blocks N for a pass of width B is then obtained with the equation:

$$N = B/ax$$

6.5.2 Harmonization

When calculating the number of blocks, if it is not an integer, upward and downward harmonized numbers of blocks are given along with corresponding concentration values.

Tolerance is of the order of a centimetre.

6.5.3 References

Larinier, Michel, Courret, D., Gomes, P., 2006. Technical guide for the design of “natural” fish passes, GHAPPE RA Report. Compagnie Nationale du Rhône / Adour Garonne Water Agency. http://dx.doi.org/10.13140/RG.2.1.1834.8562

6.6 Backwater curve for a rock-ramp fishpass

This module can be used to simulate the backwater curve of a simple macro-roughness fishway in order to determine the downstream flooding level of the fishway.

6.6.1 Operating principle

The parameters of this module are :

- The choice of the “simple” rock-ramp fishpass module among those present in the work session which will be used to perform the calculation
- The water level downstream of the pass
- The space step used to discretise the curve calculation.

N.B. : As the backwater curve can only be calculated for one set of parameters, the simple rock-ramp fishpass module cannot contain varied parameters.

The theoretical calculation carried out in the macro-roughness channel corresponds to the calculation of the water line in a uniform regime where the slope of the water is equal to the slope of the bottom of the channel. The rock-ramp fishpass module is used here to calculate the slope of the water in the non-uniform case. The fluvial backwater curve is then calculated from the water level downstream using the trapezoid integration method.

This module is based on the module for calculating the backwater curve of a section to calculate and display the results.

6.7 Rough bottom ramp

Rough-bottom ramps are generally made up of blocks of relatively uniform dimensions arranged one against the other and forming a channel of varying slope.

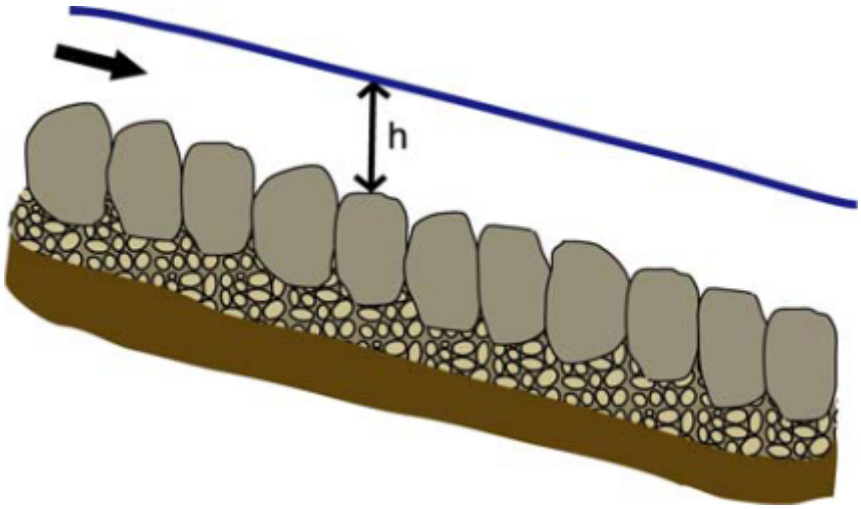

Figure 6.4: Schematic longitudinal section of a rough bottom ramp

6.7.1 Warning about the passability of the structure

In the absence of pools and protruding elements in the flow, these ramps do not provide rest areas for upstream migration fishes. Fish therefore have to swim over them in one go, generally using their maximum swimming speed. The crossability of a rough bottom ramp depends on the flow velocities, the water heights above the crest of the embankments, the 'quality' of the water surface (absence of jumps and slumps making it difficult, if not impossible, for fish to swim), and also the length of the ramp that the fish have to cover before becoming tired. This is why rough bottom ramps are not considered to be crossing devices as such (Larinier et al. 2006). This type of device can be useful (1) to make a sill directly passable by species with the best swimming ability (salmonids, even shad and lampreys) or (2) to form pre-dams combining short ramps with reduced falls and intermediate basins.

6.7.2 Calculation method

6.7.2.1 Inclined apron

The inclined apron is calculated by discretizing the pass width into several horizontal aprons whose number is determined by the parameter "Number of flow slices".

6.7.2.2 Relationship between upstream head on the crest and flow rate

The relationship between the upstream load and the flow is represented by a formula of free weir.

6.7.2.3 Relationship between water depth, flow velocity and uniform flow

From the flow supplied or calculated at the inlet, the head of water and the flow velocity in the channel are calculated using the Manning-Strickler formula for a uniform flow for a rectangular cross section equivalent to that of the ramp.

Strickler coefficient is estimated from the D_{65} size of riprap:

$$K_s = \frac{a}{{D_{65}}^{1/6}}$$

With a the **Strickler correction coefficient** function of how the riprap is placed and the level at which they are joined (Larinier et al., 2006):

- spilt rock, not grouted : 21
- riprap in a compact arrangement without jointing : 15.5
- 30% grouting : 16.7
- 50% grouting : 18

6.7.3 References

Larinier, M., J. Chorda, et O. Ferlin. 1995. « Le franchissement des seuils en enrochements par les poissons migrateurs : étude expérimentale ». GHAAPPE 95/05-HYDRE 161. irstea. https://hal.inrae.fr/hal-02575575

Larinier, Michel, Dominique Courret, et Peggy Gomes. 2006. « Guide technique pour la conception des passes à poissons “naturelles” ». Rapport GHAPPE RA. Compagnie Nationale du Rhône / Agence de l’Eau Adour Garonne. http://dx.doi.org/10.13140/RG.2.1.1834.8562

7 Baffle fishways

7.1 Baffle fishway (or baffle fishway) setup

This module allows to dimension a baffle fishway. Supported baffle fishway types are:

- plane baffles (Denil) fishway;
- “Fatou” baffle fishway;
- superactive baffles fishway;
- mixed / chevron baffles fishway.

See all the formulas used for baffle fishways.

7.1.1 Hydraulic setup

This tool allows to calculate one of the following values:

- flow through the pass (m3/s);
- upstream head (m);
- pass width (m) for plane and Fatou types.

Given the following mandatory parameters:

- pass type (Plane, Fatou, superactive, mixed);
- slope (m/m).

Parameter “Space between baffles (m)” is optional. When not given, its standard value is calculated. When given, if its value deviates by more than 10% from standard value, an error is generated.

7.1.2 Altimetric setup

Altimetric setup parameters (upstream water level and downstream water level) are optional and allow to calculate:

- pass length in horizontal projection and following the slope
- number of baffles
- apron and spilling elevations, upstream and downstream
- rake height of upstream side walls

7.1.3 Generating a baffle fishway simulation module

Results of an altimetrically setup pass may be used to generate a baffle fishway simulation module, using the ad hoc button.

7.2 Baffle fishway (or baffle fishway) simulation

This module allows to calculate different hydraulic conditions on a baffle fishway with a known geometry. This geometry may come from topographical measurements or from the result of a baffle fishway setup.

Supported baffle fishway types are:

- plane baffles (Denil) fishway;
- “Fatou” baffle fishway;
- superactive baffles fishway;
- mixed / chevron baffles fishway.

See all the formulas used for baffle fishways.

This tool allows to calculate one of the following values:

- flow through the pass (m3/s);
- upstream water elevation (m);
- upstream spilling elevation (m).

Given the following mandatory parameters:

- pass type (Plane, Fatou, superactive, mixed);
- slope (m/m).
- pass width (m);
- upstream spilling or apron elevation (m);
- downstream spilling or apron elevation (m).

7.3 Baffle fishways (or baffle fishways) calculation formulas

For calculation of:

- upstream head ha;
- water level in the pass h;
- flow Q;
- flow velocity V;
- upstream apron elevation Z_{r1};
- minimal rake height of upstream side walls Z_m

Refer to the formulas specific to each baffle fishway type:

- plane baffles (Denil) fishway;
- “Fatou” baffle fishway;
- superactive baffles fishway;
- mixed / chevron baffles fishway.

7.3.1 Upstream water elevation Z_1

$$Z_1 = Z_{d1} + h_a$$

With Z_{d1} the spilling elevation of the first upstream baffle, h_a the upstream head.

7.3.2 Pass length

Pass length along a water line parallel to the pass slope L_w equals

$$L_w = (Z_1 - Z_2)\frac{\sqrt{1+S^2}}{S}$$

with Z_1 and Z_2 the upstream and downstream water elevations, S the slope.

Pass length along the slope L_S must be a multiple of the length between two baffles P rounded to the greater integer:

$$L_S = \lceil (L_w - \epsilon)/P \rceil \times P$$

With ϵ = 1 mm to leave a margin before adding an extra baffle.

Horizontal projection of the pass length L_h thus equals:

$$L_h = \frac{L_S}{\sqrt{1+S^2}}$$

7.3.3 Number of baffles N_b

For plane and Fatou types:

$$N_b = L_S/P + 1$$

For superactive and mixed types:

$$N_b = L_S/P$$

7.3.4 Downstream apron Z_{r2} and spilling Z_{d2} elevations:

$$Z_{r2} = Z_{r1} - \frac{L_S \times S}{\sqrt{1+S^2}}$$

$$Z_{d2} = Z_{r2} + Z_{d1} - Z_{r1}$$

7.4 Plane baffles (Denil) fishway

All concepts and formulas are extracted from the following reference:

Larinier, M. 2002. “BAFFLE FISHWAYS.” Bulletin Français de La Pêche et de La Pisciculture, no. 364: 83–101. doi:10.1051/kmae/2002109

7.4.1 Geometrical characteristics

Excerpt from Larinier, 2002

7.4.2 Hydraulic laws given by abacuses

Experiments conducted by Larinier, 2002 allowed to establish abacuses that link adimensional flow Q^*:

$$Q^* = \frac{Q}{\sqrt{g}L^{2,5}}$$

to upstream head ha and the average water level in the pass h :

Abacuses of a plane baffles (Denil) fishway for a slope of 10% (Excerpt from Larinier, 2002)

Abacuses of a plane baffles (Denil) fishway for a slope of 15% (Excerpt from Larinier, 2002)

Abacuses of a plane baffles (Denil) fishway for a slope of 20% (Excerpt from Larinier, 2002)

To run calculations for all slopes between 8% and 22%, polynomes coefficients of abacuses above are themelves adjusted in the form of slope S depending polynomes.

We thus have:

$$ha/L = a_2(S)Q^{*2} + a_1(S)Q^* + a_0(S)$$

$$a_2(S) = 315.110S^2 - 115.164S + 6.85371$$

$$a_1(S) = -184.043S^2 + 59.7073S - 0.530737$$

$$a_0(S) = 15.2115S^2 - 5.22606S + 0.633654$$

And:

$$h/L = b_2(S)Q^{*2} + b_1(S)Q^* + b_0$$

$$b_2(S) = 347.368S^2 - 130.698S + 8.14521$$

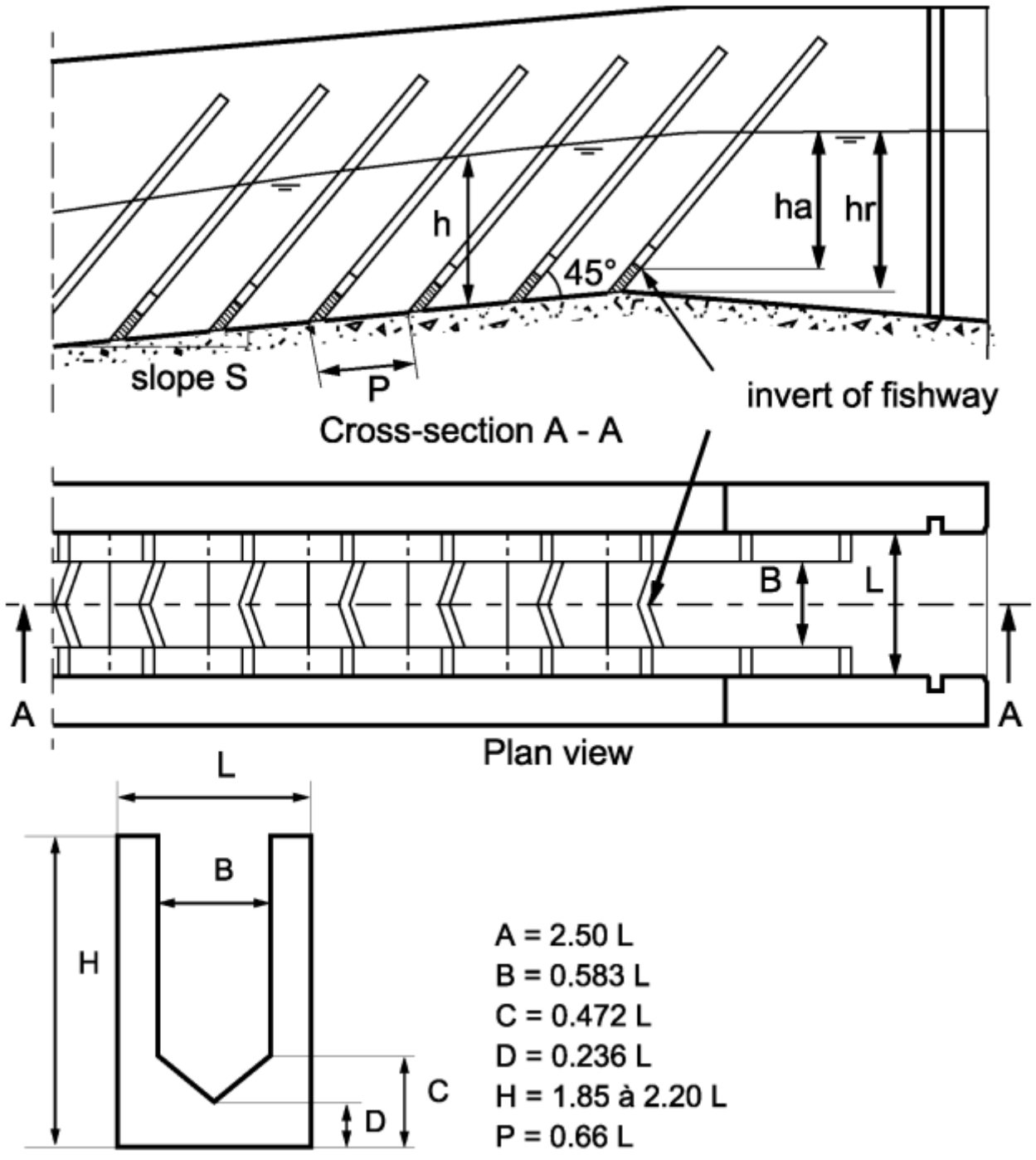

Figure 1: Characteristic parameters of a fishway with plane baffles.

Figure 7.1: Characteristics of a plane baffles (Denil) fishway

$$b_1(S) = -139.382S^2 + 47.2186S + 0.0547598$$

$$b_0(S) = 16.7218S^2 - 6.09624S + 0.834851$$

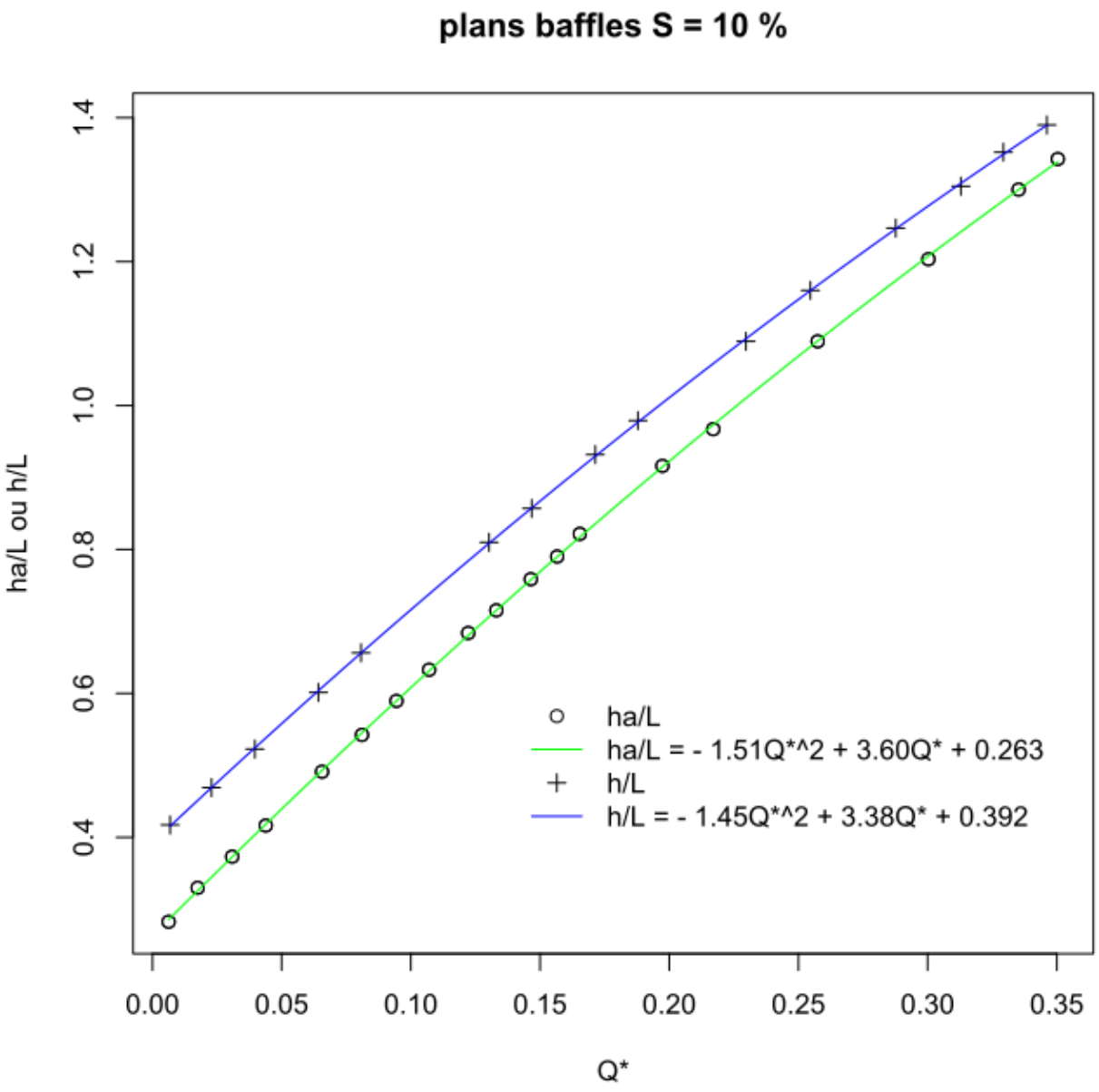

Figure 7.2: Abacuses of a plane baffles (Denil) fishway for a slope of 10%

7.4.3 Calculation of ha, h and Q

We can then use those coefficients to calculate ha, h and Q^*:

$$ha = L\left(a_2(Q^*)^2 + a_1 Q^* + a_0\right)$$

$$h = L\left(b_2(Q^*)^2 + b_1 Q^* + b_0\right)$$

Using the positive inverse function, depending on ha/L, we get:

$$Q^* = \frac{-a_1 + \sqrt{a_1^2 - 4a_2(a_0 - h_a/L)}}{2a_2}$$

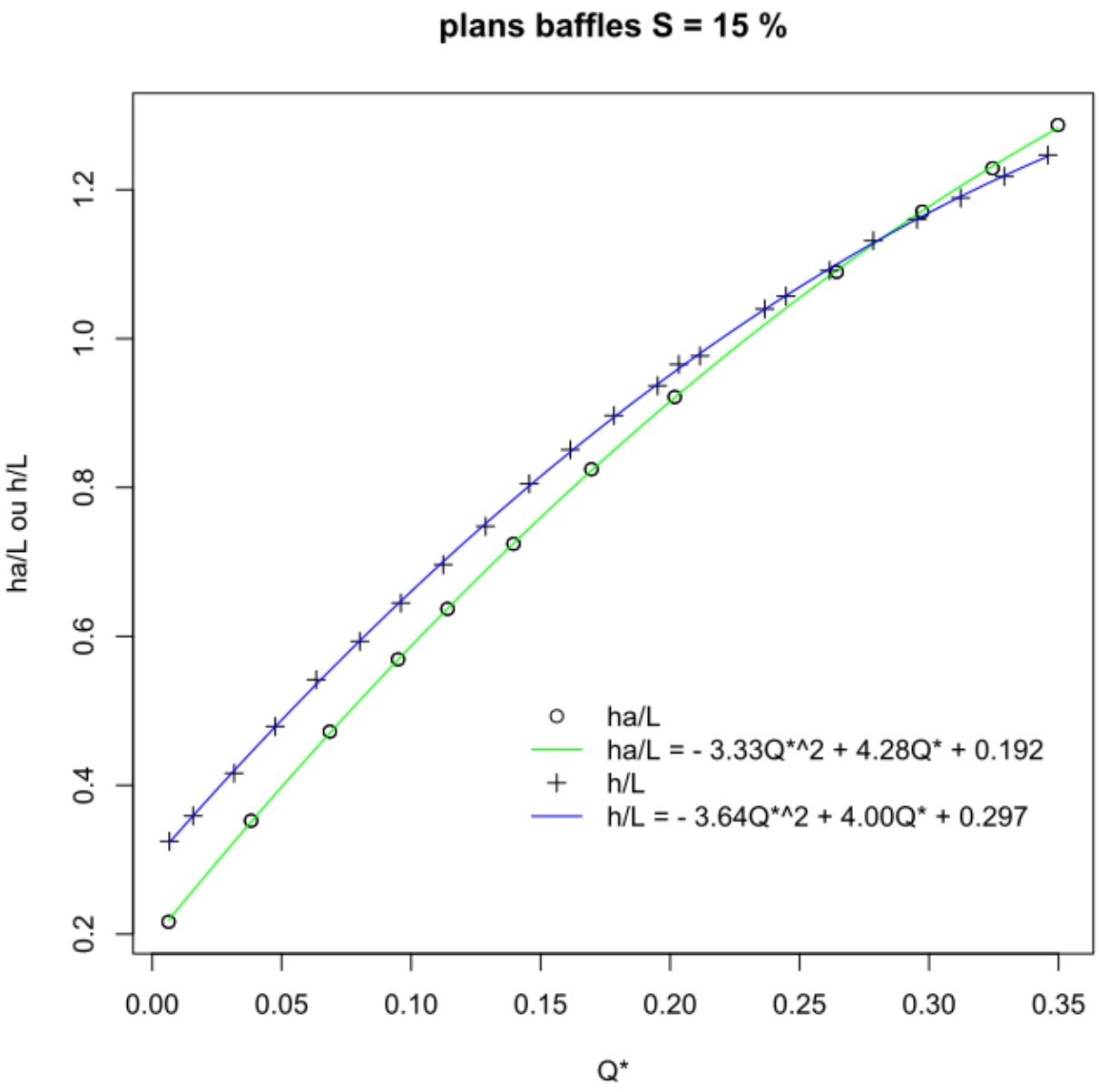

Figure 7.3: Abacuses of a plane baffles (Denil) fishway for a slope of 15%

And we finally have:

$$Q = Q^* \sqrt{g} L^{2,5}$$

Calculation limitations of Q^*, ha/L and h/L are determined based on the extremities of the abacuses curves.

7.4.4 Flow velocity

Flow velocity V corresponds to the minimum flow speed given the flow section A_w at the perpendicular of the baffle :

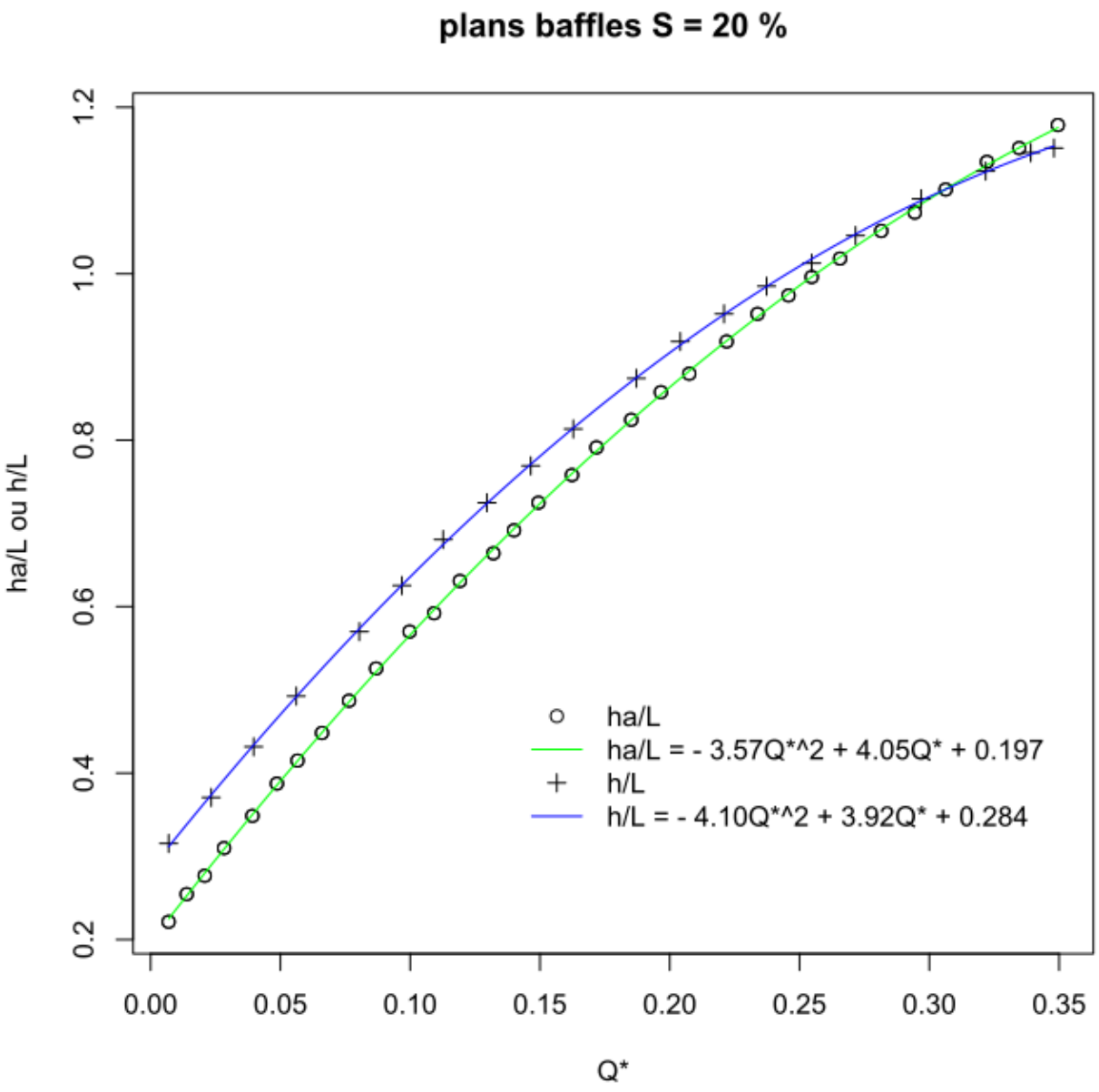

Figure 7.4: Abacuses of a plane baffles (Denil) fishway for a slope of 20%

$$V = \frac{Q}{A_w}$$

for plane baffles fishways using the notation of the schema above, we have:

$$A_w = B \times \left(h - \frac{C+D}{2} \sin(45°) \right)$$

Which gives with standard proportions:

$$A_w = L\,(0.583h - 0.146L)$$

7.4.5 Upstream apron elevation Z_{r1}

$$Z_{r1} = Z_{d1} - D\sin(45° + \arctan(S))$$

7.4.6 Minimal rake height of upstream side walls Z_m

$$Z_m = Z_{r1} + -H_{min}\sin(45° + \arctan(S))$$

7.5 “Fatou” baffle fiwhway

All concepts and formulas are extracted from the following reference:

Larinier, M. 2002. “BAFFLE FISHWAYS.” Bulletin Français de La Pêche et de La Pisciculture, no. 364: 83–101. doi:10.1051/kmae/2002109

7.5.1 Geometrical characteristics

Excerpt from Larinier, 2002

7.5.2 Hydraulic laws given by abacuses

Experiments conducted by Larinier, 2002 allowed to establish abacuses that link adimensional flow Q^*:

$$Q^* = \frac{Q}{\sqrt{g}L^{2,5}}$$

to upstream head ha and the average water level in the pass h :

Abacuses of a Fatou baffle fishway for a slope of 10% (Excerpt from Larinier, 2002)

Abacuses of a Fatou baffle fishway for a slope of 15% (Excerpt from Larinier, 2002)

Abacuses of a Fatou baffle fishway for a slope of 20% (Excerpt from Larinier, 2002)

To run calculations for all slopes between 8% and 22%, polynomes coefficients of abacuses above are themelves adjusted in the form of slope S depending polynomes.

We thus have:

$$ha/L = a_2(S)Q^{*2} + a_1(S)Q^* + a_0(S)$$

$$a_2(S) = -783.592S^2 + 269.991S - 25.2637$$

$$a_1(S) = 302.623S^2 - 106.203S + 13.2957$$

$$a_0(S) = 15.8096S^2 - 5.19282S + 0.465827$$

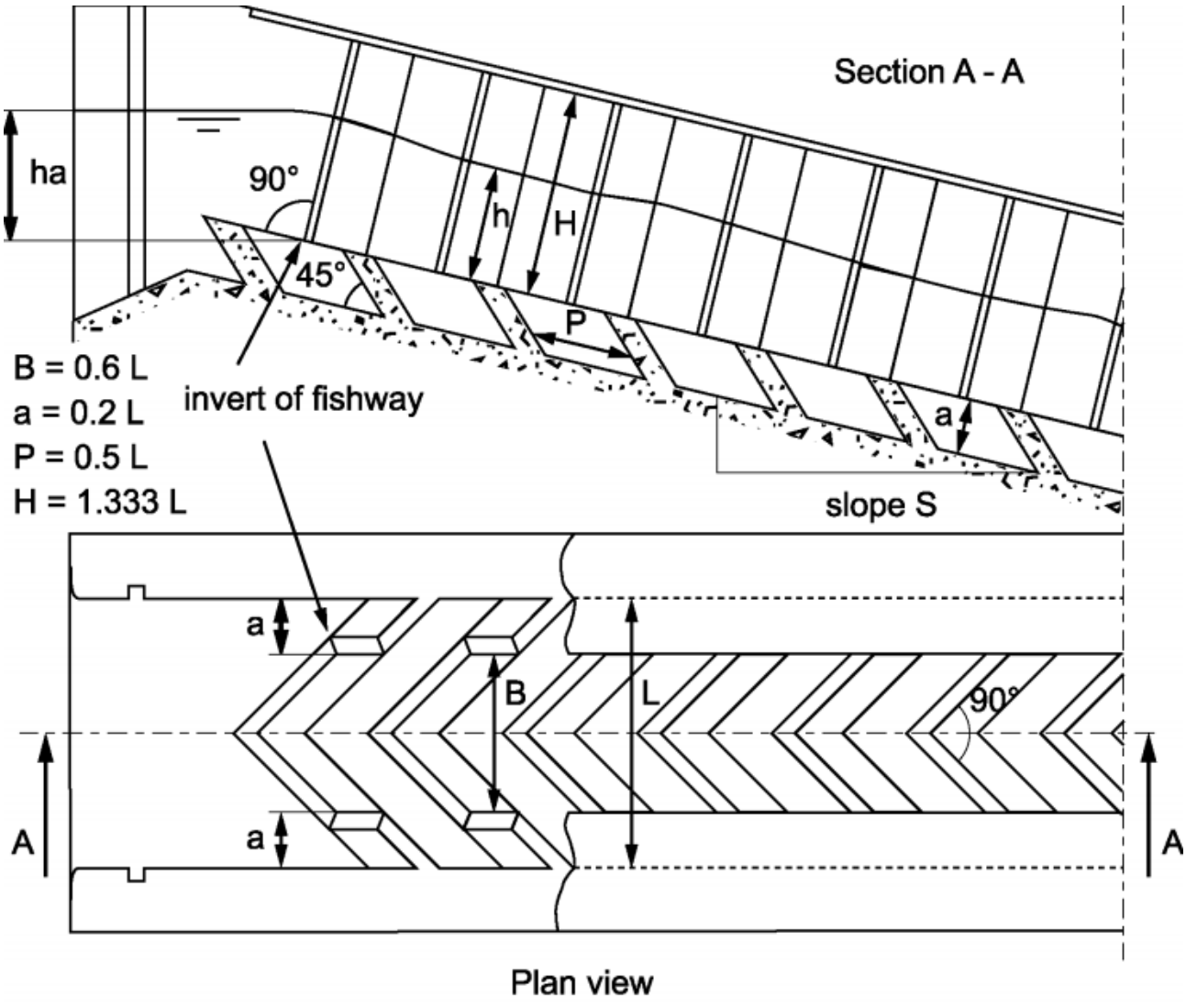

Figure 5: Characteristic parameters of the a fishway with Fatou baffles.

Figure 7.5: Characteristics of a Fatou baffle fishway

And:

$$h/L = b_2(S)Q^{*2} + b_1(S)Q^* + b_0$$

$$b_2(S) = -73.4829S^2 + 54.6733S - 14.0622$$

$$b_1(S) = 42.4113S^2 - 24.4941S + 8.84146$$

$$b_0(S) = -3.56494S^2 + 0.450262S + 0.0407576$$

7.5.3 Calculation of ha, h and Q

We can then use those coefficients to calculate ha, h and Q^*:

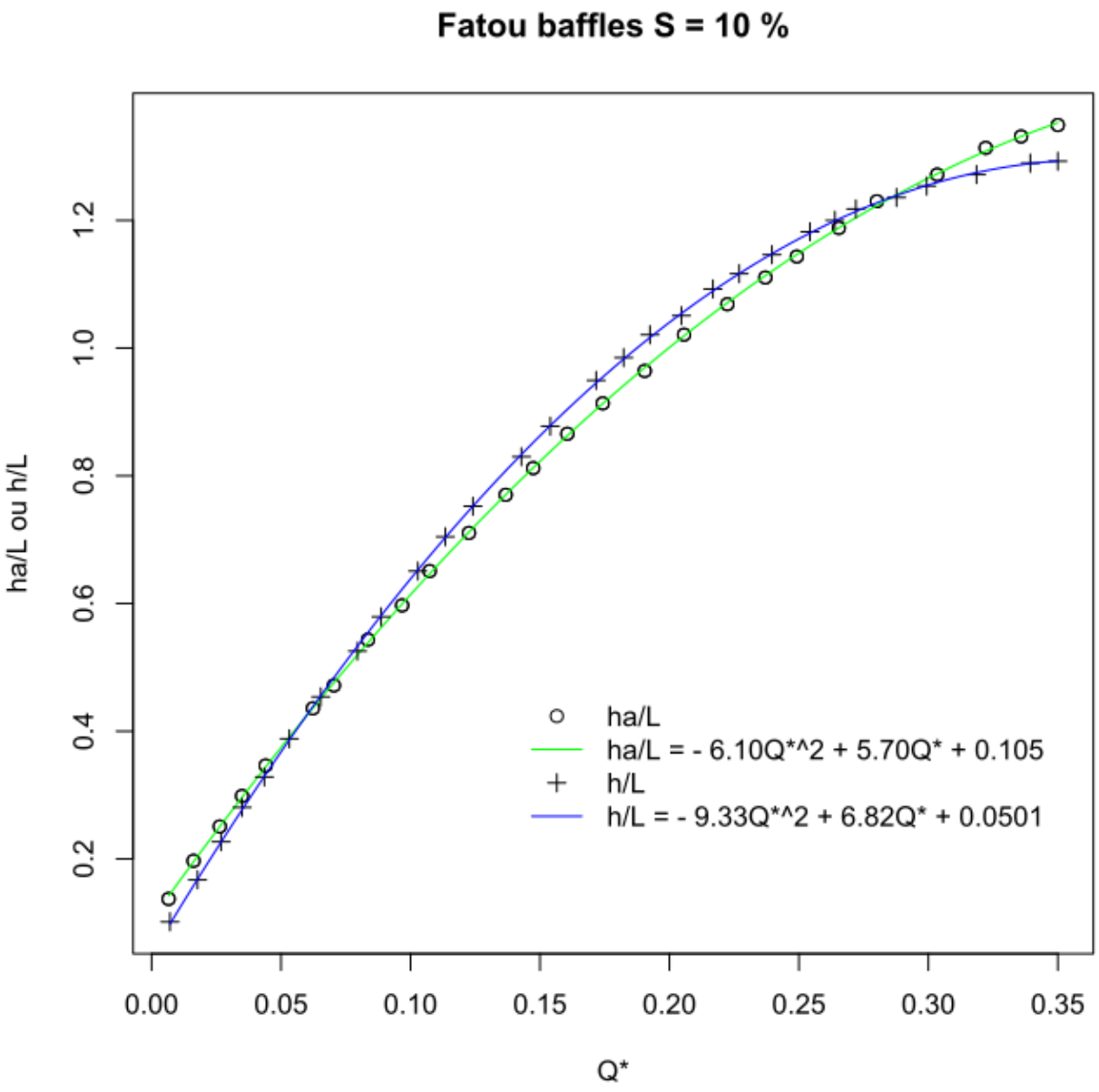

Figure 7.6: Abacuses of a Fatou baffle fishway for a slope of 10%

$$ha = L\left(a_2(Q^*)^2 + a_1 Q^* + a_0\right)$$

$$h = L\left(b_2(Q^*)^2 + b_1 Q^* + b_0\right)$$

Using the positive inverse function, depending on ha/L, we get:

$$Q^* = \frac{-a_1 + \sqrt{a_1^2 - 4a_2(a_0 - h_a/L)}}{2a_2}$$

And we finally have:

$$Q = Q^* \sqrt{g} L^{2,5}$$

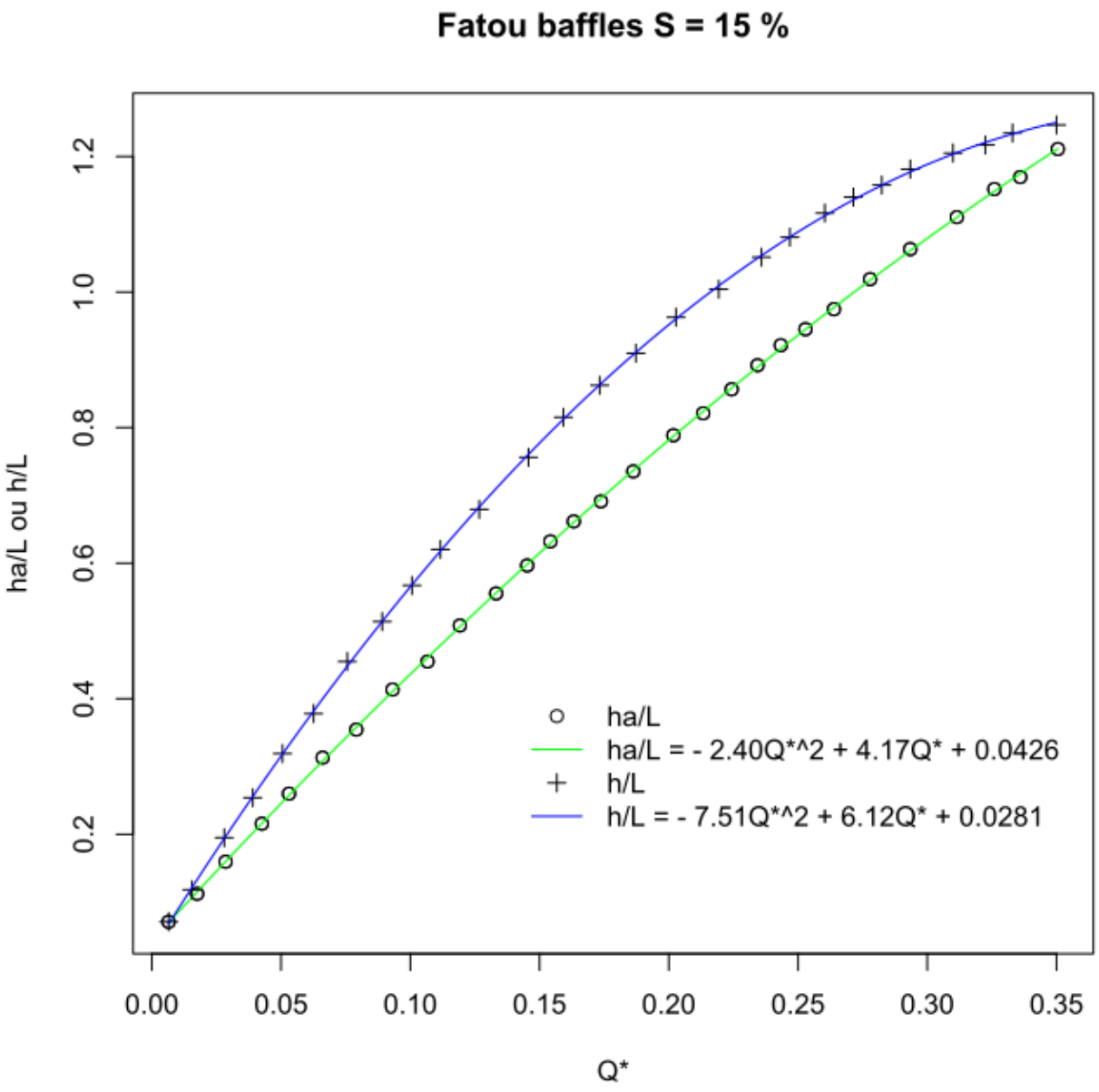

Figure 7.7: Abacuses of a Fatou baffle fishway for a slope of 15%

Calculation limitations of Q^*, ha/L and h/L are determined based on the extremities of the abacuses curves.

7.5.4 Flow velocity

Flow velocity V corresponds to the minimum flow speed given the flow section A_w at the perpendicular of the baffle :

$$V = \frac{Q}{A_w}$$

for Fatou baffle fishways using the notation of the schema above, we have:

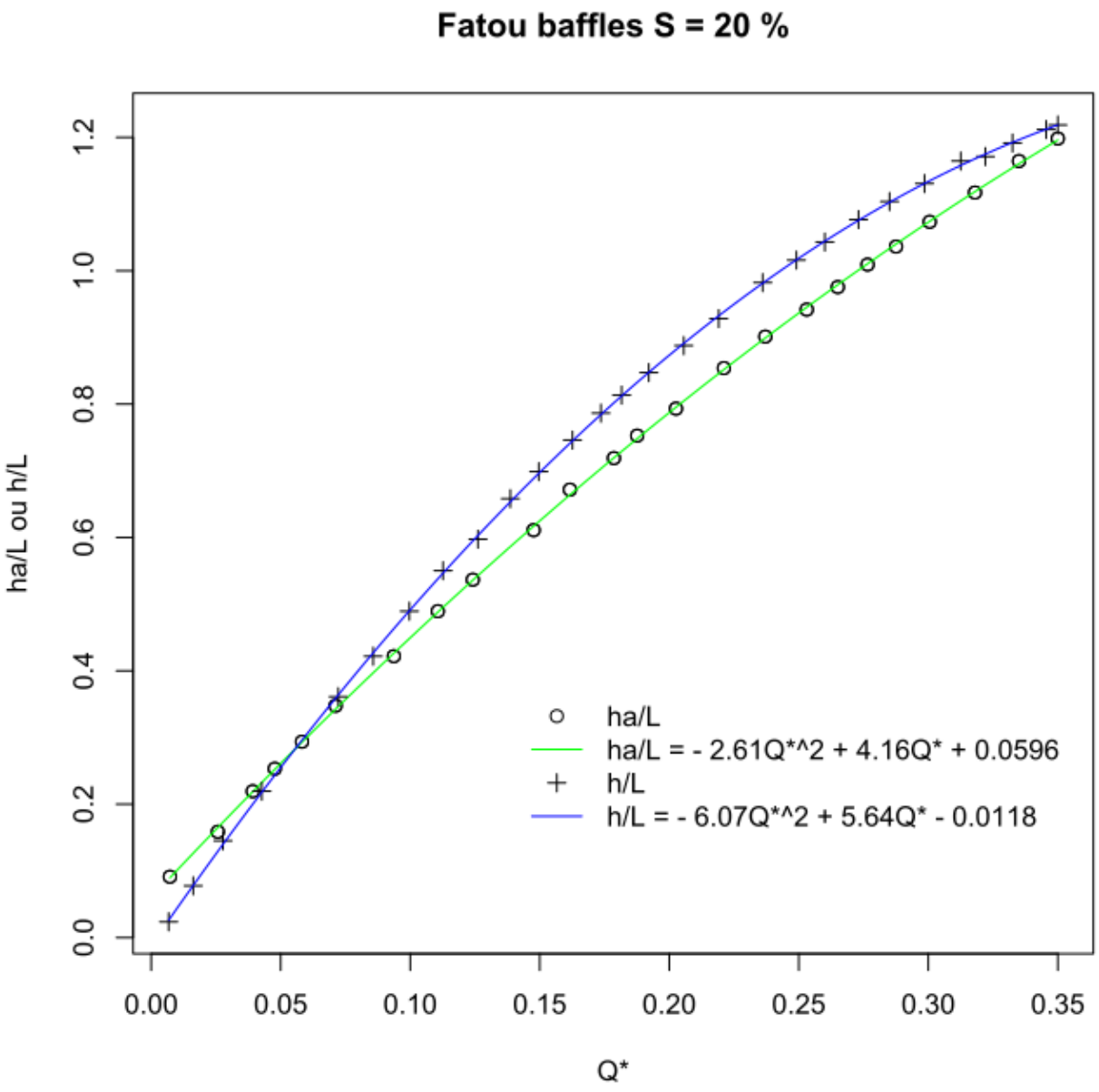

Figure 7.8: Abacuses of a Fatou baffle fishway for a slope of 20%

$$A_w = B \times h$$

Which gives with standard proportions:

$$A_w = 0.6hL$$

7.5.5 Upstream apron elevation Z_{r1}

$$Z_{r1} = Z_{d1} + \frac{0.3S - 0.2}{\sqrt{1+S^2}}$$

7.5.6 Minimal rake height of upstream side walls Z_m

$$Z_m = Z_{r1} + \frac{4L}{3\sqrt{1+S^2}}$$

7.6 Superactive baffles fishway

All concepts and formulas are extracted from the following reference:

Larinier, M. 2002. “BAFFLE FISHWAYS.” Bulletin Français de La Pêche et de La Pisciculture, no. 364: 83–101. doi:10.1051/kmae/2002109

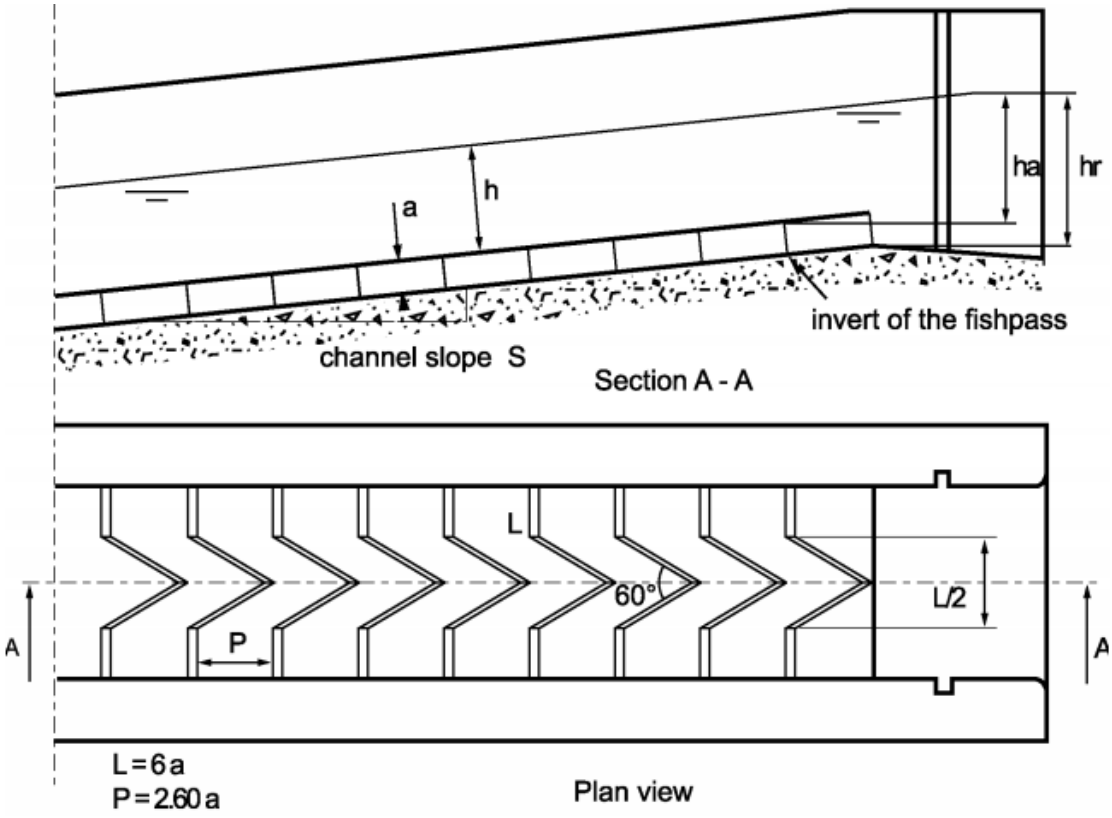

Figure 9: Characteristic parameters of a fishway with super-active-type bottom baffles.

Figure 7.9: Characteristics of a superactive baffles fishway

Excerpt from Larinier, 2002

7.6.1 Hydraulic laws given by abacuses

Experiments conducted by Larinier, 2002 allowed to establish abacuses that link adimensional flow q^* :

$$q^* = \frac{Q/L}{\sqrt{2g}a^{1,5}}$$

to upstream head ha and the average water level in the pass h :

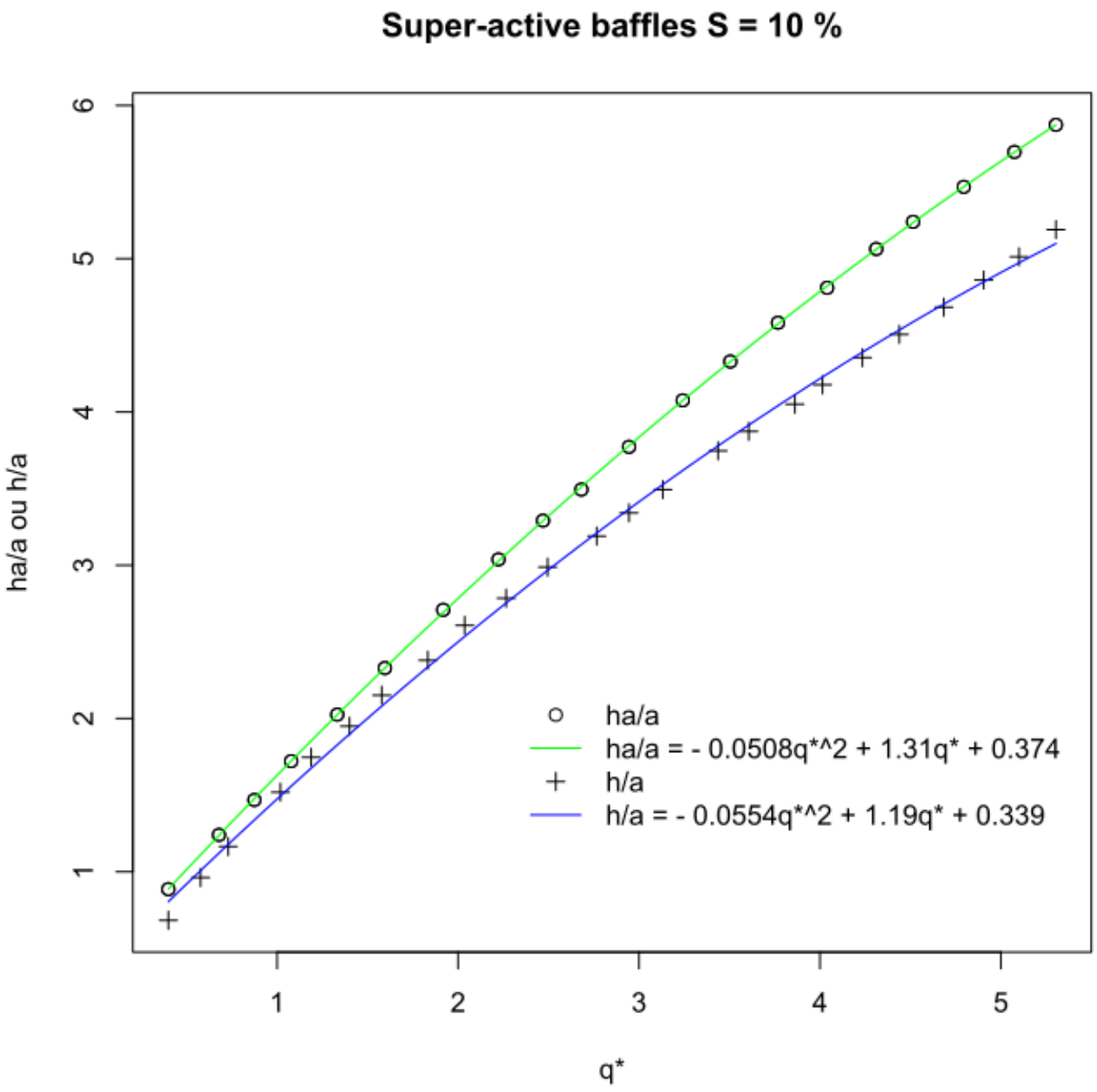

Figure 7.10: Abacuses of a superactive baffles fishway for a slope of 10%

Abacuses of a superactive baffles fishway for a slope of 10% (Excerpt from Larinier, 2002)

Abacuses of a superactive baffles fishway for a slope of 15% (Excerpt from Larinier, 2002)

To run calculations for all slopes between 8% and 22%, polynomes coefficients of abacuses above are themelves adjusted in the form of slope S depending polynomes.

We thus have:

$$ha/a = a_2(S)q^{*2} + a_1(S)q^* + a_0(S)$$

$$a_2(S) = -0.354624S - 0.0153156$$

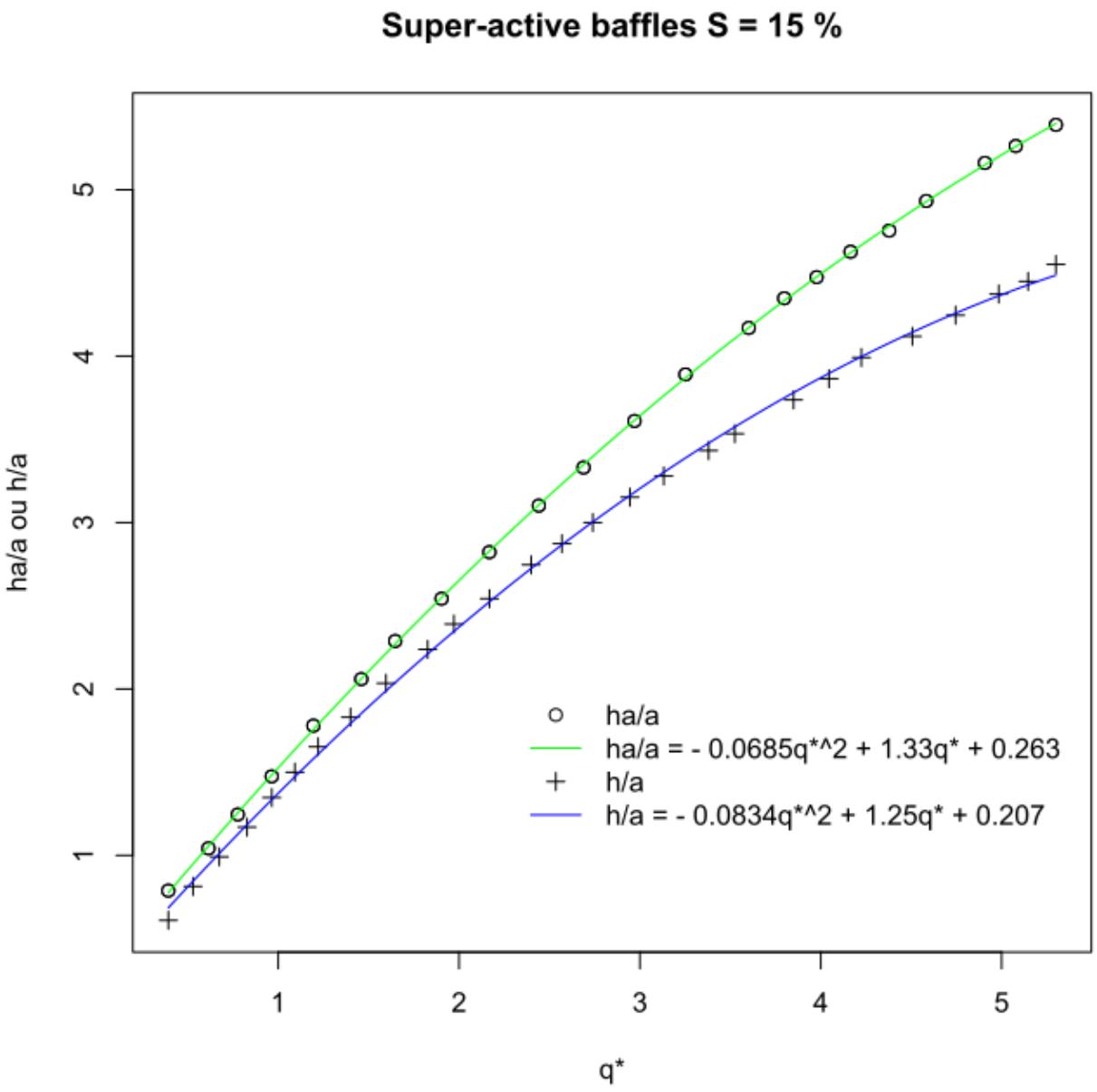

Figure 7.11: Abacuses of a superactive baffles fishway for a slope of 15%

$$a_1(S) = 0.514953S + 1.25460$$

$$a_0(S) = -2.22434S + 0.596682$$

And:

$$h/a = b_2(S)q^{*2} + b_1(S)q^* + b_0$$

$$b_2(S) = -0.559218S + 0.000504060$$

$$b_1(S) = 1.15807S + 1.07554$$

$$b_0(S) = -2.62712S + 0.601348$$

7.6.2 Calculation of ha, h and Q

We can then use those coefficients to calculate ha, h and q^*:

$$ha = a\left(a_2(q^*)^2 + a_1 q^* + a_0\right)$$

$$h = a\left(b_2(q^*)^2 + b_1 q^* + b_0\right)$$

Using the positive inverse function, depending on ha/L, we get:

$$q^* = \frac{-a_1 + \sqrt{a_1^2 - 4a_2(a_0 - h_a/a)}}{2a_2}$$

And we finally have:

$$Q = Lq^*\sqrt{g}a^{1,5}$$

Calculation limitations of q^*, ha/a and h/a are determined based on the extremities of the abacuses curves.

7.6.3 Flow velocity

Flow velocity V corresponds to the minimum flow speed given the flow section A_w at the perpendicular of the baffle :

$$V = \frac{Q}{A_w}$$

for superactive baffles fishways using the notation of the schema above, we have:

$$A_w = h \times L$$

7.6.4 Upstream apron elevation Z_{r1}

$$Z_{r1} = Z_{d1} + \frac{2.6aS - a}{\sqrt{1 + S^2}}$$

7.7 Mixed / chevron baffles fishway

All concepts and formulas are extracted from the following reference:

Larinier, M. 2002. “BAFFLE FISHWAYS.” Bulletin Français de La Pêche et de La Pisciculture, no. 364: 83–101. doi:10.1051/kmae/2002109

Excerpt from Larinier, 2002

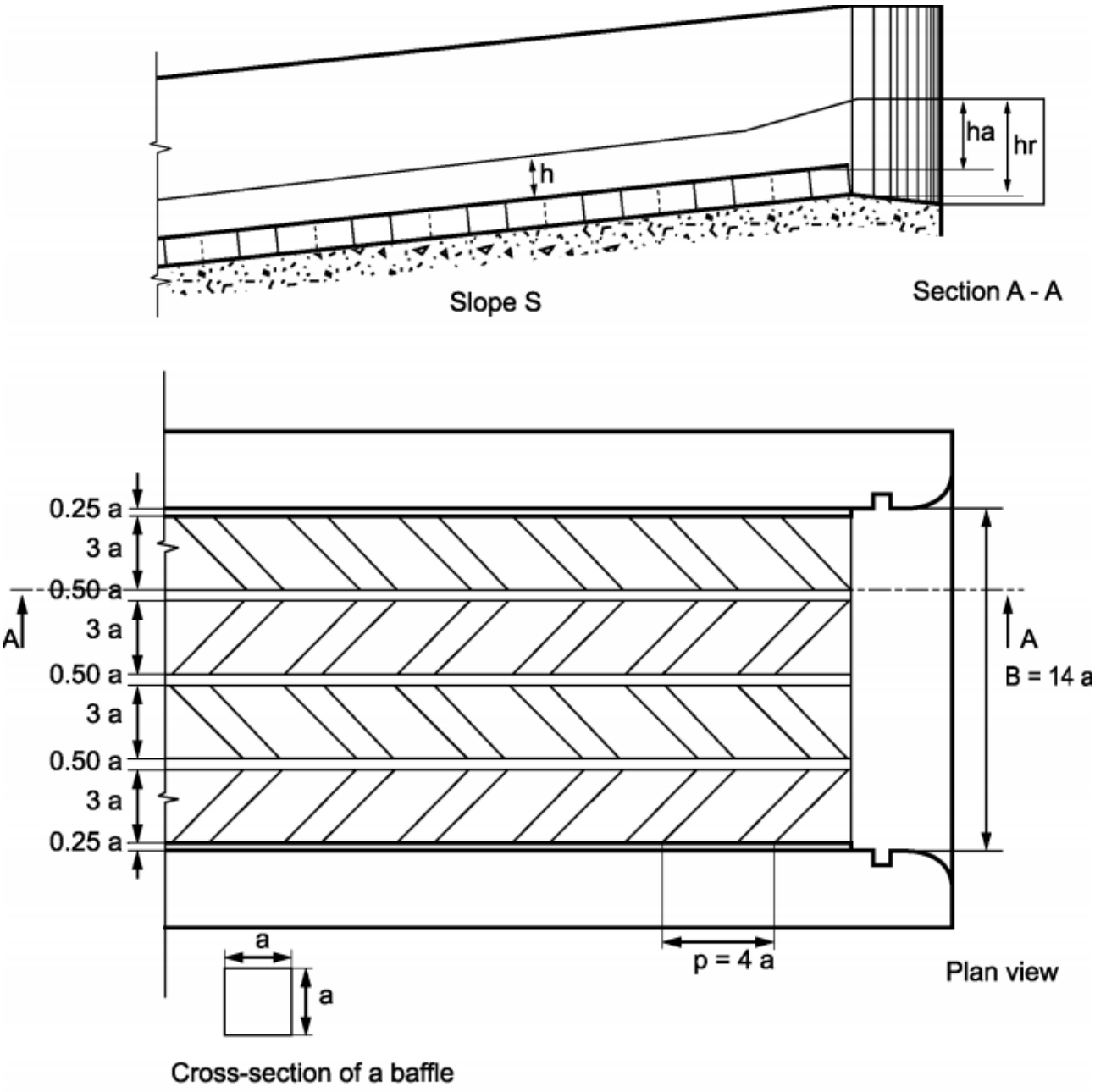

Figure 13: Characteristic parameters of a chevron baffle fishway.

Figure 7.12: Characteristics of a mixed / chevron baffles fishway

7.7.1 Hydraulic laws given by abacuses

Experiments conducted by Larinier, 2002 allowed to establish abacuses that link adimensional flow q^* :

$$q^* = \frac{Q/L}{\sqrt{2g}a^{1,5}}$$

to upstream head ha and the average water level in the pass h :

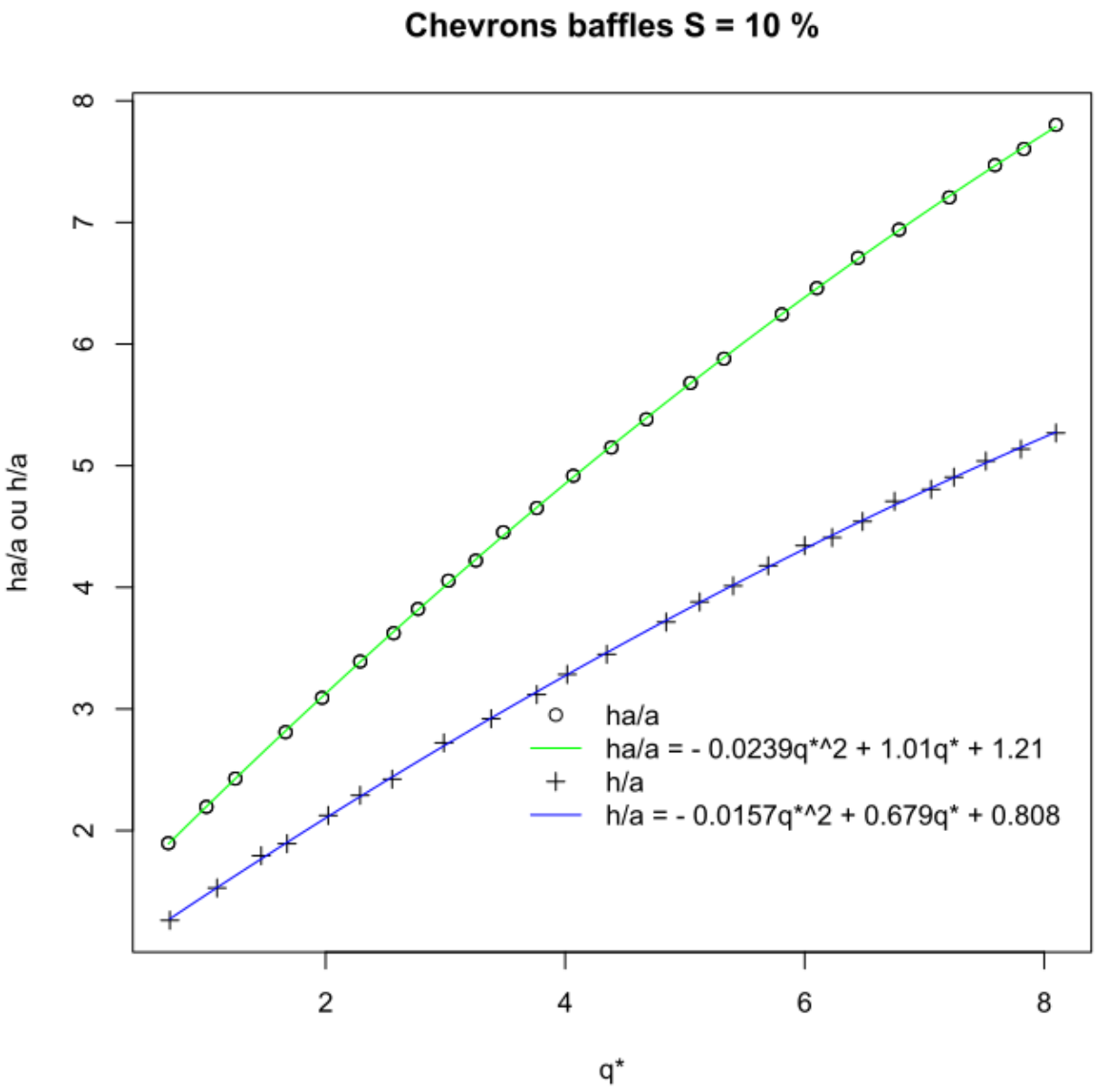

Figure 7.13: Abacuses of a mixed / chevron baffles fishway for a slope of 10%

Abacuses of a mixed / chevron baffles fishway for a slope of 10% (Excerpt from Larinier, 2002)

Abacuses of a mixed / chevron baffles fishway for a slope of 15% (Excerpt from Larinier, 2002)

To run calculations for all slopes between 8% and 22%, polynomes coefficients of abacuses above are themelves adjusted in the form of slope S depending polynomes.

We thus have:

$$ha/a = a_2(S)q^{*2} + a_1(S)q^* + a_0(S)$$

$$a_2(S) = 0.188324S - 0.0427461$$

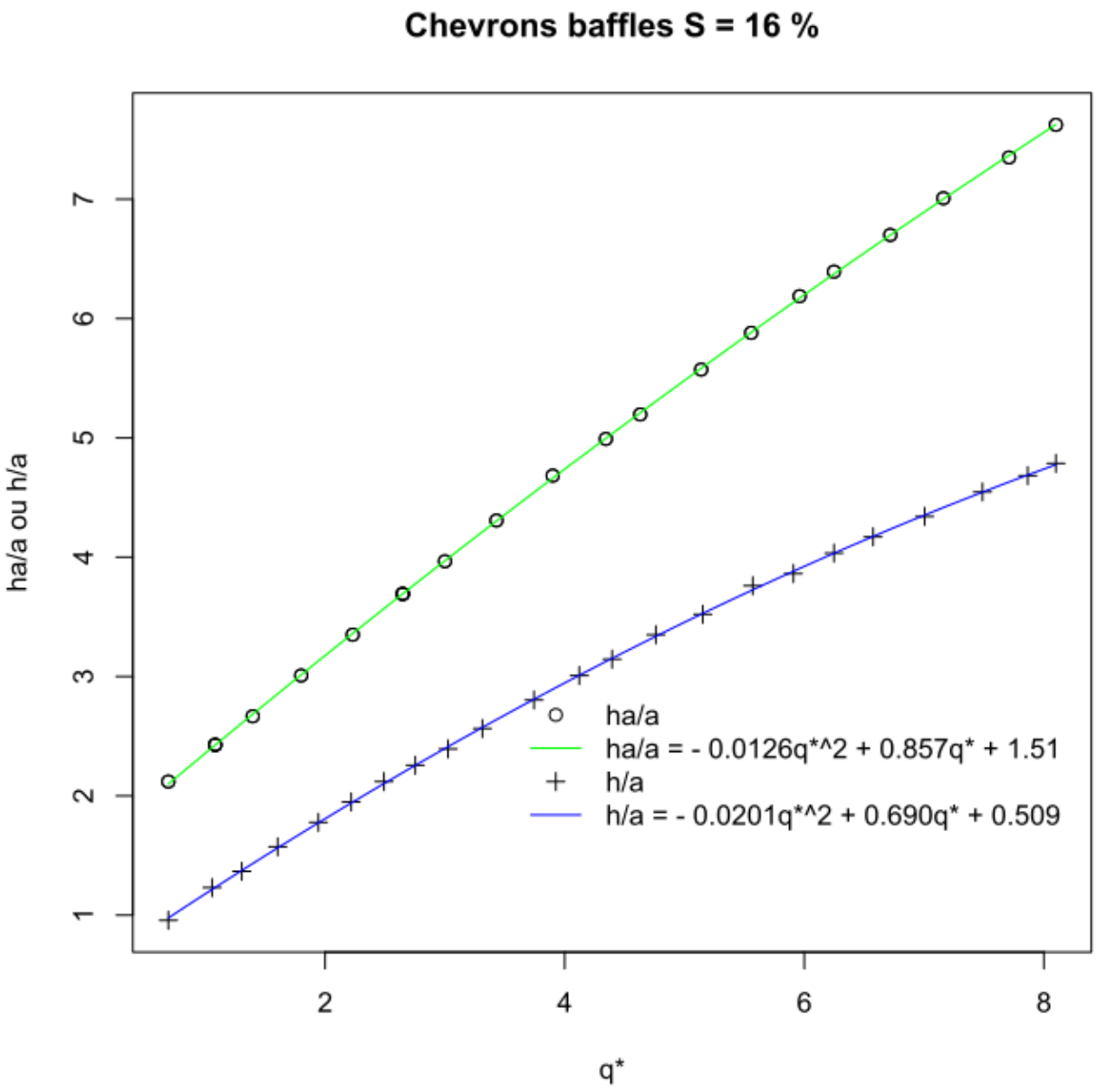

Figure 7.14: Abacuses of a mixed / chevron baffles fishway for a slope of 16%

$$a_1(S) = -2.47998S + 1.25363$$

$$a_0(S) = 5.02138S + 0.709434$$

And:

$$h/a = b_2(S)q^{*2} + b_1(S)q^* + b_0$$

$$b_2(S) = -0.0733832S - 0.00839864$$

$$b_1(S) = 0.176261S + 0.661656$$

$$b_0(S) = -4.97686S + 1.30546$$

7.7.2 Calculation of ha, h and Q

We can then use those coefficients to calculate ha, h and q^*:

$$ha = a\left(a_2(q^*)^2 + a_1 q^* + a_0\right)$$

$$h = a\left(b_2(q^*)^2 + b_1 q^* + b_0\right)$$

Using the positive inverse function, depending on ha/L, we get:

$$q^* = \frac{-a_1 + \sqrt{a_1^2 - 4a_2(a_0 - h_a/a)}}{2a_2}$$

And we finally have:

$$Q = Lq^*\sqrt{g}a^{1,5}$$

Calculation limitations of q^*, ha/a and h/a are determined based on the extremities of the abacuses curves.

7.7.3 Flow velocity

Flow velocity V corresponds to the minimum flow speed given the flow section A_w at the perpendicular of the baffle :

$$V = \frac{Q}{A_w}$$

for mixed / chevron baffles fishways using the notation of the schema above, we have:

$$A_w = h \times L$$

7.7.4 Upstream apron elevation Z_{r1}

$$Z_{r1} = Z_{d1} + \frac{3aS - a}{\sqrt{1 + S^2}}$$

8 Crossability verification

8.1 Crossability verification

8.1.1 Warning

The purpose of this tool is to carry out a simple check of the compatibility between certain fish pass sizing criteria and the passage capacities of the target fish species. It may prove useful during the design phase of a facility to ensure that the proposed design is consistent with its hydrological operating range.

However, this tool is not sufficient to fully verify the functionality of a planned or existing system, insofar as other important dimensional and hydraulic criteria are not taken into account by this module (feed flow rate and characteristics of the fish intake in terms of attractiveness, and depending on the type of system: basin aspect ratio, concentration of macro-roughness, bottom roughness, size of baffles, etc.).

This module allows to verify the capacity of different fish species to cross the following types of fish passes:

- fish ladders
- baffle fishways
- rock-ramp fishpasses

8.1.2 Principle

For each pass type, several crossability criteria are checked, expressed as threshold values (ex: minimal basin depth, for a fish ladder).

Exceeding the threshold value of a criterion leads to an explicit error mentioning the quantity concerned and the threshold value, and results in the pass not being crossable.

Some criteria such as maximal dissipated power have both an alert value (crossability is possible but not guaranteed) and a limit value (crossing the pass is impossible).

For a given pass, one can check at once the crossing capabilities of several species, over multiple modalities (variation of one or more parameters in the pass).

8.1.3 Predefined species

Several common species groups are predefined: default values are associated to crossability criteria.

Default values for some of those criteria might be missing for a species group, when the latter is considered unabled to cross the pass type the criterion is related to.

8.1.4 Custom species

The `Fish species characteristics` module allows to define custom values for all criteria, before running a pass verification.

If a criterion is applicable to the pass that is being checked, but no value was given, an error will be triggered when running the verification, leading to the pass being not crossable.

8.2 Crossability verification: Fish ladders

When verifying a fish ladder, basins and walls are sequentially tested, as well as every device of each wall. If at least one basin is not crossable, then the pass is not crossable.

Criteria differ depending on the jet type generated by the device being verified. If a wall has several devices, it will be considered crossable if at least one device is crossable.

Orifices are considered uncrossable.

For certain species, values of certain criteria are not precisely known or are subject to slight changes depending on future feedback.

8.2.1 Criteria

8.2.1.1 Diving jet support

Some species do not support diving jets. For such species, each device leading to a diving jet is marked as not crossable.

8.2.1.2 Maximum fall, in m

Basin fall must be lower than maximum fall.

8.2.1.3 Minimum slot width, in m (surface jet only)

Slot width must be greater than minimum width.

8.2.1.4 Minimum orifice surface, in m²

Orifice surface must be greater than minimum slot width (above), squared.

8.2.1.5 Minimum head on weir, in m

Head on weir must be greater than minimum head.

8.2.1.6 Minimum basin depth, in m

Basin depth must be greater than minimum depth. For diving jets, depth must be greater than twice the basin fall.

8.2.1.7 Minimum basin length, in m

Basin length must be greater than minimum length.

8.2.1.8 Recommanded maximum dissipated power and limit maximum dissipated power, in W/m³

Maximal dissipated power in the basin must be lower than limit maximum dissipated power. If it is greater than recommanded maximum dissipated power, a warning is thrown.

Important: maximum dissipated power verification is **disabled** in the current Cassiopée version.

8.2.2 Criteria values for predefined species groups

From *"Informations sur la Continuité Écologique - ICE, Onema 2014"*, and et OFB com. pers.

8.2.2.1 Common values for surface jet and diving jet

Table 8.1: List of predefined values for crossing criteria of a fish ladder

ICE group	Species	Minimum head on weir (m)	Recommanded maximum dissipated power (W/m³)	Limit maximum dissipated power (W/m³)
1	Atlantic salmon (Salmo salar)Sea or river trout [50-100] (Salmo trutta)	0.3	200	250
2	Mules (Chelon labrosus, Liza ramada)	0.2	200	250
3a	Gread shad (Alosa alosa)	0.4	150	200
3b	Shad (Alosa fallax fallax)	0.4	150	200
3c	Sea lamprey (Petromyzon marinus)	0.15	200	250
4a	River trout or sea trout [25-55] (Salmo trutta)	0.2	200	250
4b	River trout [15-30] (Salmo trutta)	0.2	200	250

ICE group	Species	Minimum head on weir (m)	Recommanded maximum dissipated power (W/m³)	Limit maximum dissipated power (W/m³)
5	Aspe (Aspius aspius)Pike (Esox lucius)	0.2	150	200
6	Common grayling (Thymallus thymallus)	0.2	200	250
7a	Common barbel (Barbus barbus)Chub (Squalius cephalus)Nase (Chondros-toma nasus)	0.2	150	200
7b	River lamprey (Lampetra fluviatilis)	0.15	130	150
8a	Common carp (Cyprinus carpio)	0.2	-	-
8b	Common bream (Abramis brama)Pike-perch (Sander lucioperca)	0.2	150	200
8c	White bream (Blicca bjoerkna)Ide (Leuciscus idus)Burbot (Lota lota)Perch (Perca fluviatilis)Tench (Tinca tinca)	0.2	130	150
8d	Common dace (Leuciscus sp but Idus)	0.2	150	200

ICE group	Species	Minimum head on weir (m)	Recommanded maximum dissipated power (W/m³)	Limit maximum dissipated power (W/m³)
9a	Bleak (Alburnus alburnus)Sprirlin (Alburnoides bipunctatus)Mediterranean barbel (Barbus meridionalis)Souffia (Telestes souffia)Crucian carp (Carassius carassius)Prussian carp (Carassius gibelio)Roach (Rutilus rutilus)Common rudd (Scardinius erythrophthalmus)South-west european nase (Parachondrostoma toxostoma)	0.2	130	150
9b	Apron (Zingel asper)Cottus spGobio spRuffe (Gymnocephalus cernuus)Brook lamprey (Lampetra planeri)Stone loach (Barbatula barbatula)Spined loach (Cobitis taenia)	0.2	130	150

ICE group	Species	Minimum head on weir (m)	Recommanded maximum dissipated power (W/m³)	Limit maximum dissipated power (W/m³)
10	Sunbleak (Leucaspius delinea-tus)European bitterling (Rhodeus amarus)Three-spined stickleback (Gasterosteus gymnu-rus)Ninespine stickleback (Pungitius laevis)Minnows (Phoxinus sp)	0.2	100	150

8.2.2.2 Surface jet

Table 8.2: List of predefined values for crossing criteria of a fish ladder, with surface jet

ICE group	Species	Maximum fall (m)	Minimum slot width (m)	Minimum basin depth (m)	Minimum basin length (m)
1	Atlantic salmon (Salmo salar)Sea or river trout [50-100] (Salmo trutta)	0.35	0.3	1	2.5
2	Mules (Chelon labrosus, Liza ramada)	0.35	0.2	1	1.75
3a	Gread shad (Alosa alosa)	0.3	0.4	1	3.5

ICE group	Species	Maximum fall (m)	Minimum slot width (m)	Minimum basin depth (m)	Minimum basin length (m)
3b	Shad (Alosa fallax fallax)	0.3	0.4	1	3.5
3c	Sea lamprey (Petromyzon marinus)	0.3	0.15	1	1.25
4a	River trout or sea trout [25-55] (Salmo trutta)	0.35	0.2	1	1.75
4b	River trout [15-30] (Salmo trutta)	0.3	0.15	0.75	1.75
5	Aspe (Aspius aspius)Pike (Esox lucius)	0.3	0.3	0.75	2.5
6	Common grayling (Thymallus thymallus)	0.3	0.2	0.75	1.75
7a	Common barbel (Barbus barbus)Chub (Squalius cephalus)Nase (Chondrostoma nasus)	0.3	0.25	0.75	2
7b	River lamprey (Lampetra fluviatilis)	0.3	0.15	0.75	1.25
8a	Common carp (Cyprinus carpio)	0.25	0.3	0.75	2.5

ICE group	Species	Maximum fall (m)	Minimum slot width (m)	Minimum basin depth (m)	Minimum basin length (m)
8b	Common bream (Abramis brama)Pike-perch (Sander lucioperca)	0.25	0.3	0.75	2.5
8c	White bream (Blicca bjoerkna)Ide (Leuciscus idus)Burbot (Lota lota)Perch (Perca fluviatilis)Tench (Tinca tinca)	0.25	0.3	0.75	2.5
8d	Common dace (Leuciscus sp but Idus)	0.25	0.3	0.75	2.5

ICE group	Species	Maximum fall (m)	Minimum slot width (m)	Minimum basin depth (m)	Minimum basin length (m)
9a	Bleak (Alburnus alburnus)Sprirlin (Alburnoides bipunctatus)Mediterranean barbel (Barbus meridionalis)Souffia (Telestes soufffia)Crucian carp (Carassius carassius)Prussian carp (Carassius gibelio)Roach (Rutilus rutilus)Common rudd (Scardinius erythrophthalmus)Southwest european nase (Parachondrostoma toxostoma)	0.25	0.25	0.75	2

ICE group	Species	Maximum fall (m)	Minimum slot width (m)	Minimum basin depth (m)	Minimum basin length (m)
9b	Apron (Zingel asper)Cottus spGobio spRuffe (Gymnocephalus cernuus)Brook lamprey (Lampetra planeri)Stone loach (Barbatula barbatula)Spined loach (Cobitis taenia)	0.2	0.15	0.5	1.25
10	Sunbleak (Leucaspius delineatus)European bitterling (Rhodeus amarus)Three-spined stickleback (Gasterosteus gymnurus)Ninespine stickleback (Pungitius laevis)Minnows (Phoxinus sp)	0.2	0.15	0.5	1.25

8.2.2.3 Diving jet

Table 8.3: List of predefined values for crossing criteria of a fish ladder, with diving jet

ICE Group	Species	Maximum fall (m)	Minimum basin depth (m)	Minimum basin length (m)
1	Atlantic salmon (Salmo salar)Sea or river trout [50-100] (Salmo trutta)	0.75	1	2
2	Mules (Chelon labrosus, Liza ramada)	0.6	0.75	1.25
4a	River trout or sea trout [25-55] (Salmo trutta)	0.4	0.75	1.25
4b	River trout [15-30] (Salmo trutta)	0.3	0.75	1
6	Common grayling (Thymallus thymallus)	0.3	0.75	1

8.3 Crossability verification: Baffle fishways (simulation)

For certain species, values of certain criteria are not precisely known or are subject to slight changes depending on future feedback.

8.3.1 Criteria

8.3.1.1 Incompatible and discouraged species

Species groups 3a, 3b and 7b are discouraged for crossing baffle fishways. This leads to a warning, but does not make the pass not crossable.

Species groups 8a, 8b, 8c, 8d, 9a, 9b and 10 are unable to cross baffle fishways.

8.3.1.2 Minimum water level, in m

Water level in the pass must be greater than the minimum water level.

8.3.2 Criteria values for predefined species groups

From *“Informations sur la Continuité Écologique - ICE, Onema 2014”*.

Table 8.4: List of predefined values for crossing criteria of a baffle fishway

ICE group	Species	Minimum water level on plane and Fatou baffles (m)	Minimum water level on superactive and chevron baffles (m)
1	Atlantic salmon (Salmo salar)Sea or river trout [50-100] (Salmo trutta)	0.3	0.2
2	Mules (Chelon labrosus, Liza ramada)	0.25	0.15
3a	Gread shad (Alosa alosa)	0.3	0.2
3b	Shad (Alosa fallax fallax)	0.25	0.15
3c	Sea lamprey (Petromyzon marinus)	0.1	0.1
4a	River trout or sea trout [25-55] (Salmo trutta)	0.25	0.15
4b	River trout [15-30] (Salmo trutta)	0.2	0.1
5	Aspe (Aspius aspius)Pike (Esox lucius)	0.3	0.2
6	Common grayling (Thymallus thymallus)	0.25	0.15
7a	Common barbel (Barbus barbus)Chub (Squalius cephalus)Nase (Chondrostoma nasus)	0.25	0.15
7b	River lamprey (Lampetra fluviatilis)	0.1	0.1

8.4 Crossability verification: Rock-ramp fishpasses

8.4.1 Compound rock-ramp fishpasses

In the case of compound rock-ramp fishpasses, each apron (reminder: inclined apron are discretised) is verified like an independent rock-ramp fishpass.

If at least one apron is crossable, the pass is considered crossable.

Maximum crossable width, wich is the maximum of the sums of the widths of contiguous crossable aprons, is given at the end of the verification.

For certain species, values of certain criteria are not precisely known or are subject to slight changes depending on future feedback.

8.4.2 Criteria

8.4.2.1 Minimum water level, in m

Water level in the pass should be greater than minimum water level.

8.4.2.2 Limit maximum flow velocity, in m/s

Maximum flow velocity in the pass should be lower than limit maximum flow velocity.

8.4.3 Criteria values for predefined species groups

From *"Informations sur la Continuité Écologique - ICE, Onema 2014"*.

Table 8.5: List of predefined values for crossing criteria of a rock-ramp fishpass

ICE group	Species	Minimum water level (m)	Limit maximum flow velocity (m/s)
1	Atlantic salmon (Salmo salar)Sea or river trout [50-100] (Salmo trutta)	0.4	2.5
2	Mules (Chelon labrosus, Liza ramada)	0.3	2.5
3a	Gread shad (Alosa alosa)	0.4	2
3b	Shad (Alosa fallax fallax)	0.4	2
3c	Sea lamprey (Petromyzon marinus)	0.15	2
4a	River trout or sea trout [25-55] (Salmo trutta)	0.3	2

ICE group	Species	Minimum water level (m)	Limit maximum flow velocity (m/s)
4b	River trout [15-30] (Salmo trutta)	0.2	2
5	Aspe (Aspius aspius)Pike (Esox lucius)	0.3	2
6	Common grayling (Thymallus thymallus)	0.3	2
7a	Common barbel (Barbus barbus)Chub (Squalius cephalus)Nase (Chondrostoma nasus)	0.3	2
7b	River lamprey (Lampetra fluviatilis)	0.15	2
8a	Common carp (Cyprinus carpio)	0.3	1.5
8b	Common bream (Abramis brama)Pike-perch (Sander lucioperca)	0.3	1.5
8c	White bream (Blicca bjoerkna)Ide (Leuciscus idus)Burbot (Lota lota)Perch (Perca fluviatilis)Tench (Tinca tinca)	0.3	1.5
8d	Common dace (Leuciscus sp but Idus)	0.3	1.5

ICE group	Species	Minimum water level (m)	Limit maximum flow velocity (m/s)
9a	Bleak (Alburnus alburnus)Sprirlin (Alburnoides bipuncta-tus)Mediterranean barbel (Barbus meridion-alis)Souffia (Telestes souffia)Crucian carp (Carassius caras-sius)Prussian carp (Carassius gibelio)Roach (Rutilus rutilus)Common rudd (Scardinius erythrophthalmus)South-west european nase (Parachon-drostoma toxostoma)	0.2	1.5
9b	Apron (Zingel asper)Cottus spGobio spRuffe (Gymnocephalus cernuus)Brook lamprey (Lampetra planeri)Stone loach (Barbatula barbatula)Spined loach (Cobitis taenia)	0.2	1.5

ICE group	Species	Minimum water level (m)	Limit maximum flow velocity (m/s)
10	Sunbleak (Leucaspius delineatus)European bitterling (Rhodeus amarus)Three-spined stickleback (Gasterosteus gymnurus)Ninespine stickleback (Pungitius laevis)Minnows (Phoxinus sp)	0.2	1.5

8.5 Crossability verification: Predefined species

From *“Informations sur la Continuité Écologique - ICE, Onema 2014”*.

Table 8.6: List of predefined group species

ICE group	Species
1	Atlantic salmon (Salmo salar)Sea or river trout [50-100] (Salmo trutta)
2	Mules (Chelon labrosus, Liza ramada)
3a	Gread shad (Alosa alosa)
3b	Shad (Alosa fallax fallax)
3c	Sea lamprey (Petromyzon marinus)
4a	River trout or sea trout [25-55] (Salmo trutta)
4b	River trout [15-30] (Salmo trutta)
5	Aspe (Aspius aspius)Pike (Esox lucius)
6	Common grayling (Thymallus thymallus)
7a	Common barbel (Barbus barbus)Chub (Squalius cephalus)Nase (Chondrostoma nasus)
7b	River lamprey (Lampetra fluviatilis)
8a	Common carp (Cyprinus carpio)

ICE group	Species
8b	Common bream (Abramis brama)Pike-perch (Sander lucioperca)
8c	White bream (Blicca bjoerkna)Ide (Leuciscus idus)Burbot (Lota lota)Perch (Perca fluviatilis)Tench (Tinca tinca)
8d	Common dace (Leuciscus sp but Idus)
9a	Bleak (Alburnus alburnus)Sprirlin (Alburnoides bipunctatus)Mediterranean barbel (Barbus meridionalis)Souffia (Telestes souffia)Crucian carp (Carassius carassius)Prussian carp (Carassius gibelio)Roach (Rutilus rutilus)Common rudd (Scardinius erythrophthalmus)South-west european nase (Parachondrostoma toxostoma)
9b	Apron (Zingel asper)Cottus spGobio spRuffe (Gymnocephalus cernuus)Brook lamprey (Lampetra planeri)Stone loach (Barbatula barbatula)Spined loach (Cobitis taenia)
10	Sunbleak (Leucaspius delineatus)European bitterling (Rhodeus amarus)Three-spined stickleback (Gasterosteus gymnurus)Ninespine stickleback (Pungitius laevis)Minnows (Phoxinus sp)

9 Downstream migration

9.1 Calculation of the head loss on a water intake trashrack

Head loss ΔH on a water intake trashrack is calculated as follows:

$$\Delta H = \xi \frac{V_1^2}{2g}$$

Upstream flow velocity V_1 is calculated from the discharge Q, the water height H_1 and the intake width B upstream the trashrack:

$$V_1 = \frac{Q}{H_1 \times B}$$

The calculation of the head loss coefficient ξ is based on the characteristics of the trashrack. For a full description of the assumptions, formulas and limitations of the method, please refer to the Raynal et al. (2012) report.

9.1.1 Conventional trashrack

Conventional trashracks: perpendicular to the flow and slightly inclined to the horizontal.

9.1.1.1 Formula

Use of the F1 formula of Raynal et al (2012) to calculate the head losses.

$$\xi = a * K_O * K_\beta$$

With:

- ξ: total head loss coefficient (-)
- a: bar shape coefficient (-), see “Bar profile” below
- K_O: blockage head loss coefficient due to bars, spacers and clogging (-)
- K_β: head loss coefficient due to the angle of the trashrack (-)

$$K_O = \left(\frac{O_C}{1 - O_C} \right)^{1.6}$$

With O_C blockage ratio due to bars, spacers and clogging (-):

$$O_C = O + (1 - O) \times C$$

With:

- O blockage ratio due to bars and spacers
- C clogging ratio

$$K_\beta = (1 - \cos \beta)^{0.39}$$

With β the angle of inclination of the trashrack in reference to the vertical (°).

9.1.2 Angled trashrack

Flow-oriented and near-vertical trashracks.

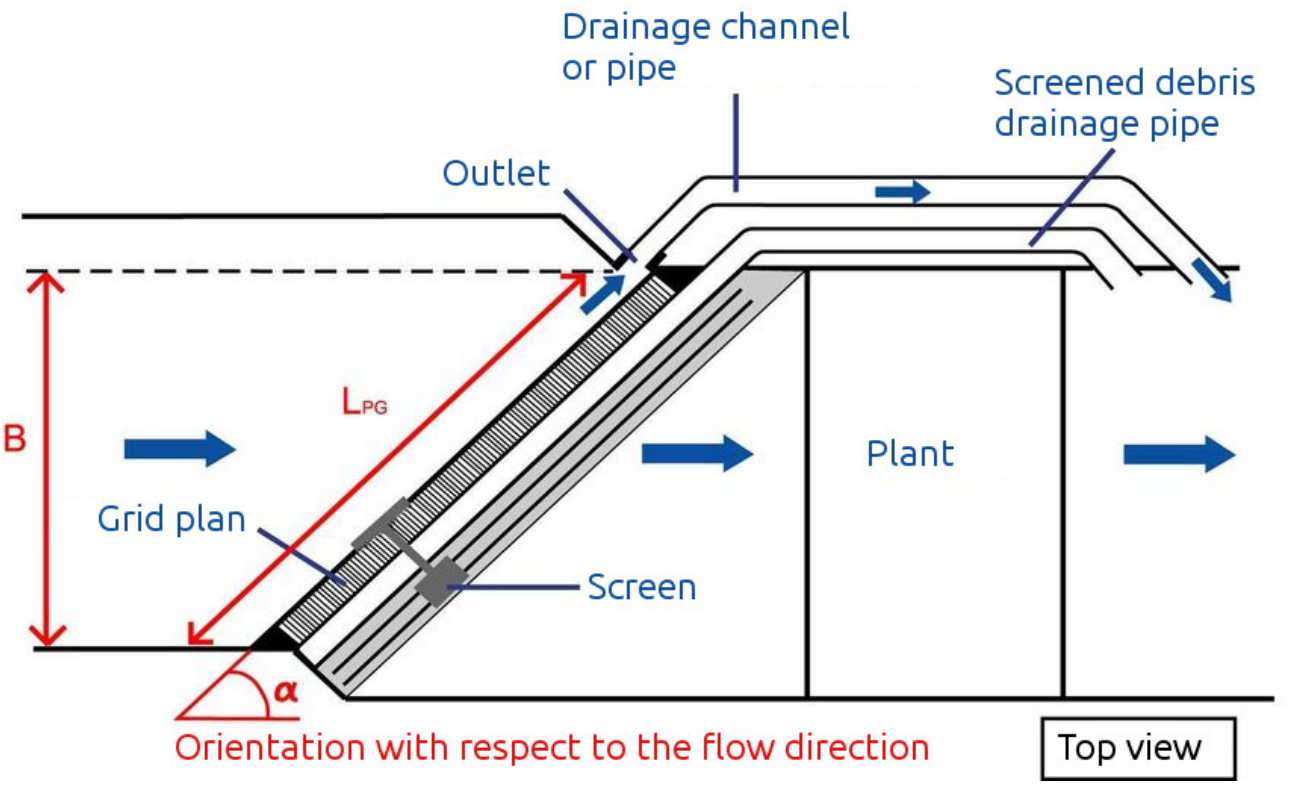

Figure 9.1: Angled trashrack

Courret, D. et Larinier, M. Guide pour la conception de prise d'eau ichtyocompatibles pour les petites centrales hydroélectriques, 2008. https:// doi.org/ 10.13140/ RG.2.1.2359.1449.

9.1.2.1 Formula

Use of the F2 formula of Raynal et al (2012) to calculate the head losses (Also in Equation (7) of Raynal et al. (2013b)).

$$\xi = a * K_O * K_\alpha$$

With K_α head loss coefficient due to inclination in reference to the horizontal (-)

$$K_\alpha = 1 + c * \left(\frac{90 - \alpha}{90}\right)^{2.35} * \left(\frac{1 - O}{O}\right)^3$$

With:

- α: inclination angle of the trashrack in reference to the horizontal (°)
- c: bar shape coefficient (-), see “Bar profile” below

9.1.3 Inclined trashrack

trashracks perpendicular to the flow, and inclined with respect to the horizontal

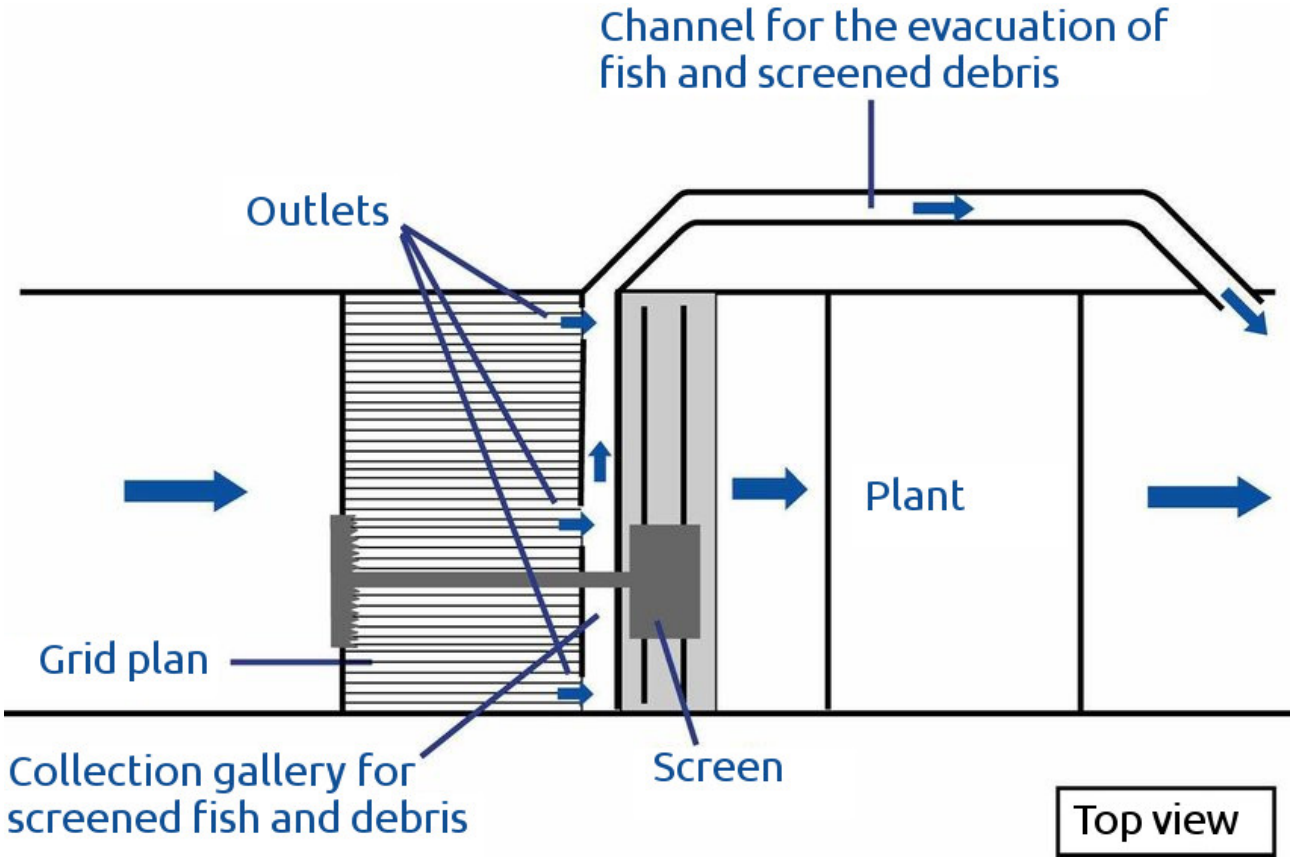

Figure 9.2: Inclined trashrack

Courret, D. et Larinier, M. Guide pour la conception de prise d’eau ichtyocompatibles pour les petites centrales hydroélectriques, 2008. https://doi.org/10.13140/RG.2.1.2359.1449.

9.1.3.1 Formula

Use of the F3 formula of Raynal et al (2012) to calculate the head losses (Also in Equation (11) of Raynal et al. (2013a)).

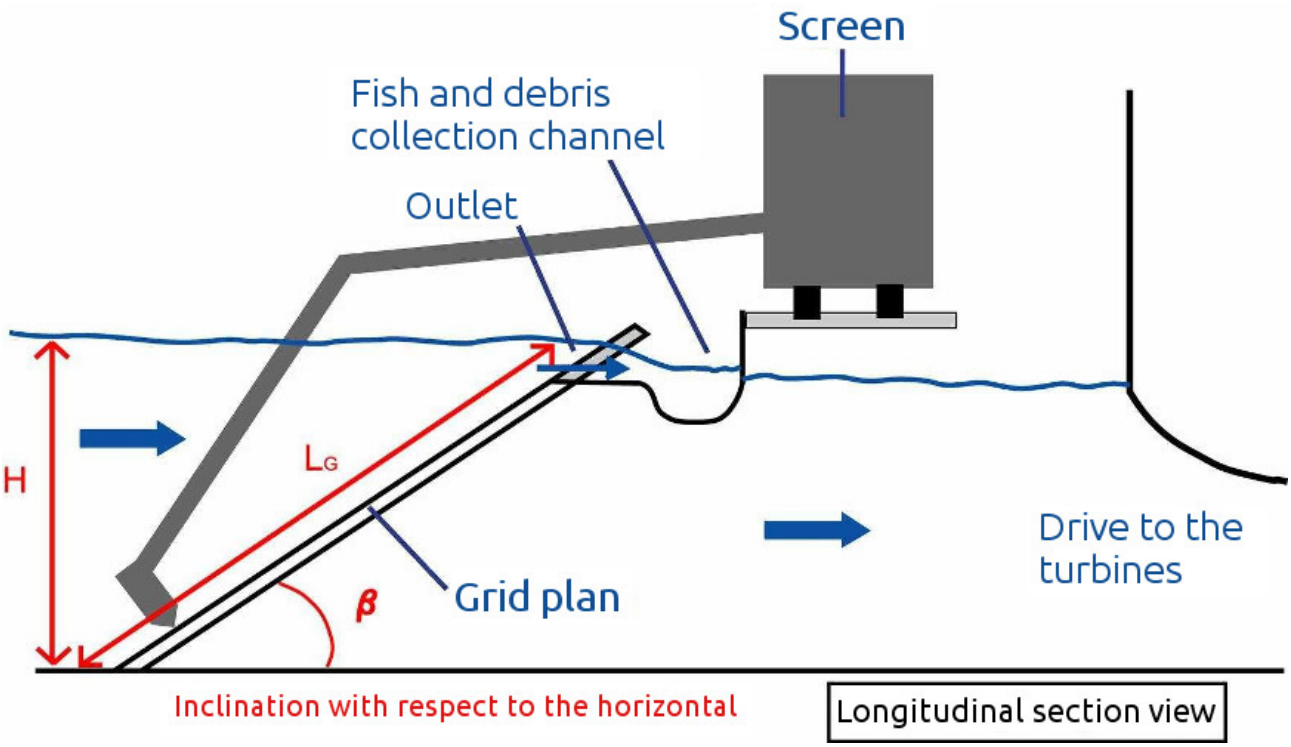

Figure 9.3: Inclined trashrack

$$\xi = a * K_b * K_\beta + K_{Fent} * K_{entH}$$

With:

- K_b: blockage head loss coefficient due to bars and clogging (-)
- K_{Fent}: spacer shape coefficient (-), see “Bar profile” below
- K_{entH}: blockage head loss coefficient due to spacers (-)

$$K_b = \left(\frac{O_{b,C}}{1 - O_{b,C}} \right)^{1.65}$$

With $O_{b,C} = O_b + (1 - O_b) \times C$ et O_b blockage ratio due to bars.

$$K_\beta = (\sin \beta)^2$$

$$K_{entH} = \left(\frac{O_{entH}}{1 - O_{entH}} \right)^{0.77}$$

With O_{entH} blockage ratio due to spacers.

9.1.4 Parameters

9.1.4.1 Elevation of the immersed vertex of the trashrack

May be different from the water level if the top of the trashrack is drowned.

9.1.4.2 Section width B

For conventional or inclined trashrack, it mMust also correspond to the width of the trashrack.

9.1.4.3 Average approach speed for the maximum turbinated flow, subtracting the upper blocked part, if any

“Maximum” value of the approach speed taken into account in the calculation of the head loss in a safety approach.

9.1.4.4 Inclination with respect to the horizontal

Conventional trashrack

Scope of the formula: $45 \leq \beta \leq 90°$

Angled trashrack

Vertical trashracks (β = 90°).

The slight inclination of the trashracks ($\beta \approx$ 75/80°), often set up for screening purposes, can be neglected.

inclined trashrack

Scope of the formula: $15° \leq \beta \leq 90°$

Recommended for fish guidance: $\beta \leq 26°$

9.1.4.5 Orientation with respect to the direction of flow

Conventional trashrack

trashracks perpendicular to the flow (α = 90°)

Angled trashrack

Scope of the formula: $30° \leq \alpha \leq 90°$

Recommended for fish guidance: $\alpha \leq 45°$

inclined trashrack

trashracks perpendicular to the flow (α = 90°)

9.1.4.6 Average normal speed for maximum turbinated flow rate V_N

Recommended to avoid plating fish on the trashrack (physical barrier) or their premature passage through (behavioural barrier): VN $\leq$ 0.5 m/s.

Angled or inclined trashrack

Above the average value calculated here, it is essential to refer to the recommendations derived from the experimental characterization of the actual velocity values.

9.1.4.7 Bar shape ratio b/p

Angled trashrack

Validity range of the formula: ratio b/p close to 0.125

9.1.4.8 Ratio of spacing / bar thickness

Angled trashrack

Scope of validity of the formula: $1 \leq e/b \leq 3$ with e space between bars.

9.1.4.9 Overall obstruction for conventional and angled trashracks

Calculated from bars + spacers + longitudinal and transverse support elements retained, it has to be determined from the trashrack plans.

Scope of validity of the formula for conventional trashracks: $0.2 \leq O \leq 0.60$

Scope of validity of the formula for angled trashracks: $0.35 \leq O \leq 0.60$

9.1.4.10 Overall obstruction for inclined trashracks

It consists of two parts.

Obstruction due to the bars and longitudinal support elements retained O_b. To be determined from the trashrack plans.. It must be higher or equal to bar blockage ratio given by $b/(b+e)$. Scope of validity of the formula: $0.28 \leq O \leq 0.53$.

Blockage ratio due to spacers. Scope of validity of the formula: $O_{entH} \leq 0.28$

9.1.4.11 Bar profile

Conventional trashrack

The shape coefficient of the bars a is 2.89 for the rectangular profile (PR) and 1.70 for the hydrodynamic profile (PH).

Angled trashrack

The shape coefficient of the bars is 2.89 for the rectangular profile (PR) and 1.70 for the hydrodynamic profile (PH).

The shape coefficient of the bars c is 1.69 for the rectangular profile (PR) and 2.78 for the hydrodynamic profile (PH).

inclined trashrack

Bar shape	Droplet	Plétina	Tadpole 8	Tadpole 10	Hydrodynamic	Rectangular
Bar coefficient A_i	2.47	1.75	1.27	1.79	2.10	3.85

After Lemkecher et al. (2020)

9.1.4.12 Average shape coefficient of spacers and transverse elements, weighted according to their respective shares

inclined trashrack

To be determined from the trashrack plans.

For example, 1.79 for cylindrical spacers, 2.42 for rectangular spacers, and around 4 for square beams and IPNs.

9.1.5 References

Raynal, S., Courret, D., Chatellier, L., Larinier, M., David, L., 2012. Définition de prises d'eau ichtyocompatibles -Pertes de charge au passage des plans de grille inclinés ou orientés dans des configurations ichtyocompatibles et champs de vitesse à leur approche (POLE RA11.02). https://continuite-ecologique.fr/wp-content/uploads/2019/11/2012_014.pdf

Raynal, S., Courret, D., Chatellier, L., Larinier, M., David, L., 2013a. An experimental study on fish-friendly trashracks–Part 1. Inclined trashracks. Journal of Hydraulic Research 51, 56–66. https://doi.org/10.1080/00221686.2012.753647

Raynal, S., Chatellier, L., Courret, D., Larinier, M., David, L., 2013b. An experimental study on fish-friendly trashracks–Part 2. Angled trashracks. Journal of Hydraulic Research 51, 67–75. https://doi.org/10.1080/00221686.2012.753646

Lemkecher, F., Chatellier, L., Courret, D., David, L., 2020. Contribution of Different Elements of Inclined Trash Racks to Head Losses Modeling. Water 12, 966. https://doi.org/10.3390/w12040966

9.2 Jet impact

This module performs a ballistic calculation of a jet while neglecting air friction. It allows to calculate the missing value among the following quantities:

- Initial velocity at the start of the jet (m/s)
- Initial slope at the start of the jet (m/m). Note that, contrary to the slope used in the free surface calculation module, this slope is positive for an upward directed jet and negative for a downward directed jet.
- Abscissa of the impact or horizontal distance travelled between the start of the jet and the point of impact (m)
- Start dimension of the jet (m)
- Water elevation (m)

The bottom elevation is used to calculate the depth and the depth to fall ratio.

9.2.1 Designing an outlet for fish evacuation

The downstream fish evacuation outlet ends with a device that empties into the plant's tail-race. This module calculates the position and velocity at the point of impact of the free fall or water vein on the surface of the tailrace water taking into account the initial angle and velocity of the jet and the drop height.

Excerpt from Courret and Larinier (2008), p.24:

> Speeds in the structure and at the point of impact in the tailrace must remain below about 10 m/s, with some organizations even recommending that they not exceed 7-8 m/s (ASCE 1995). (...) The head between the outlet and the water body must not exceed a dozen metres to avoid any risk of injury to fish on impact, whatever their size and mode of fall (free fall or fall in the water vein) (Larinier and Travade 2002). The discharge must also be made in an area of sufficient depth to avoid any risk of injury from mechanical shock. Odeh and Orvis (1998) recommend a minimum depth of about a quarter of the fall, with a minimum of about 1 m.

9.2.2 Formulas used

9.2.2.1 Fall height

$$H = 0.5 * g * \frac{D^2}{\cos\alpha^2 * V_0^2} - \tan\alpha * D$$

With:

- H: height of fall (m) which corresponds to the difference in height between the jet's departure and the water surface.
- g: acceleration of gravity = 9.81 m.s-2
- D: horizontal distance travelled between the start of the jet and the point of impact (m)
- α : angle of shooting in relation to the horizontal (°)
- V_0 : initial speed (m/s)

9.2.2.2 Impact abscissa (horizontal distance covered)

$$D = \frac{V_0}{g * \cos\alpha}\left(V_0 * \sin\alpha + \sqrt{(V_0 * \sin\alpha)^2 + 2 * g * H}\right)$$

9.2.2.3 Flight time

$$t = \frac{D}{V_0 \cos\alpha}$$

9.2.2.4 Horizontal speed at impact

$$V_x = V_0 \cos\alpha$$

9.2.2.5 Vertical speed at impact

$$V_z = V_0 \sin\alpha - t * g$$

9.2.2.6 Speed at impact

$$V_t = \sqrt{V_x^2 + V_z^2}$$

9.2.3 References

Courret, Dominique, and Michel Larinier. Guide for the design of ichthyocompatible water intakes for small hydroelectric power plants, 2008. https://doi.org/10.13140/RG.2.1.2359.1449

10 Mathematical tools

10.1 Operators and trigonometric functions

The basic mathematical operators and functions provided by Cassiopeia make it possible above all to facilitate the link between the results of one calculation module and the input into another in the case of a sequence of calculations between several modules. The provided example “Weir jet length” shows the use of the “Linear function” module.

10.1.1 Linear function

The linear function module solves the equation of a line:

$$y = ax + b$$

Three parameters must be entered and the module calculates the missing parameter.

10.1.2 Sum and product of powers

This module allows to write an equation summing powers in the form ax^n with a, x, and n of real numbers.

In the case of a sum the equation solved by the module is written:

$$y = \sum_{i=1}^{k} a_i x_i^{n_i}$$

In the case of a product the equation solved by the module is written:

$$y = \prod_{i=1}^{k} a_i x_i^{n_i}$$

All parameters must be entered except the last one which is the value calculated in the equation.

10.1.3 Trigonometric function

This module allows to calculate the value of a trigonometric function or its inverse.

The equation solved by this module is written:

$$y = f(x)$$

With f, a trigonometric function and x an angle in degrees or radian.

The “Operation” parameter allows to choose the operator among the available functions: cos, sin, tan, cosh, sinh and tanh. The “Unit” parameter is used to choose between degree and radian.

10.2 Multi-module solver

The multi-module solver allows to calculate the value of an input parameter of a module depending on a calculation chain made up of several modules for which a target value for an output calculated parameter is sought.

The diagram below shows the example of a calculation chain comprising two modules. The module `x` takes the parameter `Input x` and calculates the parameter `Output x`. The `y` module takes the `Input y` parameter and calculates the `Output y` parameter. The `Input y` parameter is linked to the `Output x` parameter. The problem to be solved by the solver is to get the value of the `Input x` to obtain a target value in `Output y`.

```
graph LR
Ix([Input x])
x[Module x]
Ox([Output x / Input y])
y[Module y]
Oy([Output y])
Ix --> x
x --> Ox
Ox --> y
y --> Oy
Oy -..->|Input x for a target value Output y ?| Ix
```

To solve this problem, the characteristics of the target parameter must be defined which include:

- The module and its calculated parameter (here the module `y` calculating `Output y`);
- The target result which can be the parameter calculated by the module or one of its complementary results (Here `Output y`);
- The desired target value.

It is also necessary to define the characteristics of the searched parameter:

- The searched parameter is to be chosen from the list of input parameters of the modules of the session (Here the `Input x` parameter of the `x` module);
- An initial value of this parameter to start the calculation.

The initial value chosen must be close enough to the solution because there is no guarantee that the function resulting from the sequence of calculations is continuous and monotonous.

Examples of the use of the multi-module solver are given in the example sessions “Channel flow with structures” and “Critical slope of a channel”. The notes of these sessions describe the sequence of the modules and the use of the solver.

11 Numerical methods

11.1 Runge-Kutta diagram of order 4

The Runge-Kutta scheme of order 4 is based on an approximation of the derivative to a higher order (order 4). The principle of discretization is the same as for the Euler method, but we will make some additional calculations to approach the derivative:

- we know the function f, a point t_i where we know y_i
- we can therefore calculate $f_1 = y'_i = f(y_i, t_i)$ (cf. Euler=pente method to the point (t_i, y_i))
- we calculate $f_2 = f(y_i + \frac{1}{2}\Delta t f_1, t_i + \frac{1}{2}\Delta t)$ (estimated value in the middle of the interval, with the slope taken in t_i)
- we calculate $f_3 = f(y_i + \frac{1}{2}\Delta t f_2, t_i + \frac{1}{2}\Delta t)$ (estimated value in the middle of the interval $t_{i+1/2}$, with the slope taken in $t_{i+1/2}$
- we calculate $f_4 = f(y_i + \Delta t f_3, t_i + \Delta t)$ (estimated value in t_{i+1}, with the slope taken in $t_{i+1/2}$
- we then have $y_{i+1} \simeq y_1 + \frac{1}{6}\Delta t(f_1 + 2f_2 + 2f_3 + f_4)$
- you can then iterate (solve step by step) to move to the next point. The problem is initialized from t_0 where we know y_0 (boundary condition).

It is clear that the method is much more precise. Even with a much higher calculation step, the solution is approached correctly, whereas the Euler method gives results very far from the exact solution. We also note that, between the discretization points, the solution was approached by line segments (although we may have more advanced interpolation if we need to know intermediate values).

The program can be written as follows, using the Scilab scientific calculation software:

```
// Program for solving a differential equation
// Equation to be solved: dy/dt=f(y,t)

// Definition of the function f
a=-0.1;
function z=f(y,t);z=a*y; endfunction

// Boundary condition:
t0=0;
y0=1;

// Time discretization
tmax=50;
```

```
dt=5;

// Number of discretization steps
N=(tmax-t0)/dt;
// Indices
ii=1:N+1;
t=(ii-1)*dt; // time vector

// time vector with a finer step, for the exact solution
t2=0:tmax;

// Solution by Euler method, noted ye
ye(1)=y0; // boundary condition
for i=1:N
  ye(i+1)=ye(i)+dt*f(ye(i),t(i));
end

// Solution by RK4 method, noted yrk4
yrk4(1)=y0; // boundary condition
for i=1:N
  f1=f(yrk4(i),t(i));
  f2=f(yrk4(i)+f1*dt/2,t(i)+dt/2);
  f3=f(yrk4(i)+f2*dt/2,t(i)+dt/2);
  f4=f(yrk4(i)+f3*dt,t(i)+dt);
  yrk4(i+1)=yrk4(i)+dt*(f1+2*f2+2*f3+f4)/6;
end

Solution mapping //
scf(2)
plot(t2,exp(a*t2),'k-',t,ye,'kd-',t,yrk4,'ks-')
title('Resolution by Runge-Kutta method of'order 4 - dy/dt=-0.1y')
xlabel('t')
ylabel('y')
legend('Exact solution','Euler method, dt=5','RK4 method, dt=5')
```

11.2 Explicite Euler method

To describe an evolutionary process, or the profile of a water line, for example, we often have to solve a first-order ordinary differential equation (EDO). This equation writes how a function varies, at a given point (an instant or a point in space), knowing the value of this mathematical function, the problem to be solved is written:

$$\begin{cases} \frac{dy}{dt} &= f(y,t) \\ y(t=t_0) &= y_0 \end{cases}$$

where $\frac{dy}{dt}$ refers to the derivative with respect to t of the function y (which depends on the variable t); the variable y_0 is called the boundary condition; it conditions the final solution of the equation.

As we often do not know an analytical solution to this problem, we will use approximate methods to estimate the solution. So we make a discretization of the variable t. We note the discretization step, and solve the problem at the points t_0, $t_1 = t_0 + \Delta t$, $t_2 = t_0 + 2\Delta t$, ..., $t_n = t_0 + n\Delta t$ where n is an integer.

The explicit Euler method is the most intuitive; it consists in considering that, from a point t_i to a point t_{i+1}, the function evolves linearly, with a trajectory that is the one that can be calculated at point t_i.

The problem is solved as follows:

- we know the function f, a point t_i where we know y_i
- so we can calculate $y'_i = f(y, t)$
- we then estimate the value of y at point $t_{i+1} = t_i + \Delta t$: $y_{i+1} \simeq y_i + y'_i \Delta t$
- you can then iterate (solve step by step) to move to the next point. The problem is initialized from t_0 where we know y_0 (boundary condition).

We can feel that this scheme will only work well if Delta is not too big. Values of too high Δt can give completely false results, leading to erroneous physical interpretations. However, its interest is its simplicity, and it can be easily implemented on a table.

11.2.1 Example application: exponential process

Consider the following (simple) problem:

$$\begin{cases} \frac{dy}{dt} &= -ay \\ y(t = t_0) &= y_0 \end{cases}$$

So we have here $f(y, t) = -ay$. The analytical solution is easily solved, giving $y(t) = y_0 \exp(-a(t - t_0))$. The problem can be solved by the Euler method:

- we choose Δt (for example, $\Delta t = 1$)
- calculate $y_1 = y_0 - ay_0 \Delta t$
- calculate $y_2 = y_1 - ay_1 \Delta t$ etc.

It can be seen that the resolution is not very precise; this is linked to the calculation step being too large given the method chosen and the equation to be solved.

11.3 Trapezes integration method

The integral form of the ordinary first-order differential equation is written:

$$\int_{t_i}^{t_{i+1}} \frac{dy}{dt} = \int_{t_i}^{t_{i+1}} f(y, t)$$

Trapezes methods gives:

$$y_{i+1} \simeq y_i + \frac{y'_i + y'_{i+1}}{2} \Delta t$$

11.4 Brent's method

See definition on Wikipedia

11.5 Newton's method

See definition on Wikipedia

12 Historique des versions

4.19.1 - 06/05/2025

12.0.0.1 Correction de bogues

- Régime uniforme: Affichage erroné des résultats quand un des paramètres varie (jalhyd#381, nghyd#681)

12.0.0.2 Changements internes

- Remove .htaccess file on deployment server (nghyd#680)

4.19.0 - 03/03/2025

12.0.0.3 Nouvelles fonctionnalités

- Ajout de la passe à rugosité de fond (jalhyd#340)
- RugoFond: Ajouter un avertissement sur les lignes d'eau trop élevées (jalhyd#379, nghyd#675)
- Espèce personnalisée : grouper les critères de PAB (nghyd#457)
- Documentation > Lois d'ouvrages: homogénéiser schémas, formules et noms des lois (nghyd#512)
- Solveur: Résultat ciblé: ne pas proposer le paramètre calculé (nghyd#669)

12.0.0.4 Correction de bogues

- Courbe de remous - génération section paramétrée : la pente de fond n'est pas copiée (jalhyd#366)
- Macrorugo Complexe: Non convergence du calcul (jalhyd#368)
- Solveur: absence de message d'erreur à la non convergence (jalhyd#369)
- Solveur: Les select d'une session chargée ne s'initialise pas (jalhyd#374, nghyd#668)
- Non fonctionnement des tests E2E suite à la mise à jour de NodeJS (nghyd#646)
- Documentation > HTML: Les formules ne s'affichent pas dans le chapitre méthodes numériques (nghyd#653)
- Documentation > PDF: erreur de notes de bas de page (nghyd#655)
- Cassiopée doesn't work for languages other than French and English (nghyd#667)
- Rugofond Multiple/Macrorugo complexe: affichage des unités sur les résultats complémentaires (nghyd#676)

12.0.0.5 Changements internes

- Non fonctionnement des tests E2E suite à la mise à jour de NodeJS (nghyd#646)
- Optimize waiting time for starting e2e tests (nghyd#647)
- Mise à jour vers Angular 15 (nghyd#659)
- Tests E2E: Error: Couldn't find a matching Chrome browser for tag "121.0.6167.184" on platform "Linux" (nghyd#661)
- E2E tests are failing for one month (nghyd#678)

4.18.0 - 2024-01-30

12.0.0.6 Nouvelles fonctionnalités

- Ajout du module courbe de remous d'une passe à macro-rugosité (jalhyd#325, nghyd#609, nghyd#650, nghyd#654)
- Add bundle maker for CassiopeeR (jalhyd#360)
- Chargement d'une session: Afficher la page de note si elle existe au lieu du diagramme des modules (nghyd#649)
- PreBarrage: autoriser les cotes de seuil inférieures à la cote de fond du bassin amont (jalhyd#353, nghyd#634)
- Electron: ajouter un message d'avertissement de transition vers PWA (nghyd#640)

12.0.0.7 Correction de bogues

- L'URL https://cassiopee.g-eau.fr/cassiopee-releases/ est accessible aléatoirement (nghyd#624)
- PWA: Les bloqueurs de tracker empêchent la mise à jour de l'application (nghyd#633)
- Vérificateur: la vérification ne devrait pas être possible quand aucune espèce n'est sélectionnée (jalhyd#349, nghyd#637)
- Prebarrage: erreur de calcul de la somme des débits sur plusieurs branches (jalhyd#351)
- MacroRugo: erreur de calcul du Strickler équivalent (jalhyd#361)
- Documentation PDF: erreurs à la compilation (nghyd#656)

12.0.0.8 Documentation

- Grilles: ajouter les schémas de profil issus de Lemkecher et al. (2020) (nghyd#594)
- Ajouter un exemple de passe à rangées périodiques (nghyd#635)
- Vérificateur: ajouter un avertissement à l'utilisation (nghyd#643)
- Mise à jour du logo de l'UMR G-EAU (nghyd#651)

12.0.0.9 Changements internes

- Update chartjs zoom plugin to v2.0.1 (nghyd#638)
- Importer le DockerFile utilisé pour le CI/CD de Cassiopée dans ngHyd (nghyd#639, nghyd#648)
- Clean npm dependencies (jalhyd#356)
- CI: automatically publish jalhyd package on NPM (jalhyd#359)

4.17.1 - 2023-11-20

12.0.0.10 Correction de bogues

- Cloisons: le champ “Cote de l’eau amont” n’est pas vide par défaut (jalhyd#355, nghyd#623)
- Le séparateur décimal est passé à la virgule sur certaines configurations (nghyd#628)

12.0.0.11 Changements

- Modifier l’avertissement de limite d’ennoiement de Villemonte (jalhyd#350, nghyd#629)

12.0.0.12 Changements internes

- CI: change cache strategy for node modules (jalhyd#358, nghyd#630)

4.17.0 - 2023-05-30

12.0.0.13 Nouvelles fonctionnalités

- Structure : Ajout d’une erreur sur l’ennoiement (jalhyd#302, nghyd#614)
- Conduites en charge : ajout de la loi de Strickler (jalhyd#215, nghyd#596)
- Ajout d’une redirection vers https pour les adresses http (nghyd#587)
- Courbe de remous : rendre facultatif l’une des deux conditions limites en cote (jalhyd#343, nghyd#610)
- Courbe de remous: visualiser les profils de sections (nghyd#496)
- Courbe de remous: renommer la ligne d’eau en ZW et fournir le tirant d’eau d’après celle ci (jalhyd#333)

12.0.0.14 Changements

- Prébarrages : interdire de supprimer le dernier bassin (nghyd#582)
- PAB: Alignement à droite des cellules numériques dans le tableau des bassins et cloisons (nghyd#583)
- PAB: Optimisation du tableau : déplacement de la colonne “cote de radier amont” (nghyd#615)

12.0.0.15 Correction de bogues

- Documentation : Les formules de math ne s’affichent pas dans la version anglaise (nghyd#608)
- Perte de charge : les paramètres de loi ne sont pas modifiés quand on change le type de perte (nghyd#611)
- Solveur multimodule : le module existe toujours après suppression (jalhyd#342, nghyd#601)
- Notes de session : la note ne s’affiche pas directement (nghyd#602)
- PWA : l’application ne se met pas à jour (nghyd#604)
- Traduction des résultats : tous les libellés ne sont pas modifiés quand on change de langue (nghyd#586)

- Un paramètre cible d'un lien ne doit pas se lier à un autre paramètre (jalhyd#341, nghyd#605)
- Application PWA inaccessible hors ligne (nghyd#588)
- Régression : le fichier de session n'enregistre plus le type de section (nghyd#592)
- PAB : la précision d'affichage a une influence sur la valeur des paramètres (nghyd#543)
- Le bouton calculer est activé malgré un champ en erreur (nghyd#616)
- Solveur multimodule : impossibilité d'utilisation sur un seul module (nghyd#606)
- PreBarrage: Changement intempestif des paramètres d'ouvrage au changement d'équation (nghyd#620)
- PreBarrage: il n'y a plus aucun résultat au niveau des cloisons (nghyd#619)
- Passe à macrorugosités: des champs ne sont pas liables avec le module "Concentration de blocs" (jalhyd#345)
- Passe à macrorugosité: la largeur doit avoir un centimètre de tolérance (jalhyd#344)
- Structure: le chargement d'une session loi d'ouvrages avec Q varié remet Q en mode fixé (nghyd#603)
- Structure: résultat du calcul de la cote amont dépendant de la cote initiale pour un débit nul (jalhyd#219)
- Passe à bassins : message non défini dans la légende des graphiques (nghyd#584)
- Les résultats ne sont pas réinitialisés quand on modifie des paramètres globaux (jalhyd#331, nghyd#574)
- PreBarrage: Doublement des avertissements (jalhyd#348)

12.0.0.16 Documentation

- Passe à ralentisseurs : ajouter de liens vers les pages de documentation des types de passes (nghyd#598)
- Perte de charge : documentation du module (nghyd#597)
- Modification de la documentation sur le coefficient de débit d'une fente (nghyd#595)
- Ajout d'une documentation pour l'installation de Cassiopée PWA (nghyd#617)
- Perte de charge: Il manque l'aide dans le module perte de charge (nghyd#593)
- Ajouter le numéro de version de Cassiopée sur la documentation (nghyd#578)

12.0.0.17 Changements internes

- Restructurer Lechapt et Calmon pour de nouvelles lois de pertes de charge (jalhyd#334, jalhyd#590, nghyd#585)
- Migration des tests e2e vers WebDriverIO (nghyd#618)
- Documentation: localisation des dépendances javascript dans un seul dossier (nghyd#612)
- Optimiser l'affichage des unités (jalhyd#338)
- Fusionner les "select" avec "source" et les "select_custom" (jalhyd#328, nghyd#483)
- Docker: Supprimer les dépendances à l'application Android (cassiopee2-integration#12)
- Supprimer les dépendances et la chaîne de compilation pour l'application Android (nghyd#580)
- Suppression des warnings à la compilation (nghyd#579)
- Tests E2E: Vérifier la cohérence entre le json de description des calculettes et le flag visible des paramètres (nghyd#550)
- Thème Angular Material personnalisé : avertissements dart-sass à la compilation (nghyd#414)

4.16.3 - 2023-01-11

12.0.0.18 Correction de bogues

- Lechapt et Calmon : erreur de sélection de matériau (jalhyd#337, nghyd#589)

4.16.1 - 2022-11-16

12.0.0.19 Correction de bogues

- Un paramètre lié ne change pas d'état après la suppression du module cible (jalhyd#329, nghyd#571)
- Le mode lié d'un paramètre de section est perdu quand on change le type de section (jalhyd#329, nghyd#572)

12.0.0.20 Documentation

- Rajouter François Grand comme auteur de la documentation PDF (nghyd#573)
- Ajouter les références pour les schémas des lois d'ouvrages (nghyd#575)

4.16.0 - 2022-10-12 (Anguilla anguilla)

12.0.0.21 Nouvelles fonctionnalités

- PAB : ajout de la charge et l'ennoiement dans le tableau de résultat et l'export (jalhyd#324, nghyd#518)
- Courbe de remous (et bief) : remontée d'une erreur quand le pas de discrétisation est supérieur à la longueur du bief (jalhyd#316, nghyd#565)
- Section paramétrée : profil de section : option axes orthonormés (nghyd#497,nghyd#568)
- URL de routeur "/loadsession" pour charger un exemple (nghyd#476)
- Deploy devel branch on cassiopee-dev.g-eau.fr (nghyd#564)

12.0.0.22 Correction de bogues

- Les caractères UTF8 ne sont pas imprimés dans la doc PDF (nghyd#556)
- PréBarrages: La sélection de l'amont ou l'aval n'est pas visible au premier clic (nghyd#560)
- Solveur: le paramètre recherché n'est pas conservé (nghyd#555)
- PAB: Bugs de format du tableau NgPrime (nghyd#562)
- Section paramétrée: crash de l'appli sur variation de paramètre (jalhyd#319, nghyd#561)
- Module avec une section : le mode champs vide ne fonctionne pas (jalhyd#327, nghyd#569)
- Déplacement du paramètre calculé lors de la duplication d'un Nub (jalhyd#322, nghyd#567)
- Lois d'ouvrages : mauvaise gestion du paramètre calculé sur suppression d'ouvrage (jalhyd#321, nghyd#566)

12.0.0.23 Changements

- Ouvrages: modification des types d'ouvrages (ajout de seuil/orifice rectangulaire, vanne rectangulaire renommée en vanne de fond rectangulaire) (jalhyd#326, nghyd#511)
- Prébarrages : regroupement de la saisie des bassins (nghyd#522)

12.0.0.24 Documentation

- corrections diverses (nghyd#559)
- MacroRugo : ajout d'un schéma rugosité de fond (nghyd#524)
- Lois d'ouvrages : définition seuil mince/épais (nghyd#514)
- Ajout d'un tableau synthétiques des lois d'ouvrages (nghyd#513)
- MAJ de la documentation des grilles avec les données de Lemkecher et al. (2020) (nghyd#438)

12.0.0.25 Changements internes

- Mise à jour vers Angular 14 (nghyd#500)
- CI : MAJ de l'image Docker vers Debian Bullseye compatibilité TLS) (cassiopee2-integration#10)
- Angular : compilation avec Ivy (nghyd#369)
- Déplacer le répertoire Jalhyd dans celui de Nghyd (nghyd#558)
- Déménagement de l'intégration continue sur les serveurs gitlab à Lyon (nghyd#557)
- Mise à jour de Chartjs (nghyd#554)
- MAJ vers PrimeNG 10 (nghyd#481)

4.15.1 - 2022-07-04

12.0.0.26 Nouvelles fonctionnalités

- Structure: Modification de l'avertissement ennoiement (jalhyd#314, nghyd#520)
- Dialogue de paramètre variable : pouvoir valider avec la touche entrée (nghyd#541)
- Journal de calcul repliable (nghyd#519)

12.0.0.27 Changements

- MacroRugo: changer cote de radier par cote de fond (nghyd#523)
- PAB, MacroRugo complexe et Prébarrages: modifier le message d'erreur synthétique (nghyd#517)
- Error 404 on language files load (nghyd#499)

12.0.0.28 Correction de bogues

- Plantage PAB si un paramètre est passé en mode variable puis annulé (nghyd#549)
- Liens inaccessibles pour certains modules (jalhyd#289, nghyd#547)
- Plantage du calcul sur modules liés (jalhyd#286)
- PréBarrages: les champs ne sont pas vides à la création du module (jalhyd#310, nghyd#546)

- L'annulation de la saisie du mode "Varier" mémorise les valeurs non valides (nghyd#545)
- PréBarrages: les changements de couleur du schéma ne sont pas instantanées (nghyd#544)
- Crash sur annulation du dialogue d'édition du paramètre variable pour un paramètre initialement en calcul (nghyd#542)
- Le passage en mode varier devrait systématiquement ouvrir la boite de dialogue (nghyd#537)
- Lois d'ouvrages: les champs ne sont pas vide à l'ajout d'un ouvrage (nghyd#536)
- PAR Calage et Simulation: répétition des paramètres dans le résultat (nghyd#535)
- PAB nombre: mauvaise colonne de résultat (jalhyd#304, nghyd#534)
- MacroRugo complexe: le graphique des vitesses moyennes entre les blocs ne s'affiche pas (nghyd#533)
- Cote amont/aval de bief: le bouton "détail d'une section hydraulique" ne fonctionne pas toujours (nghyd#504, jalhyd#311)
- PréBarrages: les valeurs erronées ne sont pas conservées (nghyd#501)
- Solveur multimodule: le choix du paramètre recherché n'est pas maintenu à l'écran (nghyd#486)
- Log : améliorer la synthèse de journal (jalhyd#308)
- Les liens erronés sont remplacés par d'autres liens (nghyd#551)
- PAB: Lancement du calcul possible avec des champs invalides (nghyd#552, jalhyd#317)

12.0.0.29 Changements internes

- Path error in stable deployment version on the dev server nghyd#540

4.15.0 - 2022-05-04 (Salmo trutta)

12.0.0.30 Nouvelles fonctionnalités

- PAB : Variation du débit d'attrait (nghyd#431)
- Ajouter un bouton "Annuler" sur la saisie des paramètres variables (jalhyd#300, nghyd#507)
- Prébarrages : mettre les enfants invalides en rouge dans le schéma (jalhyd#298, nghyd#484)

12.0.0.31 Changements

- Fente Larinier : laisser le coefficient de débit vide (nghyd#515)
- Cloisons : Générer une PAB : vider les champs (jalhyd#306, nghyd#516)

12.0.0.32 Correction de bogues

- Courbe de remous: crash de l'application sur données erronées (jalhyd#307, nghyd#532)
  Deux bugs en un, l'appli crashe quand :
  - la hauteur de berge dépasse une certaine valeur avec des paramètres corrects pour effectuer un calcul (par exemple les valeurs par défaut)
  - les deux cotes de l'eau se situent sous les cotes de fond amont et aval
- Sections : non convergence du calcul du tirant d'eau critique (jalhyd#301, nghyd#528)
- Remettre le paramètre dans son état initial quand le dialogue "Varier" est annulé (nghyd#508)

- Prébarrages: les champs ne sont pas vides lors des ajouts de bassins et cloisons (nghyd#503)
- Mode “champs vides par défaut” : changer le type d’un ouvrage (ex: dans Cloisons) remplit les champs (nghyd#480)
- PréBarrages : perte du focus lorsqu’on édite un paramètre d’un enfant (cloison ou bassin) (nghyd#469)

12.0.0.33 Documentation

- Cloisons : il manque l’aide contextuelle pour les lois de débit (nghyd#529)
- Documentation : corrections (nghyd#498)

12.0.0.34 Changements internes

- Nightly build: clean folder before installation (nghyd#495)
- Transfert du site de production sur OVH (nghyd#505)
- Plantage des tests e2e sur le chargement des exemples (nghyd#530, nghyd#531)
  - Les champs des exemples chargés sont vides lorsque le mode “champ vides” est activé.
  - Les tests e2e plantent par manque de temporisation
- CI : les jobs build en schedule de master et devel plantent (nghyd#527)
- CI : affiner la gestion du cache (nghyd#526)

4.14.2 - 2021-03-25

12.0.0.35 Nouvelles fonctionnalités

- Passe à macro-rugosité: Retour aux formules utilisées dans la v4.13.1 (jalhyd#297, nghyd#493)

12.0.0.36 Correction de bogues

- Passe à macro-rugosité: error de calcul de la vitesse max (jalhyd#294)
- Graphiques: lorsqu’on relance un calcul les axes ne se mettent pas à jour (nghyd#489)

12.0.0.37 Documentation

- Macrorugo : Documentation de Cd0 avec schéma (nghyd#492)

4.14.1 - 2021-02-17

12.0.0.38 Nouvelles fonctionnalités

- Passe à macro-rugosité: Changer Cd0 pour Cx et ajuster Cd0 aux données expérimentales (jalhyd#291)

12.0.0.39 Correction de bogues

- Vérificateur de passe: message erroné pour les passes à macro-rugosités submergées (jalhyd#292)

4.14.0 - 2021-02-16 (Scomber scombrus)

12.0.0.40 Nouvelles fonctionnalités

- Passe à macro-rugosité: Mise à jour des formules de calcul (jalhyd#283)
- Passe à macro-rugosité: Ajout de la vitesse moyenne entre les blocs (jalhyd#285)
- Passe à macro-rugosité: Ajout du Strickler équivalent dans les résultats liables à des Strickler (jalhyd#287)
- Passe à macro-rugosité: ajout d'un avertissement pour les concentrations en dehors de l'intervalle validé par les expérimentations (jalhyd#284)
- Vérificateur: Les passes à macro-rugosité submergées sont non franchissables (jalhyd#290)

12.0.0.41 Correction de bogues

- Passe à macro-rugosité: Calcul de la puissance dissipée erroné (jalhyd#282)
- Crash au chargement d'un module contenant une parenthèse dans son nom (nghyd#487)
- Electron: l'icône de l'application n'est plus reconnue (nghyd#485)

12.0.0.42 Documentation

- Documentation du solveur multi-module et des modules de calcul mathématiques (nghyd#433)
- Macrorugo : documenter le coefficient de forme Cd0 (nghyd#477)
- MacroRugo: erreur de formule de correction de Cd dans la documentation (nghyd#488)
- Documentation du module de calcul de la cote amont / aval d'un bief (nghyd#490)

4.13.1 - 2020-10-02

12.0.0.43 Correction de bogues

- PreBarrage: Distribution des débits erronée sur exemple simple (jalhyd#279)
- PreBarrage: erreur de calcul sur Z2 > Z1 initiale (jalhyd#280)
- Prebarrage : avec Chrome (et electron) le schéma est mal rendu (nghyd#482)

4.13.0 - 2020-09-24 (Michel Larinier)

12.0.0.44 Nouvelles fonctionnalités

- Module Pré-barrage (jalhyd#32, jalhyd#269, jalhyd#268, jalhyd#243, jalhyd#246, nghyd#395, nghyd#430, nghyd#456, nghyd#455, jalhyd#275, jalhyd#276, jalhyd#277, jalhyd#278, nghyd#452, nghyd#470, nghyd#451)

- Simplification de l'architecture des composants de résultats Angular (nghyd#418, nghyd#466, nghyd#465)
- Modifier les titres et descriptions de "Passes à bassins" et "Passes à macro-rugosités" (nghyd#478)
- Ajouter des mots-clés "maths" pour les outils mathématiques (moteur de recherche) (nghyd#474)

12.0.0.45 Correction de bogues

- Electron : la détection de mise à jour disponible ne fonctionne plus (nghyd#462)
- Débit lié au débit en calcul d'un PréBarrage : erreur dans CalcSerie() (jalhyd#274)
- Cloisons : changer le type d'ouvrage pour Seuil Triangulaire casse le fieldset (nghyd#479)

12.0.0.46 Documentation

- Prébarrages (nghyd#467)
- Aide du Jet / de la pente : mentionner l'inversion de la pente pour le module Jet (nghyd#475)
- Ajouter à l'accueil de la documentation un chapitre "contact, bugs, remarques…" (nghyd#472)

4.12.1 - 2020-09-15

12.0.0.47 Correction de bogues

- Lien vers la documentation cassé sur Chrome et Edge (nghyd#458)
- Macrorugo : en mode "champs vides par défault", L est en calcul avec une valeur initiale vide (nghyd#459)
- Grille : différencier Ob de O pour les grilles inclinées (jalhyd#273)
- Fermeture d'un module Jet calculé : plante l'application (nghyd#460)
- Déversoir dénoyé : Infinity pour des largeurs de lit faible et sur variation (jalhyd#272)

12.0.0.48 Documentation

- Lechapt-Calmon : documentation du coefficient de pertes de charges singulières (nghyd#338)

4.12.0 - 2020-09-09 (Les critères de Francis Blanche - ils peuvent le faire !)

12.0.0.49 Nouvelles fonctionnalités

- Vérification des critères de franchissement des passes à poissons (jalhyd#204, nghyd#60, jalhyd#236, jalhyd#251, jalhyd#238, jalhyd#252, jalhyd#250, jalhyd#258, jalhyd#247, jalhyd#239, jalhyd#249, jalhyd#248, jalhyd#254, jalhyd#235, jalhyd#237, nghyd#402, jalhyd#216, nghyd#426)
- Moteur de recherche sur la page d'accueil (nghyd#428)
- Améliorer le système de traduction (nghyd#223)
- Labels des paramètres : lire l'unité dans le modèle et non dans les fichiers de traduction (nghyd#417)

- Cloisons : remplacement de la loi Cunge80 par la loi CEM88D (jalhyd#264)

12.0.0.50 Correction de bogues

- Cordova : la notification de mise à jour ne fonctionne plus (nghyd#436)
- Conditionner le passage en mode CALC aux liens déjà définis, pour éviter les boucles (nghyd#181)
- Solveur : le paramètre recherché, si c'est un extraResult, ne s'initialise pas correctement lors du chargement d'une session (jalhyd#263)
- Solveur : this.prms.X is undefined (jalhyd#262)
- Exemple "débit d'un chenal avec ouvrages" : plusieurs bugs (nghyd#446)
- PAR, générer une simulation à partir d'un calage : NaN (nghyd#447)
- Paramètres liés d'un enfant à l'autre d'un même module : boucle infinie si la source varie (nghyd#444)
- JaLHyd : dans createStructure(), définir automatiquement le structureType en fonction de la loiDebit
- Lors de la vérification d'une passe à bassins variée, bug sur la vérification de charge minimale (jalhyd#265)
- PAB, calcul de cloison qui échoue : l'erreur ne dit pas quelle cloison est en cause (jalhyd#267)
- Vérification d'une PAB variée : erreur dans la vérification des critères obligatoires (jalhyd#266)
- Vérification de PAB : rendre la largeur minimale d'échancrure obligatoire (jalhyd#270)

12.0.0.51 Documentation

- Documentation de la vérification des passes (nghyd#434)
- Traduire la documentation des PAR (nghyd#443)
- Harmonisation de l'indentation des fichiers (nghyd#409)

12.0.0.52 Mises à jour de dépendances

- Angular 10
- Cordova 10
- Electron 10
- Mathjax 3 (nghyd#416)

4.11.1 - 2020-08-11

12.0.0.53 Nouvelles fonctionnalités

- Lois d'ouvrages: ajouter le n° d'ouvrage dans les logs (jalhyd#260, nghyd#442)

12.0.0.54 Correction de bogues

- Erreur de formulation de la loi de Cunge en orifice dénoyé (jalhyd#259)
- Définition de la valeur initiale d'un calcul (nghyd#440)
- Structure et Dever : exposer les résultats pour liage (jalhyd#255)

- Déversoirs dénoyés: Ajouter les liens vers les lois de débit (nghyd#437)

12.0.0.55 Documentation

- Mise à jour de la documentation de la loi de Cunge (nghyd#441)

4.11.0 - 2020-07-28 (Puisque tu PAR)

12.0.0.56 Nouvelles fonctionnalités

- Calage d'une passe à ralentisseurs (jalhyd#34, jalhyd#223, jalhyd#225, jalhyd#226, jalhyd#232, jalhyd#233, jalhyd#234, jalhyd#240, nghyd#365, nghyd#394, nghyd#408, nghyd#422, nghyd#423, nghyd#424, nghyd#425)
- Simulation d'une passe à ralentisseurs (jalhyd#201, jalhyd#229, nghyd#366, nghyd#382, nghyd#394, nghyd#425)
- Bief : lier les paramètres de section pour les Sections Paramétrées générées (nghyd#380)
- Permettre de lier des paramètres de sections de types identiques, sans utiliser les familles (jalhyd#203, nghyd#379)

12.0.0.57 Correction de bogues

- Lien entre deux paramètres de section : la valeur n'apparaît pas dans le tableau de résultats (nghyd#381)
- Désactiver le suivi Matomo lorsqu'Angular n'est pas en mode "prod" (nghyd#412)
- Corriger le coefficient de débit de la vanne submergée (jalhyd#231, nghyd#421)
- Cloisons : une pelle (négative) est calculée pour les orifices, ce qui donne lieu à des avertissements (jalhyd#242)
- Empêcher de créer des liens vers des paramètre invisibles (jalhyd#244)
- MRC : après un calcul varié, il n'y a plus d'eau sur certains radiers (jalhyd#253, nghyd#432)

12.0.0.58 Documentation

- Passes à ralentisseurs (nghyd#398)

4.10.6 - 2020-07-21

12.0.0.59 Nouvelles fonctionnalités

- Transférer les fonctionnalités de cassiopee-2-integration dans Gitlab-CI (nghyd#374)

12.0.0.60 Correction de bogues

- Lechapt-Calmon : ne plus proposer de matériau "NONE" (jalhyd#230)

12.0.0.61 Documentation

- Renommer les lois d'ouvrage (nghyd#419)
- Erreur dans l'équation de Cunge
- Corrections mineures sur Vanne Dénoyée

4.10.5 - 2020-06-30

12.0.0.62 Nouvelles fonctionnalités

- Renommer les lois triangulaires "dénoyées" en "(Villemonte)" (jalhyd#210, nghyd#393)
- Lois d'ouvrages: ajout du seuil triangulaire épais (jalhyd#211, nghyd#399)
- Régime Uniforme, conduite circulaire: provoquer une erreur fatale si la conduite est en charge (jalhyd#214, nghyd#406)
- Cunge 1980 : ajout dans les cloisons et modification du coefficient de débit à 1 (jalhyd#220, jalhyd#221, nghyd#404)

12.0.0.63 Correction de bogues

- PAB : résultats cassés (nghyd#392)
- PAM : Supprimer le lien rugosité de fond (nghyd#391)
- Cloisons : avertissement si les cotes de radier des seuils se situent sous la cote de radier du bassin amont (jalhyd#217)
- Absence d'erreur en cas de code de langue manquant dans les listes déroulantes (nghyd#400)
- Contrôler le domaine de définition lors de l'affectation de .singleValue (jalhyd#218)
- Ouverture de vanne et liens : bug sur longueur du paramètre varié (jalhyd#222)
- Exemple "Longueur de jet d'un déversoir" cassé (jalhyd#224)
- Exemple 3 : l'affichage de graphique clignote (nghyd#407)
- Définition de la pente (jalhyd#212)

12.0.0.64 Documentation

- Documentation de la pente (nghyd#397)
- Documentation de la loi Cunge80 (nghyd#403)
- Documentation des grilles: il manque la définition des variables (nghyd#401)

4.10.4 - 2020-04-17

12.0.0.65 Nouvelles fonctionnalités

- Régime uniforme: ajouter un bouton pour créer une section paramétrée (nghyd#386)
- Cordova : notifications de mise à jour (nghyd#384)

12.0.0.66 Correction de bogues

- Section paramétrée: le tirant d'eau critique ne converge pas sur une section circulaire fermée (jalhyd#209)

- Régime uniforme: erreur de calcul de la vitesse (jalhyd#206, jalhyd#207)
- Impact de jet: problème de gestion des erreurs fatales (jalhyd#205)
- Unité du coefficient de Strickler (jalhyd#208)
- Robustifier le solveur sur la recherche de l'intervalle de départ (jalhyd#164)
- Champ vide à la création d'un module: les champs de section ne sont pas vides quand on choisit un type de section (nghyd#388)
- Section paramétrée: Ajouter le tirant d'eau dans le schéma en coupe de la section (nghyd#389)
- Saisie paramètre qui varie: message d'erreur persistant sur le champ min (nghyd#385)
- Cordova : version erronée (nghyd#383)

12.0.0.67 Documentation

- Fusionner "Section paramétrée" et "Variables hydrauliques" (nghyd#390)
- Sections : documentation du champ Hauteur de berge

4.10.3 - 2020-03-12

12.0.0.68 Nouvelles fonctionnalités

- Nouveau raccourci clavier Alt+G pour afficher le diagramme des modules
- Diagramme des modules : lien vers les notes
- Test e2e des exemples officiels (nghyd#373)
- Exemples types mis à jour, avec notes

12.0.0.69 Correction de bogues

- Calcul d'un module aval qui casse les résultats du module amont (nghyd#371)
- Astérisques sur les champs non-obligatoires (nghyd#368)
- Exemple "Débit d'un chenal avec ouvrages" : impossible de calculer la cote amont dans le module "Cotes d'un bief" (jalhyd#202)
- Déversoirs et Lois d'ouvrages : liens erronés vers la documentation du seuil dénoyé
- Jet : ne pas remplir "sous" la ligne de fond, lorsque sa cote est négative (nghyd#372)
- Passage en mode calcul d'un paramètre dont la singleValue est undefined (nghyd#367)
- Marges sur les titres de Fieldset, Fieldset container, PAB Table
- Désactivation des notifications lorsqu'on vide la session (nghyd#375)
- Chargement d'un Solveur avant ses Nubs cibles
- Sélection de la cible du Solveur lorsque le Nub calculé n'a pas de paramètre calculé (ex: Section Paramétrée) (nghyd#378)
- Section Paramétrée : tableau de résultats fixes en plusieurs exemplaires lors de l'utilisation avec le Solveur (nghyd#377)
- Bief : calcul des sections amont et aval (nghyd#376)

4.10.2 - 2020-02-25

12.0.0.70 Correction de bogues

- Correction de liens erronés vers la documentation

12.0.0.71 Documentation

- Documentation : ajout de liens vers la page de téléchargement

4.10.1 - 2020-02-25

12.0.0.72 Correction de bogues

- Electron : erreur de détection de mise à jour (comparaison chaînes semver)

4.10.0 - 2020-02-24 (Langue Hilare Neuve)

12.0.0.73 Nouvelles fonctionnalités

- Solveur : cibler un résultat complémentaire (nghyd#363, jalhyd#188)
- *Monkey test* sur les interfaces (nghyd#235)
- Lechapt-Calmon : ajouter un avertissement lorsque la vitesse est en dehors de l'intervalle [0.4, 2] (jalhyd#192)
- Rendre plus générique la gestion des listes déroulantes (nghyd#359)
- Automatiser les chemins de configuration depuis le CalculatorType (nghyd#358)

12.0.0.74 Correction de bogues

- Certains liens doivent être cliqués deux fois (nghyd#364)
- Solveur : interdire de travailler sur un Nub dont le résultat est varié (jalhyd#198)
- Paramètre varié et lien à un résultat varié simultanément (jalhyd#199)
- Parfois lorsqu'on charge une session, le bouton Calculer reste grisé (nghyd#349)
- PAB : parfois le type de jet est undefined (jalhyd#196)
- Export XLSX : retirer "help" des entêtes de colonnes (nghyd#360)
- Chargement de session : selon l'ordre des paramètres, le paramètre calculé n'est pas correctement défini

12.0.0.75 Documentation

- Générer la documentation en PDF (nghyd#348)

12.0.0.76 Mises à jour de dépendances

- Angular 9 (nghyd#354)
- Typescript 3.7 (jalhyd#197)
- mise à jour de toutes les dépendances jalhyd/nghyd sauf Mermaid (provoque un bug) et Mathjax (adaptations importantes nécessaires)

4.9.0 - 2020-01-15 (On Fusionne Bien)

12.0.0.77 Nouvelles fonctionnalités

- Nouveau module "Concentration de blocs" (jalhyd#185)

- Lechapt-Calmon : ajout des pertes de charge singulières (nghyd#352, jalhyd#172)
- Simplification du code des Formulaires (nghyd#353)
- Passage de l'AFB à l'OFB : changement de logo, de nom, d'URL

12.0.0.78 Documentation

- Documentation utilisateurs en anglais (nghyd#321)
- Réorganisation de la documentation utilisateurs (nghyd#355)
- Documentation développeurs (nghyd#317)
- Exemples de code Typescript et Javascript pour le développement d'applications en ligne de commande basées sur JaLHyd
- Diagramme de classes simplifié de JaLHyd

12.0.0.79 Mises à jour de dépendances

- Jasmine 3.5
- Karma 4.4

4.8.1 - 2019-12-20

12.0.0.80 Nouvelles fonctionnalités

- Dever: Ajout d'un avertissement si la cote de radier d'un ouvrage est sous la cote de fond du lit (jalhyd#179)
- Strickler: Ajout d'une aide contextuelle (nghyd#332)
- Grille: permettre les calculs partiels (nghyd#336)
- MacroRugo: Ajout d'avertissement sur l'adéquation taille des cellules - largeur de la rampe (jalhyd#174)
- Documentation lois d'ouvrages manquantes (nghyd#342)
- Champs vides à la création d'un module (nghyd#331)
- Dever: Calcul du débit corrigé en utilisant la charge dans les formules (jalhyd#52, nghyd#345)
- Grille: Ajouter le coefficient de forme des barreaux dans les résultats complémentaires (jalhyd#178)
- Grille: Ajouter un profil de barreaux personnalisé (nghyd#334)
- PAB: Ajouter la position du radier des seuils sur le graphique du profil en long (jalhyd#171)
- Impact de jet: Modification des champs de hauteurs (jalhyd#181)
- Hydraulique à surface libre: ajouter un avertissement quand ça déborde (jalhyd#180)
- Cloisons: Ajouter le calcul de la pelle (jalhyd#169)
- MacroRugoCompound: radier incliné - Ajouter le calcul du dévers latéral (jalhyd#177)
- MacroRugo: Supprimer les débits et vitesses du guide technique (jalhyd#177)
- MacroRugo: Domaine de définition de Cd0 (jalhyd#175)
- PAB nombre: Ajout du nombre de chutes harmonisé (jalhyd#167)
- MacroRugoComplexe: modification du libellé des champs (nghyd#333)
- PAB: Export du tableau de géométrie au format XLSX (jalhyd#170)
- MacroRugo: transition douce entre régime émergent et régime submergé (jalhyd#191)

12.0.0.81 Correction de bogues

- Parfois, lorsque le débit varie, la PAB n'a pas d'eau à l'aval pour certaines valeurs de débit (jalhyd#187)
- Lorsqu'on vide un champ, si on change de page, au retour le champ est à nouveau rempli (nghyd#343)
- Impact de chute: Erreur de calcul de la chute nécessaire pour atteindre l'abscisse d'impact (jalhyd#183)
- Impact de jet: non prise en compte de l'angle (jalhyd#182)
- Grille: Pas d'invalidation des résultats sur le choix du profil des barreaux (nghyd#335)
- MacroRugoCompound: radier incliné - changer la répartition des cellules (jalhyd#173)

4.8.0 - 2019-11-26 (Affine et forte à la fois, par amour du remous)

12.0.0.82 Nouvelles fonctionnalités

- Module Fonction affine (jalhyd#160, nghyd#319)
- Module Trigonométrie (jalhyd#161)
- Module Somme et produit de puissances (jalhyd#162)
- Loi Déversoir noyé (jalhyd#165, nghyd#318)
- Logo animé lors du chargement de l'application (nghyd#322)

12.0.0.83 Correction de bogues

- MacroRugo: définition de la valeur par défaut de Cd0 à 1.2 (jalhyd#166)
- Échec du calcul en chaîne dans certains cas (nghyd#325)
- Remous : suppression de LargeurBerge dans le log (nghyd#326)
- Remous : les tirants d'eau critique et normal sont erronés sur le graphique (nghyd#327)
- Remous : une fois calculé, chaque rechargement du module ajoute une copie des logs (nghyd#324)
- Remous : en fluvial uniquement avec forte pente, les abscisses sont fausses (nghyd#328)
- Calcul en chaîne : ERR inopiné dans le tableau de résultats fixes (nghyd#329)

4.7.0 - 2019-10-29 (AGB - Agence Grolandaise pour la Biodiversité)

12.0.0.84 Nouvelles fonctionnalités

- Solveur multi-modules (jalhyd#152, nghyd#301)
- Nouvelle loi d'ouvrage: Orifice Dénoyé (jalhyd#156, nghyd#311)
- Script de déploiement d'une nouvelle version (sur Aubes) (cassiopee2-integration#9)
- Documentation lois d'ouvrages CEM88 V et D (nghyd#315)
- Remous: connecter le ressaut sur un seul point lorsque le ressaut est court (une seule abscisse) (nghyd#312)

12.0.0.85 Correction de bogues

- Lois d'ouvrages: bug à l'affichage des résultats variés lorsque le calcul échoue (jalhyd#163)

- PAB : problème de cotes sur les cloisons (jalhyd#158)
- Calcul en chaîne: stopper la chaîne si une erreur survient (jalhyd#155)
- Diagramme de Jet / de Section : problème de rafraîchissement (nghyd#308)
- Remous : il manque parfois une abscisse (jalhyd#147)

12.0.0.86 Mises à jour de dépendances

- chartjs-plugin-zoom 0.7.4

4.6.1 - 2019-10-15

12.0.0.87 Nouvelles fonctionnalités

- Suivi des comportements des utilisateurs à l'aide de Matomo (sur Aubes) (nghyd#306)
- Documentation: faciliter l'accès à l'application plutôt qu'à GitLab (nghyd#307)

12.0.0.88 Mises à jour de dépendances

- chartjs-plugin-zoom 0.7.4

4.6.0 - 2019-10-14 (Bluefish délavé)

12.0.0.89 Nouvelles fonctionnalités

- Ajout du module Bief (jalhyd#55, nghyd#299)
- Ajout du module Grille (jalhyd#114, nghyd#289)
- Ajout du module Impact de Jet (jalhyd#112, nghyd#287)
- Ajout du module : Pente (jalhyd#143, nghyd#295)
- Passage des courbes de remous en cotes (jalhyd#146, nghyd#298)
- SectionParametree: remplacement de Yf et Yt par Ycor (jalhyd#145, nghyd#297)
- Régime uniforme: ajout de la vitesse moyenne (jalhyd#139)
- Page d'accueil: ajout du logo du pôle (IMFT), remplacement du texte nghyd#208)
- Tests e2e sur les messages de langues absents (nghyd#294)
- Ajout de la possibilité d'un bouton d'aide dans les résultats (nghyd#293)
- Electron : mise à jour automatique (nghyd#250)
- Intégration continue : exécution des tests e2e (nghyd#278)
- Préférences: applicaton de "precision" et "newtonMaxIter" à la Session en cours (jalhyd#40, nghyd#286)
- Lorsqu'un paramètre varie, ajout dans le log global d'un résumé des erreurs/avertissements (jalhyd#140)

12.0.0.90 Correction de bogues

- MacroRugo: écart des débits en submergé (jalhyd#154)
- MacroRugo: non convergence du calcul pour les faibles profondeurs (jalhyd#144)
- Remous : crash avec paramètre lié à un résultat non calculé (jalhyd#151)
- Remous : lorsque la longueur du bief n'est pas un multiple du pas de discrétisation, exécuter le calcul sur la dernière abscisse tout de même (jalhyd#153)

- Remous: parfois le premier point de la courbe torrentielle est absent (jalhyd#148)
- Cordova: le zoom sur les graphiques n'est pas réinitialisable (nghyd#270)
- Chargement de session : déduire le type de structure (nodeType) de la loi de débit (nghyd#265)
- Lechapt-Calmon : effacer les résultats lorsqu'on change de matériau (nghyd#291)
- Lois d'Ouvrages: les logs ne s'affichent pas (jalhyd#120, nghyd#284)
- Lois d'ouvrages: calculer un paramètre enfant en variant la cote aval fait planter les résultats (nghyd#285)

12.0.0.91 Mises à jour de dépendances

- chartjs-plugin-zoom 0.7.4
- ngx-markdown 8.2.1
- electron 6.0.10

4.5.0 - 2019-09-09 (Fish ramps that rock!)

12.0.0.92 Nouvelles fonctionnalités

- Passe à macro-rugosité complexe (jalhyd#35, nghyd#271)
- Réorganisation des onglets par glisser-déposer (nghyd#206)
- Raccourcis clavier (nghyd#192)
- Ajout des graphiques de type "Points" (nghyd#118)
- Passe à bassins: Supprimer simultanément plusieurs bassins (nghyd#269)
- Sessions exemples (nghyd#165)
- Diagrammes des modules de calcul et de leurs liens (nghyd#140)
- Amélioration de la précision d'affichage (nghyd#281, nghyd#29)
- Ouverture d'un fichier de session pour chargement : prévenir si le fichier est vide ou mal formé (nghyd#264)

12.0.0.93 Correction de bogues

- Lechapt-Calmon : le sélecteur de matériaux n'a plus de sélection par défaut (nghyd#276)
- Lechapt-Calmon : enregistrement de la propriété "matériaux" (jalhyd#138)
- Lois d'ouvrages: plantage sur deux paramètres qui varient (nghyd#273)
- Passe à bassins: prise en compte de la longueur des bassins dans l'interpolation (nghyd#268)
- Passe à bassins: il manque l'édition de la cote de radier de la cloison aval (nghyd#277)
- Résultats fixés: l'unité des paramètres calculés n'est pas affichée (nghyd#274)

4.4.2 - 2019-08-06

12.0.0.94 Nouvelles fonctionnalités

- Boutons d'aide sur tous les éléments graphiques (nghyd#157)
- Chargement de session: ouverture automatique du premier module nouvellement chargé
- Touche Tab dans un champ de saisie: le texte est surligné (nghyd#259)

- Simplification des fichiers de session
- Graphique : afficher tous les paramètres d'une même famille simultanément (nghyd#246)
- Réorganisation du format des résultats (jalhyd#128)
- Erreur au chargement de session avec lien sur des paramètres calculés (nghyd#263)
- Enregistrement de session partielle avec liens tronqués: enregistrer les valeurs courantes des paramètres (jalhyd#133)

12.0.0.95 Correction de bogues

- Documentation de la passe à Macrorugosités
- Enregistrement de session: dédoublonner les messages concernant les dépendances
- nodeType est lu depuis la Section et plus depuis le Nub parent (jalhyd#124)
- Electron / Cordova : script npm pour mettre à jour les mimetypes dans dist/index.html (nghyd#258)
- Passe à bassins : traduction
- Graphiques : ne pas représenter les données de type ENUM (nghyd#260)
- Remous : l'itérateur d'abscisses est en retard sur le dessin du graphe (nghyd#267)

4.4.1 - 2019-07-30

12.0.0.96 Nouvelles fonctionnalités

- Passe à bassins : ajouter un accès rapide aux différents panneaux (table, résultats, graphiques...) pour éviter de faire défiler péniblement (nghyd#237)
- Passe à bassins : permettre d'ajouter / dupliquer un ouvrage pour plusieurs cloisons à la fois (nghyd#243)
- Passe à bassins : ajouter la nature du jet (nghyd#245)
- Lois d'ouvrages: Ne pas écraser les valeurs par défaut du coefficient de débit au changement de loi (nghyd#225)
- Lois d'ouvrages: Ajouter le type de jet dans les résultats complémentaires des ouvrages (jalhyd#92)
- Amélioration du titre et de l'icône de l'application (nghyd#257)

12.0.0.97 Correction de bogues

- Ne pas exposer les paramètres de cloisons pour les rendre liables (nghyd#247, jalhyd#111)
- Passe à macro-rugosités : erreur de calcul (nghyd#247)
- Passe à bassins : Le journal de calcul ne s'efface pas quand les données d'entrée changent (nghyd#241)
- Courbes de remous : les inputs ne sont plus pris en compte (nghyd#256)
- Invalidation de calcul bien qu'absence de lien de résultat (jalhyd#98)
- Lois d'ouvrages: Erreur de calcul des lois de seuil / vanne (jalhyd#118)
- Lechapt-Calmon : le sélecteur de matériaux ne charge plus les coefficients, depuis la 4.4.0a (nghyd#231)
- Cloisons: Erreur de calcul de la charge (jalhyd#127)
- Cloisons: Erreur de calcul de la cote de radier si la charge est en calcul (jalhyd#126)
- Passe à macro-rugosité: Écart entre le débit calculé et celui du guide technique (jalhyd#113)

- Passe à macro-rugosité: Erreurs de calcul (jalhyd#85)
- Paramètre varié : le champ d'édition de la liste de valeurs s'affiche mal (nghyd#244)
- Paramètres liables : parfois le mat-select est trop étroit et on ne sait pas ce qu'on est en train de choisir (nghyd#248)

12.0.0.98 Mises à jour de dépendances

- Angular 8.1.2

4.4.0 - 2019-07-16 (Basse à Sapins)

12.0.0.99 Nouvelles fonctionnalités

- Module "Passe à bassins"
- Plusieurs paramètres peuvent varier simultanément
- Implémentation de la vanne levante
- Implémentation de la loi de Villemonte sur les seuils triangulaires et triangulaires tronqués
- Remplacement de la cote de radier par la charge sur les seuils de cloisons
- Remplacement de la dichotomie par la méthode de Brent
- Simplification de la loi Kivi pour les cloisons et les PAB
- Déploiement avec Electron : paquets installables pour Windows 32 bits et Linux (.deb)
- Déploiement avec Cordova : paquet .apk (non signé) pour Android
- Zoom sur les graphiques
- Bouton d'aide dans la barre de navigation, lorsque la session est vide
- Carte de bienvenue lorsque la session est vide: logos et mentions légales
- Système de rapport de bugs par email
- Paramètres liés: affichage de la valeur, icônes d'information
- Compilation: allègement de la bibliothèque Mathjax embarquée
- Magnifique icône en SVG
- Option pour désactiver les notifications à l'écran
- Nouveaux tests

12.0.0.100 Correction de bogues

- Correction erreur de calcul de ZDV
- Corrections d'erreurs liées au cycle de vie d'Angular
- Structures en parallèle: interdiction de supprimer le dernier ouvrage
- Mode plein écran compatible avec les navigateurs plus anciens
- Amélioration de la robustesse de l'enregistrement / chargement de session
- Suppression du lissage sur les graphiques de type "scatter"
- Nettoyage de code
- Limitation de la précision numérique à différents endroits

4.3.0 - 2019-04-12 (Éditions LLL)

12.0.0.101 Nouvelles fonctionnalités

- Module “Passe à bassin : chute”
- Module “Passe à bassin : nombre de bassins”
- Amélioration du filtre de choix des paramètres liables
- Vérification de la cohérence des paramètres liés au chargement de session
- Validation et invalidation en cascade des modules de calcul liés
- Calcul en cascade automatique des modules de calculs liés
- Transfert de ngHyd vers JaLHyd des mécanismes gérant les états des paramètres des modules de calcul
- Ajout des tags de version dans le panneau latéral
- La touche TAB permet de passer directement d’un champ de saisie à un autre
- Le bouton “+” disparaît sur la page d’accueil

12.0.0.102 Correction de bogues

- Divers bogues autour des paramètres liés
- Mise à jour intempestive des paramètres calculés dans le formulaire de saisie
- Précision d’affichage des données dans les infobulles

4.2.0 - 2019-03-11

12.0.0.103 Nouvelles fonctionnalités

- titres courts pour les modules, suffixe numérique automatique
- Lechapt-Calmon : amélioration du sélecteur de matériau
- affichage des valeurs liées
- détection de la langue du navigateur
- mémorisation des paramètres par le navigateur
- mécanisme de langue de secours pour les modules non traduits
- paramètres variables : courbe d’évolution
- graphiques de résultats : choix libre de l’abscisse et de l’ordonnée

12.0.0.104 Correction de bogues

- déplacement de la sérialisation au niveau du modèle (JaLHyd)
- nouvelle gestion des langues: plus robuste, charge moins de fichiers inutiles, ajout d’un cache
- meilleure gestion de la session et de la hiérarchie (ouvrages en parallèle / parent)
- gestion homogène de la touche entrée dans les formulaires : déclenche le calcul
- la précision Pr est traitée comme un paramètre normal
- simplification de la gestion des types d’ouvrages
- désérialisation des ouvrages en parallèle
- validation des ouvrages en parallèle
- validation des paramètres variables
- simplification et suppression de code inutilisé
- affichage des icônes et polices hors-ligne
- conservation du type de graphe lorsqu’on change de module
- ajout de tests exhaustifs sur le calcul des paramètres et le clonage des modules

4.1.0 - 2019-02-20

12.0.0.105 Nouvelles fonctionnalités

- interface : angular-material, angular-flex, charte graphique Irstea
- nouvelle page de liste, modules groupés par thèmes
- ajout du module Passe à Enrochement
- bouton pour vider la session
- bouton pour cloner un module de calcul
- fichier de configuration JSON, gestion d'une langue par défaut
- paramètre variable : amélioration des listes de valeurs
- affichage des graphiques et des tableaux de résultats en plein écran
- export des graphiques en PNG
- export des tableaux de résultats vers Excel
- utilisation de chaînes pour les UID
- utilisation de routerLink et des fragments d'URL (#)
- ajout de tests e2e avec Protractor
- limitation de la précision dans les graphiques

12.0.0.106 Correction de bogues

- redirection des URL invalides vers /list
- chargement de paramètres liés
- sauvegarde et chargement des valeurs des paramètres
- IDs uniques dans les champs de formulaires
- nettoyage du code (tslint)
- suppression de code inutilisé
- renommage et simplification de classes
- amélioration de la traduction

12.0.0.107 Mises à jour de dépendances

- Angular 7.2
- Compodoc
- angular-material
- angular-flex
- suppression de MDBootstrap
- suppression de FontAwesome

4.0.0 - 2018-07-23

13 Legal notice and terms of use

13.1 Editor

The site cassiopee.g-eau.fr hereinafter referred to as “Cassiopée” is published by the UMR G-EAU (Mixed Research Unit “Water Management, Actors, Uses”):

UMR G-EAU 361 rue Jean-François Breton BP 5095 34196 Montpellier Cedex 5
France Tel: +33 (0) 4 67 04 63 00

Director of publication: Marcel Kuper, Director of the UMR G-EAU

Development Project Manager: David Dorchies

Developers: David Dorchies, François Grand, Mathias Chouet, Jean-Pascal Aubry

Cassiopée is a tool proposed by OFB (French Office for Biodiversity) within the framework of the OFB-Irstea conventions (Action n°100 of the 2016-2018 convention and Action n°21 of the 2019-2021 convention).

13.2 Hosting

UMR G-EAU 361 rue Jean-François Breton BP 5095 34196 Montpellier Cedex 5
France

13.3 Contents of the Cassiopée software

The OFB and the UMR G-EAU offer access to calculation tools in the field of hydraulics and more specifically tools to assist in the sizing of fish passes.

Internet users’ access to the Cassiopee site and tools is free and unlimited for all private and professional uses, as long as this access is made only through the tools and interfaces of the site cassiopee.g-eau.fr.

Unless otherwise stated, the intellectual property of the content of the pages is held by the Institut national de Recherche en Sciences et Technologies pour l’Environnement et l’Agriculture (IRSTEA).

13.4 Limitation of liability

The UMR G-EAU undertakes to provide the necessary and reasonable means to ensure or make ensure continuous access to the cassiopee.g-eau.fr website and its contents for the user.

However, the UMR G-EAU cannot be held liable to users in the event of interruption, failure or possible lack of quality of Cassiopée's services for any reason whatsoever, including for reasons of maintenance, upkeep or updating of the servers.

Unless otherwise stated, the contents of Cassiopee are published for information purposes only, excluding any guarantee as to their accuracy or suitability for the specific needs of users of the site cassiopee.g-eau.fr. The contents of Cassiopée do not in any way engage the responsibility of the producers in the event of direct or indirect damage resulting from their non-conformity with the reality on the ground.

If you notice an error or omission in the tools and content of Cassiopée, please report it via the "Report a problem" feature available in the main menu of Cassiopée.

13.5 Users' personal information

13.5.0.1 Data collected by Cassiopée

The cassiopee.g-eau.fr site does not collect any personal data about the user except the IP address of the machine used to connect to the site and the calculation modules used by the user and the number of calculation run.

The data and calculations carried out by Cassiopée are entirely carried out on the user's machine and are not transmitted to the server or any other third party.

Submitting a bug report via the "Report an issue" feature invites the user to send by email the content of his current work session to the Cassiopée development team. The user can choose not to transmit his session by deleting the text of the email below the line `--- Status of the current session - do not modify the text below ---`. The email address provided by the user to the development team will not be shared with third parties or used for any purpose other than to contact the user in connection with the reported problem.

13.5.0.2 Data stored on the user's terminal

Cassiopée does not store any information on the user's terminal except the application settings if they are explicitly saved by the user.

All or part of the user's working session can be saved by the user on any medium at his convenience (json file) and then loaded for later use.

13.6 Hypertext links

13.6.0.1 Links from cassiopee.g-eau.fr to other sites

The links inserted in the pages of the site cassiopee.g-eau.fr to third party sites are provided for information purposes only. The content of the sites at which these links point does not engage the responsibility of the UMR G-EAU.

13.6.0.2 Link to cassiopee.g-eau.fr

The establishment of a hyperlink to Cassiopée is free and open on condition that this hyperlink allows the opening of a new viewing window and that the display of the URL cassiopee.g-eau.fr in the new window is readable by the Internet user as soon as it is opened and throughout the access to Cassiopée's data.

UMR G-EAU reserves the right to delete any hyperlink to Cassiopée that may harm its editorial policy or its image.

13.7 Brands and logos

The brands and logos appearing on the site make it possible to inform as to the origin of the data and software used; they have no advertising character and are the property of their respective owners.

13.8 Screenshots and prints

The content produced by Cassiopée (calculation results, tables, graphs, etc.) can be reused and distributed on any medium without any limitation.

Cassiopée's documentation is published underCC BY-NC-ND 4.0 License which authorizes to copy, distribute, communicate all or part of the documentation by any means and in any format under the conditions that it is credited with a link to the license, it is not used commercially, and that it is not modified.

13.9 Free software

13.9.0.1 License of the Cassiopée calculation module

Cassiopée is based on a library called JaLHyd (for JAvascript Library for HYDraulics) developed in Typescript by the Cassiopée development team. This library is published under GNU AGPL 3 license and the source code is available on request from the Cassiopée editor.

13.9.0.2 Third-party tools and libraries

Cassiopée has been developed using many libraries and free software tools including:

- Typescript
- Visual Studio Code

- Angular
- Angular Material
- Chart.js
- MathJax

List of Figures

List of Tables

UMR G-EAU
361 rue J-F Breton - BP 5095
34196 Montpellier cedex 5
tél. : +33(0)4670400

Rejoignez-nous sur :

www.g-eau.fr
www.inrae.fr

Institut national de recherche pour
l'agriculture, l'alimentation et l'environnement

INRAE
la science pour la vie, l'humain, la terre